Am J Cancer Res 2021;11(1):277-296
www.ajcr.us /ISSN:2156-6976/ajcr0119919

Original Article

Epigenetically silenced linc00261 contributes to the metastasis of hepatocellular carcinoma via inducing the deficiency of FOXA2 transcription

Zhanjun Chen[1,2*], Leyang Xiang[1*], Zhigang Hu[1], Huohui Ou[3], Xiao Liu[4], Lili Yu[5], Wancheng Chen[5], Lei Jiang[5], Qiangfeng Yu[1], Yinghao Fang[1], Yuyan Xu[1], Qin Liu[1], Yu Huang[6], Xianghong Li[1], Dinghua Yang[1]

[1]Unit of Hepatobiliary Surgery, Department of General Surgery, Nanfang Hospital, Southern Medical University, Guangzhou 510515, Guangdong Province, China; [2]Department of General Surgery, Affiliated Baoan Hospital of Shenzhen, Southern Medical University, Shenzhen 518101, Guangdong Province, China; [3]Department of Hepatobiliary Surgery, Shunde Hospital, Southern Medical University (The First People's Hospital of Shunde), Foshan 528308, Guangdong Province, China; [4]Department of General Surgery, Foresea Life Insurance Guangzhou General Hospital, Guangzhou 511356, Guangdong Province, China; [5]Cancer Research Institute, Guangdong Provincial Key Laboratory of Cancer Immunotherapy, School of Basic Medical Sciences, Southern Medical University, Guangzhou 510515, Guangdong Province, China; [6]Department of Laboratory Medicine, Nanfang Hospital, Southern Medical University, Guangzhou 510515, Guangdong Province, China. [*]Equal contributors.

Received August 9, 2020; Accepted November 25, 2020; Epub January 1, 2021; Published January 15, 2021

Abstract: Hepatocellular carcinoma (HCC) is one of the most common malignancies worldwide. In recent decades, long non-coding RNAs (lncRNAs) have attracted increasing attention and have been reported to play important roles in human cancers, making them ideal candidates for precise disease assessment and treatment. Our previous study found that the loss of linc00261 was significantly correlated with the malignant biological behaviors of HCC, particularly MVI, and serves as an excellent independent prognostic factor for recurrence-free survival. In this study, our in-depth research demonstrated that linc00261 inhibits epithelial-mesenchymal transition (EMT) in liver cancer cells, thereby suppressing migration, invasion, and the formation of lung metastatic lesions. Moreover, linc00261 and its neighbor gene *FOXA2* were positively correlated in HCC, the gain- and loss-of-function analyses indicated that linc00261 transcriptionally promotes the expression of FOXA2. Additionally, bioinformatic analysis and rescue assays confirmed that linc00261 partially suppresses migration, invasion, and EMT by upregulating FOXA2 expression. Molecular mechanism studies showed that linc00261 transcriptionally upregulates FOXA2 in *cis* by recruiting SMAD3. Finally, we identified EZH2 is responsible for linc00261 transcription repression via modulating trimethylation of H3K27 at Lys27 (H3K27Me3), both EZH2 and H3K27Me3 were negatively correlated with linc00261 expression in HCC. In conclusion, these findings demonstrated a crucial role of linc00261 in HCC metastasis, and that EZH2/linc00261/FOXA2 axis might reveal potential prognostic factors and be applied as therapeutic targets for HCC metastasis.

Keywords: Hepatocellular carcinoma, metastasis, linc00261, FOXA2, EZH2

Introduction

Primary liver cancer is the sixth most frequent cancer and fourth leading cause of cancer-related death worldwide; 75-85% of these cases are hepatocellular carcinoma (HCC) [1]. Although various therapeutic options are available, such as surgical resection, liver transplantation, ablation, transarterial chemoembolization, radiotherapy, and systemic treatments involving multidisciplinary approaches, tumor recurrence and metastasis remain the main factors resulting in poor prognosis [2]. A better understanding of the risk factors and molecular mechanisms underlying HCC progression is necessary to advance diagnostic and therapeutic inventions.

Long non-coding RNAs (lncRNAs) post-transcriptionally modulate gene expression by affect-

ing mRNA stability, functioning as miRNA sponges, and regulating translation in the cytoplasm; however, they are more able to activate or repress gene transcription in *cis* or *trans* by interacting with various chromatin-modifying complexes in the nucleus [3-5]. Our previous study discovered a long intergenic noncoding RNA (lincRNA), linc00261, which is significantly associated with the presence of microvascular invasion (MVI) and dysregulated in HBV-related HCC; the loss of linc00261 in HCC tissues was correlated with worse post-operative recurrence-free survival (RFS) in HBV-related HCC and enhanced cellular motility and invasion in HCC cells [6], which possibly results from the inhibition of Notch signaling through the suppression of Notch-1 and Hes-1 expression [7]. However, the precise effect and underlying mechanism of linc00261 on HCC progression, as well as the reason of linc00261 downregulation in HCC, is not well-understood.

Accumulating studies have suggested that the loss of differentiation-associated transcription factors (such as GATA3, ELF5, and NKX2-1) and embryonic cell fate regulating transcription factors (such as SOX2, MYC, KLF4, FOXA2, and OCT4) induces stem cell-like properties, which are related to metastasis initiation [8]. Interestingly, these development-associated transcription factors are always preferentially surrounded by lincRNAs in vertebrates [9], whereas only approximately 3% of all human lincRNAs are positively correlated with their neighboring genes [10]. Therefore, it is rare that development-associated lincRNAs influence cancer metastasis by interacting with neighboring genes encoding development-associated transcription factors. Encoding one of the pioneer transcriptional factors in liver specification, *FOXA2* was found to be located upstream of linc00261 and induced by linc00261 during endoderm differentiation [11, 12]. In lung adenocarcinoma, FOXA2 also inversely induce linc00261 expression, their expression are together triggered by DNMT1 through CpG island methylation of the entire lnc00261-FOXA2 locus [13]. Moreover, FOXA2 and its targets are central modulators of the sexual dimorphism of HCC, indicating that FOXA2 is tightly coupled with HCC initiation or progression [14]. Besides, FOXA2 was recently reported to be involved in regulating AFP production both in AFP-producing gastric adenocarcinomas and HCC cells [15]. Some studies have also demonstrated crucial suppressive roles for FOXA2 in HCC metastasis [16, 17]. Taken these together, linc00261/FOXA2 axis is supposed to regulate HCC progression, yet it has not been systemically explored.

EZH2 (Enhancer of zeste 2) is the key subunit of PRC2 (ploycomb repressive complex 2), which catalyzes trimethylation of H3K27 at Lys27 (H3K27Me3) via its SET domain, and then triggers the recruitment of PRC1 complex to the promoter region of target genes, ultimately results in the compression of chromosomes and silencing of target genes [18]. It also causes transcriptional inhibition through a variety of histone independent mechanisms. For example, EZH2 directly recruits DNMT1 and DNMT3A/B to the promoter region of the target gene, causes methylation of the promoter CpG island, thus interferes the binding of transcriptional factors to the promoter and regulating the transcription of target genes [19]. EZH2 is commonly overexpressed in a number of caners, and correlated with tumor aggressiveness and poor prognosis, including HCC [2, 3]. It induces gene silencing of many tumor suppressors, such as miRNAs (miR-101, miR-622, miR-34a) [20, 21] and lncRNAs (SPRY4-IT1, lncRNA-SVUGP2) [22, 23]. However, little is known about the effect of EZH2 on the epigenetic regulation of linc00261 in HCC.

In this study, we further discovered that the loss of linc00261, partially suppressed by EZH2 mediated H3K27Me3, might be a key risk factor for the generation of metastasis-initiating cells. Subsequent exploration of the potential mechanism underlying linc00261-associated HCC metastasis showed that it transcriptionally upregulates the expression of its neighbor gene, a known tumor suppressor, *FOXA2*, by interacting with the transcriptional factor SMAD3, thereby restraining HCC metastasis.

Materials and methods

Patients and tissue specimens

Patients with hepatitis B virus-related HCC who underwent radical resection between November 2010 and November 2016 in Nanfang Hospital, Southern Medical University were enrolled in this study. HCC and adjacent non-

cancerous tissues (exceeding the outer edge of tumor at least 2 cm) were obtained immediately after resection. The specimens were stored in liquid nitrogen until subjected for real-time quantitative PCR (RT-qPCR) analysis or were paraformaldehyde-fixed and paraffin-embedded. All patients included in this study satisfied the following inclusion criteria: (a) treatment-naïve before surgery; (b) diagnosed pathologically and serologically as having hepatitis B virus-related HCC, and without hepatitis C virus infection; (c) the complete clinical parameters and follow-up data were well-documented. The Ethical Committee of Nanfang Hospital, Southern Medical University approved the usage of tissues from patients with HCC for retrospectively analysis at January 15th, 2018 (NFEC-2018-004). As required by the Declaration of Helsinki (6th revision, 2008), written consent was signed by each patient.

For cohort 1 (n=100), fresh HCC and adjacent noncancerous tissues were used for linc00261 relative expression determination by RT-qPCR. For cohort 2 (n=79), paraformaldehyde-fixed and paraffin-embedded HCC and adjacent noncancerous tissues were subjected to immunohistochemical staining. Overlapping cases (n=44) between cohorts 1 and 2 were evaluated by both assays.

Patient follow-up

After discharge from the hospital, the patients were further monitored for survival analysis via regular outpatient follow-up. Relapse was diagnosed based on increased post-operative serum alpha-fetoprotein levels and the presence of space occupying lesion in or out of the liver, using at least one imaging examination (ultrasonic examination, computed tomography scan, or magnetic resonance imaging). Follow-up began on the date of surgery and terminated on August 31, 2017.

Hematoxylin-eosin (HE) staining and immunohistochemical staining

Paraffin-processed sections with 3 μm thickness were prepared and mounted onto polylysine-coated slides, and then dewaxed in xylene and rehydrated in gradient alcohol. For HE staining, the slides were subsequently stained with hematoxylin and eosin according to standard protocols. For immunohistochemical staining, the antigens were firstly retrieved in citric acid buffer (PH6.0) by microwave antigen retrieval. After that, they were immersed in 3% H_2O_2, blocked with 5% BSA solution, and incubated with primary rabbit polyclonal antibodies (Supplementary Table 5) overnight at 4°C. The following day, the sections were incubated with horseradish peroxidase-conjugated goat-anti-rabbit secondary antibody (ZSGB-BIO, Beijing, China), and developed with peroxidase substrate diaminobenzidine (DAB; ZSGB-BIO). The pathological histology and expression of target proteins were observed under an upright microscope (Olympus, Tokyo, Japan). The expressions of target proteins were evaluated semi-quantitatively by multiplying the scores of staining intensity and positive rate as we previously reported [24].

Immunofluorescence staining

Cells at logarithmic phase were planked on coverslips. After adherence, cells were fixed in 4% paraformaldehyde for 20 min, permeabilized with 0.3% Triton X-100 diluted with PBS buffer for a specified interval set (without this step for membrane proteins, 10 min for cytosolic proteins and 30 min for nuclear proteins), and blocked with 3% BSA in PBS buffer for 1 hour at room temperature. Then, cells were incubated with primary antibodies (Supplementary Table 5) overnight at 4°C, and with Alexa fluor 594-conjugated goat-anti-rabbit secondary antibody (Proteintech) for 1 hour at room temperature in the dark. In the end, nuclei were stained using 4',6-diamidino-2-phenylindole (DAPI; Solarbio, Beijing, China) and images were captured under an inverted fluorescence microscope (Olympus).

FISH

The expression and localization of linc00261 in tissues and cell lines were determined as the instructions obtained from Exonbio (Guangzhou, China) who designed and synthesized linc00261-specific probes (targeting 3409-4497nt of linc00261 and labeled with digoxin). Briefly, the paraffinized sections were dewaxed with xylene and rehydrated in gradient alcohols, digested with 0.25% pepsin solution for 30 min at 37°C. For cell lines, the coverslips were incubated with 4% paraformaldehyde and permeabilized with 0.3% Triton X-100 for 20 min. Then, the sections/cell slides were prehybridized with hybridization solution (Exonbio)

for 2 hours at 55°C followed with refixation with 4% paraformaldehyde. In the meanwhile, the probes diluted with hybridization solution (1: 100) were denatured for 5 min at 85 ± 2°C and kept at 37°C for use in a temperature-controlled water bath. Next, the sections/cell slides were incubated with denatured probes overnight at 37°C, blocked with 3% BSA, and incubated with rhodamine-conjugated IgG fraction monoclonal mouse anti-digoxin (Exonbio) for 1 hour at 37°C in the dark. Nuclei were stained using DAPI (Solarbio) and images were captured under an inverted fluorescence.

RNA pull-down assay and mass spectrometry (MS) analysis

RNA pull-down assay was conducted using Pierce TM Magnetic RNA-Protein pull-down kit (20164; Thermo Scientific, MA, USA). Briefly, linc00261 was firstly transcribed in vitro and 3'-end labeled with a single desthiobiotinylated cytidine bisphosphate using T4 RNA ligase. Then, the labeled RNA was captured by magnetic beads and incubated with MHCCLM3 cell lysates. The same amount of 3'untranslated-region of androgen receptor RNA was used as the negative control, the sequence was as follow: 5'-CUGGGCUUUUUUUUUCUCUUUCUCUCCUUUCUUUUUCUUCUUCCCUCCCUA-3'. After washing and elution, the RNA-binding proteins was separated by 10% SDS-PAGE and visualized using silver staining. Ultimately, the proteins were identified with MS and western blotting analyses. For evaluation of the MS results, samples from 3 replications were merged and subjected for MS detection. Each peptide identified has a score, pep_expect, If the pep_expect score < 0.05, it was considered that this peptide matches with its target protein. The ultimate results of linc00261 potentially binding proteins refers to Supplementary File 1. For verifivation of the binding between linc00261 and SMAD3 (Abcam, Cambridge, England), the proteins retrieved in the RNA pull-down assay were subjected to western blotting for 3 times.

RNA immunoprecipitation (RIP)

MHCCLM3 cells were subjected to RIP assay according to the protocol of using RNA Binding Protein Immunoprecipitation Kit (BersinBio, Guangzhou, China). Briefly, cells were lysed in polysome lysis buffer containing protease inhibitor and RNase inhibitor. After removal of DNA, the lysates were divided into three groups (IP, IgG and Input groups), and the former two were respectively immunoprecipitated with equal amount of anti-SMAD3 rabbit antibody and control IgG at 4°C overnight, and incubated with prepared protein A/G beads at 4°C for 1 hour. Then, RNA was extracted from the protein-RNA complexes and applied to the subsequent RT-qPCR. U1 snRNP and GAPDH were used as control, and the primers were the same as above. The experiment was repeated for 3 times.

Chromatin immunoprecipitation (CHIP)

To evaluate the binding of SMAD3 to the promoter region of FOXA2, and EZH2, H3K27Me3 to the promoter region of linc00261, CHIP assay using SimpleChIP® Enzymatic Chromatin IP Kit (Agarose Beads; Cell signaling technology, MA, USA; CST9002) was performed with MHCCLM3 and HepG2 cell lines, respectively, according to the manufacturer's instruction for 3 times. Control rabbit IgG and antibodies against SMAD3 (Abcam), EZH2 (Cell signaling Technology) and H3K27Me3 (Cell signaling Technology) were presented in Supplementary Table 5. The purified DNA was further used for RT-qPCR with a subset of primers targeting FOXA2 and linc00261 promoters (Supplementary Table 6).

The other materials and methods, such as cell lines and culture conditions, cell proliferation assay, plate colony-forming assay, Transwell migration and invasion assays, RNA extraction and RT-qPCR, Western blotting, subcellular fractionation and quantification of RNAs, establishment of transient knockdown models, lentivirus construction and transfection, and in situ tumor model, refers to the Supplementary Materials and Methods.

Statistical analysis

All results were presented as the mean ± standard error of mean and analyzed using SPSS Statistics 20.0 software (SPSS, Inc., Chicago, IL, USA). The enumeration data were analyzed by χ^2-test. The measurement data obtained from two groups were compared by Student's *t* test or Mann-Whitney U test, and analysis of variance followed with least significant difference-*t* test or Dunnett's T3 test were used to compare multiple groups. Pearson correlation

was used to analyze the correlation coefficient between two groups. Survival data were assessed by the Kaplan-Meier method and log-rank test was used to evaluate the difference. Univariate and multivariate analyses were based on the Cox proportional hazards regression model. $P < 0.05$ was considered as statistically significant.

Results

Downregulation of linc00261 is associated with HCC progression as an independent risk factor

To study the effect of linc00261, we consulted online databases to examine its expression in various adult normal tissues and cancerous tissues. First, the NCBI gene database revealed that linc00261 was annotated as specifically-expressed in endoderm-derived adult tissues/organs, with the liver showing the highest level compared to that in other organs or tissues (Supplementary Figure 1A). Then, we determined that patients with lower linc00261 levels in cancerous tissues had poorer overall survival in colon adenocarcinoma, HCC, lung adenocarcinoma, pancreatic adenocarcinoma, and uterine corpus endometrial carcinoma (Supplementary Figure 1B, 1C) as shown in the sequencing data of *Oncolnc* (http://www.oncolnc.org/) [25]. Our previous preliminary study suggested that linc00261 can serve as a prognostic biomarker to predict postoperative outcomes in patients with HCC [6]. To further explore its expression and clinical significance, we measured its expression in another cohort with HCC. The results showed that linc00261 was downregulated in 32.0% of patients (**Figure 1A**). Further, Chi-square and Mann-Whitney U tests revealed that patients with tumor sizes ≥ 5 cm or with MVI had lower linc00261 expression (Supplementary Table 1 and **Figure 1B-E**) and that patients with lower relative linc00261 expression had a shorter RFS than those with higher expression (median ± standard deviation, 7.89 ± 2.59 *vs.* 31.34 ± 13.40 months; **Figure 1F**). Moreover, univariate and multivariate Cox regression analyses indicated that tumor number (95% confidence interval [CI], 1.350-5.436; P=0.005), MVI (95% CI, 1.065-4.595; P=0.033), differentiation (95% CI, 0.306-0.824; P=0.006), and relative linc00261 expression (95% CI, 0.294-0.978; P=0.042) were independent prognostic factors of RFS in patients with HCC (Supplementary Table 2).

Microvascular invasion (MVI), usually defined as the presence of microscopic tumor emboli within the portal or hepatic veins of the surrounding liver tissues close to the HCC lesions, has been regarded as the early stage of HCC intra- and extra-hepatic metastasis, which markedly increases the risk of post-operative recurrence and death [26-28]. We further screened HE-stained slides in patients with MVI; specifically, three cases with MVI within the noncancerous liver tissues were selected and subjected to further fluorescence in situ hybridization (FISH) analysis, which demonstrated that linc00261 was downregulated in cells undergoing MVI compared to expression in normal liver cells (**Figure 1G**, **1H**).

Linc00261 suppresses migration, invasion, and EMT in HCC cell lines

The previously mentioned results indicated that the downregulation of linc00261 in liver tumor cells was significantly associated with MVI, thereby contributing to metastatic recurrence. To further understand the potential underlying mechanism, gene ontology (GO) analysis were conducted using *DAVID* (https://david.ncifcrf.gov/tools.jsp) [29] with linc00261 negatively co-expressed mRNAs in HCC obtained from *cBioPortal* [30, 31]. Interestingly, the analyses of biological process (BP), cellular component (CC), and molecular function (MF) showed that linc00261 was significantly associated with cell-cell adhesion (BP, CC, and MF), extracellular matrix disassembly (BP), microtubule-based movement (BP), and microtubule motor activity (MF); further, the cell-cell adhesion-associated co-expressed mRNA counts ranked among the highest levels, indicating that linc00261 is closely related to cell motility, EMT, and even cancer metastasis (Supplementary Figure 2A).

Based on RT-qPCR detection in a series of cell lines (Supplementary Figure 2B), we constructed linc00261-knockdown models using MHCCLM3 and SNU-449 cell lines (Supplementary Figure 2C), as well as models stably overexpressing linc00261 based on HepG2 and SMMC-7721 cell lines (Supplementary Figure 2D). Neither linc00261 knockdown or overexpression influence the proliferation, as revealed

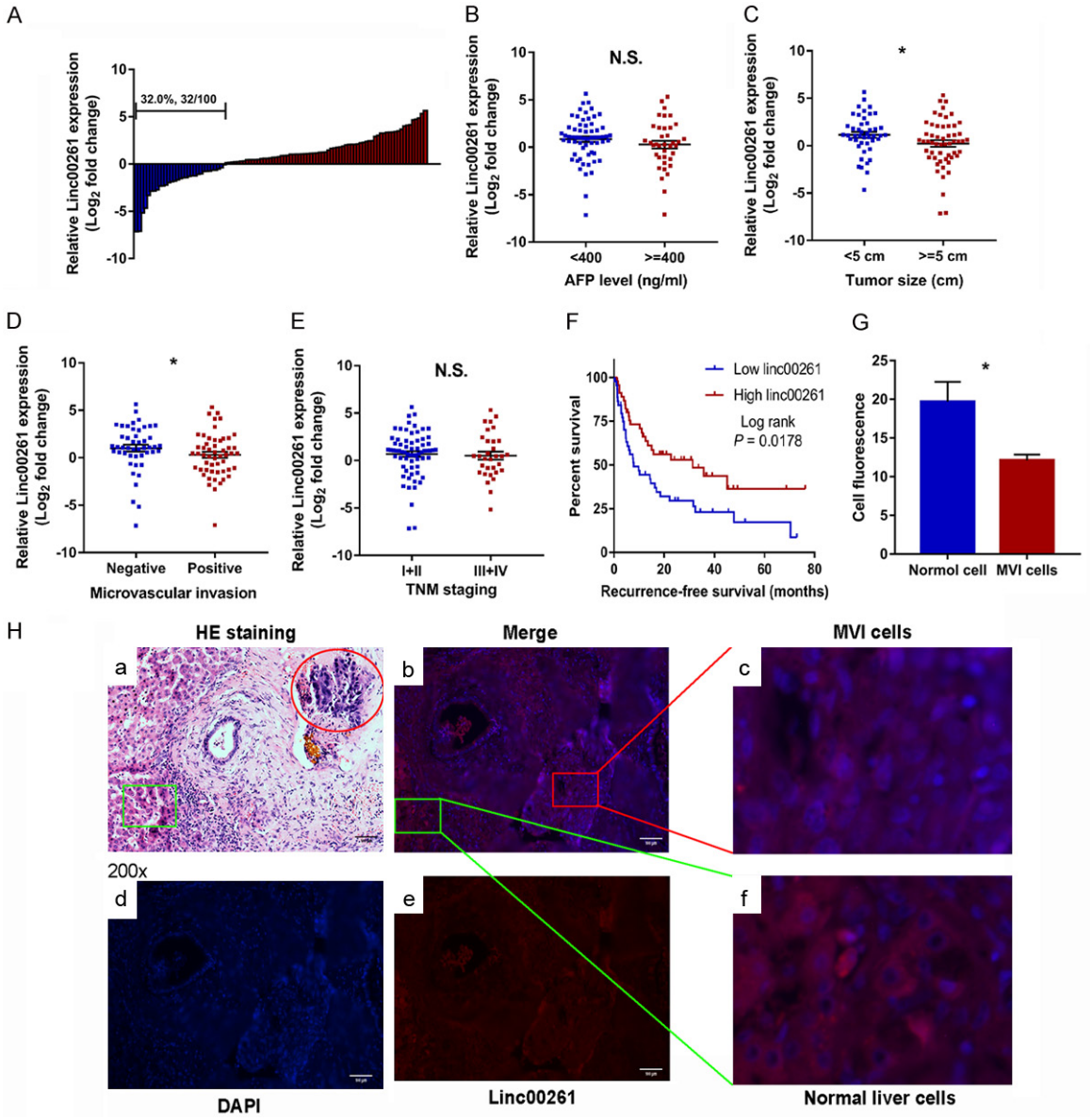

Figure 1. Linc00261 expression in patients with HCC and the relationship with clinicopathological parameters and survival. (A) Linc00261 was down-regulated in 32.0% (32/100) patients with HCC determined by RT-qPCR; (B-E) Linc00261 expression was compared in patients with different pre-operative AFP levels (B), tumor size (C), MVI status (D) and TNM staging (E) determined by RT-qPCR and Mann-Whitney U test; (F) Recurrence-free survival was analyzed by Kaplan-Meier method in HCC patients with different relative linc00261 expression (n=91); (G) Linc00261 expression comparison between normal liver cells and MVI cells evaluated by FISH and t-test (n=3); (H). Representative images of linc00261 staining by FISH in noncancerous liver tissues. In H(a) the red circle displays the MVI cells in the portal vein, and the green box indicates the normal liver cells. N.S. not significant; *$P < 0.05$.

by CCK-8 and plate clone formation assays (Supplementary Figure 2E-G); however, migration and invasion were significantly promoted after linc00261 knockdown (**Figure 2A**), and obviously suppressed after overexpressing linc00261 (**Figure 2B**). We also determined the expression of EMT-associated proteins in linc00261-overexpressing and knockdown cells. The knockdown of linc00261 promoted ZEB1 and vimentin expression and suppressed E-cadherin expression (**Figure 2C**, **2D**), whereas its overexpression resulted in the opposite effects on ZEB1, E-cadherin and Vimentin expressions (**Figure 2E-G**). Additionally, ectopic expression of linc00261 in SMMC-7721 cells significantly inhibited the formation of lung metastatic lesions in male Biocytogen-NOD-PrkdcscidIL2rgtm1/Bcgen (B-NDG) mice based

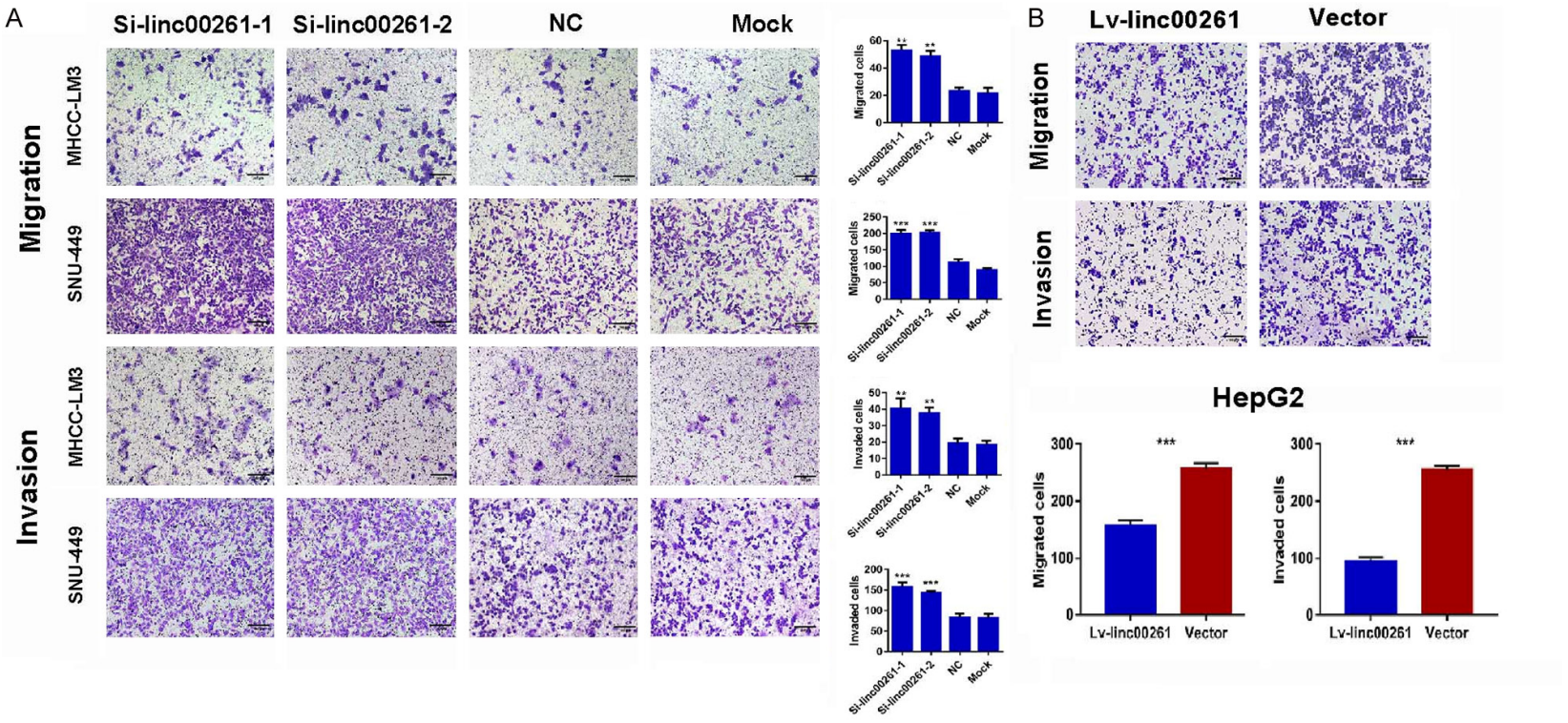
A
Si-linc00261-1
Si-linc00261-2
NC
Mock
Migration
Invasion
MHCC-LM3
SNU-449
Migrated cells
Invaded cells
B
Lv-linc00261
Vector
HepG2
Migrated cells
Invaded cells

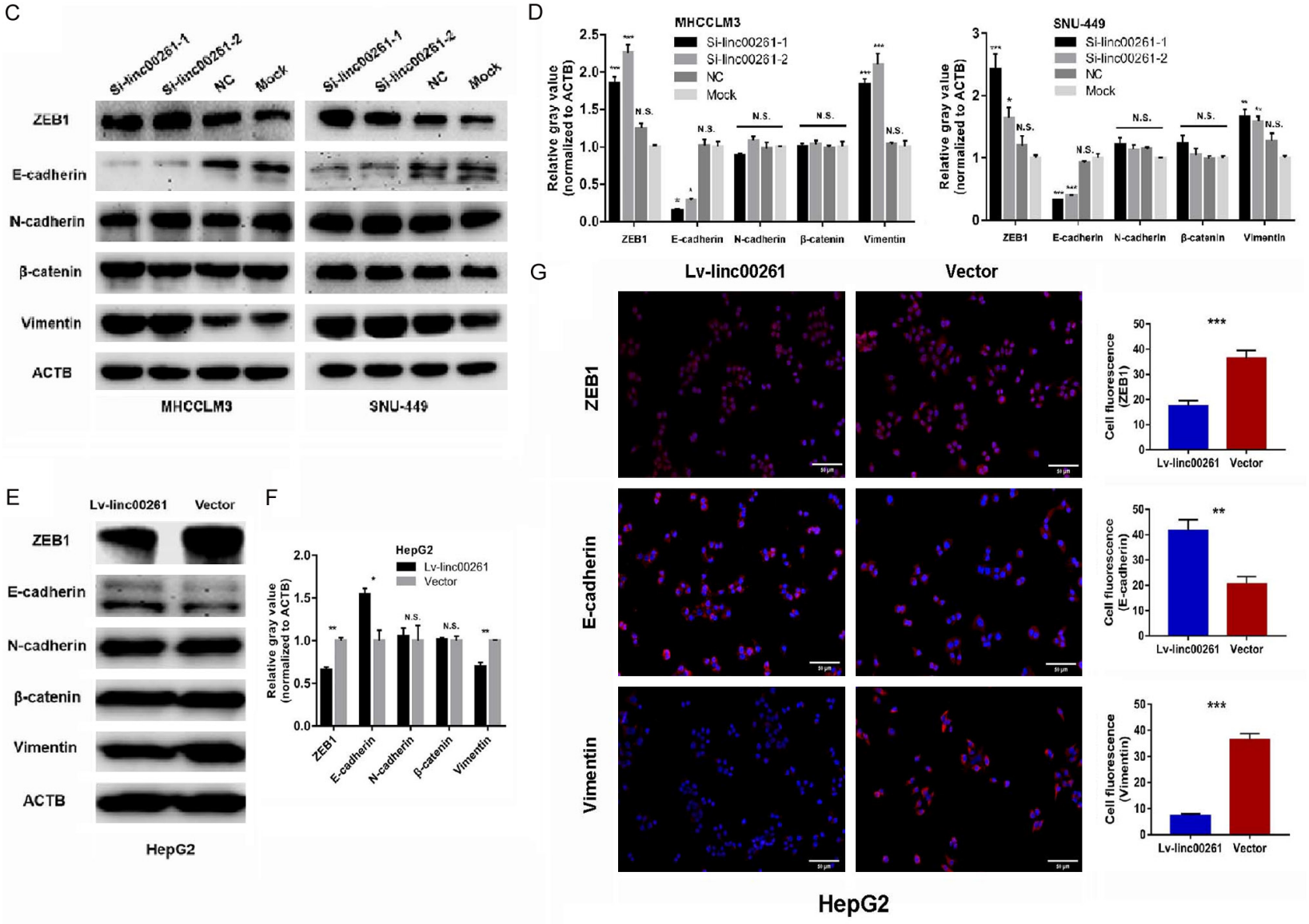

Figure 2. Linc00261 overexpression suppressed migration, invasion and EMT process in HCC cell lines. (A) Representative images and statistical analyses of migration and invasion assays after linc00261 knockdown in MHCCLM3 and SNU-449 cells; (B) Representative images and statistical analyses of migration and invasion assays after linc00261 overexpression in HepG2; (C-F) The protein expressions of epithelial (E-cadherin) and mesenchymal associated markers (N-cadherin,

β-catenin and Vimentin)/transcription factor (ZEB1) determined by western blotting after linc00261 knockdown in MHCCLM3 and SNU-449 (C) or linc00261 overexpression in HepG2 (E), as well as the comparisons of gray values of these proteins using ANOVA (D and F); (G) Representative images and statistical analyses (t-test) of ZEB1, E-cadherin and Vimentin expression evaluated by immunofluorescence after linc00261 overexpression in HepG2 (n=3). N.S. not significant; *P < 0.05; **P < 0.01; ***P < 0.001. The original western blotting images refers to Supplementary Figure 5.

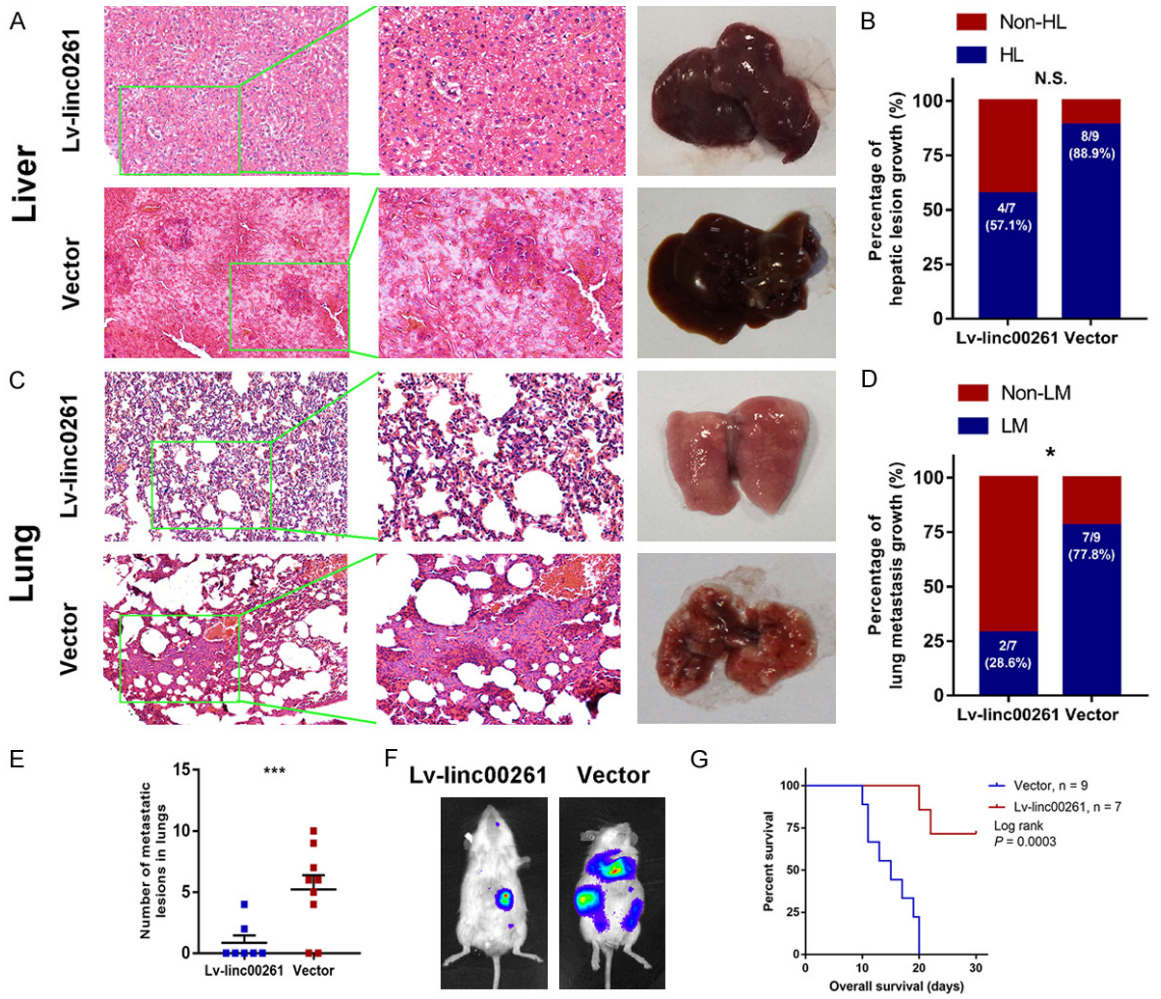

Figure 3. Forced expression of linc00261 in SMMC-7721 significantly suppresses lung metastasis and results in early death in B-NDG mice. Nine and 7 B-NDG mice were separately implanted with SMMC-7721-vector and -Lv-linc00261 cells in the livers and maintained in SPF-grade condition. (A) The representative microscope photos of the livers of B-NDG mice revealed by HE staining (A, left) and the gross specimens (A, right); (B) Comparison of the hepatic lesions growth rates between two groups using chi-square test; (C) The representative microscope photos of the lungs of B-NDG mice revealed by HE staining (C, left) and the gross specimens (C, right); (D and E) Comparisons of the lung metastatic lesions growth rates (D; chi-square test) and the tumor numbers (E; t-test) between two groups; (F) The representative images of *in vivo* orthotopic (in the livers) and metastatic (in the lungs) tumors of B-NDG mice; (G) Overall survival comparison of B-NDG mice after SMMC-7721 cells implantation using Kaplan-Meier method. B-NDG, Biocytogen-NOD-PrkdcscidIL2rgtm1/Bcgen; HL, hepatic lesion; LM, lung metastasis; N.S. not significant; *P < 0.05; ***P < 0.001.

in-situ tumor model, although few liver orthotopic xenograft tumors were observed (**Figure 3A-F**). Mice implanted with SMMC-7721-vector cells showed earlier death compared to that in the linc00261-overexpressing groups (**Figure 3G**).

Linc00261 suppresses migration, invasion, and EMT by upregulating its neighboring gene, FOXA2

It is well-known that lincRNA transcriptionally regulates neighbor gene expression in *cis* by

interacting with transcription factors [5, 32]. *FOXA2* is located upstream of linc00261 in the genome. Thus, we examined FOXA2 expression in another HCC cohort (cohort 2; n=79), which showed that FOXA2 protein was primarily localized in the nucleus and was significantly decreased in HCC tissues compared to that in adjacent noncancerous tissues (Supplementary Figure 3A, 3B). Further, FOXA2 protein levels were negatively associated with MVI (P=0.045), portal vein tumor thrombus (P=0.015), and TNM stage (P=0.008) (Supplementary Table 3); in addition, patients with lower FOXA2 protein levels in HCC tissues had a shorter RFS compared to those with higher levels (Supplementary Figure 3C). Univariate and multivariate Cox regression analyses indicated that portal vein tumor thrombus (95% CI, 1.330-7.432; P= 0.009), differentiation (95% CI, 0.091-0.586; P=0.002), and FOXA2 protein expression (95% CI, 0.152-0.706; P=0.004) were independent prognostic factors for RFS (Supplementary Table 4). Furthermore, the knockdown of FOXA2 promoted the migration and invasion capabilities of HCC cells (Supplementary Figure 4A-C), suppressed expression of the epithelial marker E-cadherin, and increased levels of the mesenchymal markers ZEB1, β-catenin, and vimentin (Supplementary Figure 4D). These results confirmed that FOXA2 plays a suppressive role in HCC metastasis.

To explore whether linc00261 suppresses HCC metastasis by modulating its neighboring gene *FOXA2*, correlation analysis between linc00261 and *FOXA2* mRNA based on RNA sequencing data using *GEPIA* (http://gepia.cancer-pku.cn/detail.php?gene=) [33] was performed, indicating that they were positively correlated in both normal liver (P=0.00039, r=0.48; **Figure 4A**, left) and HCC tissues (P=7.6E-32, r=0.56; **Figure 4A**, right); data from a series of cell lines and tissues from patients with HCC (n=44, intersection of the previous two cohorts) also demonstrated a strong correlation between linc00261 and FOXA2 mRNA (**Figure 4B**, **4C**) and protein (**Figure 4D**). Next, linc00261 localization was evaluated by RT-qPCR following the separation of nuclear and cytoplasmic RNA fractions (**Figure 4E**), as well as by FISH (**Figure 4F**), which demonstrated that linc00261 was present in both the nucleus and cytoplasm, but primarily in the nucleus. Further, knockdown of linc00261 significantly attenuated FOXA2 expression at the mRNA level (**Figure 4G**), whereas the ectopic expression of linc00261 upregulated FOXA2 expression at the mRNA level (**Figure 4H**); and the FOXA2 protein expression altered in accordance with mRNA in both linc00261 knockdown and overexpression experiments (**Figure 4I-K**). Moreover, linc00261- and FOXA2-co-expressed mRNAs in patients with HCC were separately obtained from *cBioPortal* (http://www.cbioportal.org/) [30, 31]. Genes co-expressed with linc00261 significantly overlapped with those co-expressed with FOXA2 (**Figure 5A**), and the common negatively co-expressed mRNAs were significantly enriched in the following terms as revealed by GO analysis: cadherin binding involved in cell-cell adhesion, extracellular matrix disassembly and collagen catabolic process (BP), cell-cell adherens junction (CC), and cadherin binding involved cell-cell adhesion (MF) (**Figure 5B**) [29]; this was in agreement with our previous findings (Supplementary Figure 2A). Ultimately, rescue experiments showed that knockdown of FOXA2 in Lv-linc00261-HepG2 cells could abrogate the inhibitory effect of linc00261 on migration, invasion, and EMT (**Figure 5C**, **5D**).

Linc00261 interacts with SMAD3 to activate the transcription of FOXA2

Considering the positive regulatory effect of linc00261 on FOXA2 expression at both the mRNA and protein levels, we predicted the involvement of chromatin-modifying complexes controlling *FOXA2* transcription. To understand the potential mechanism, we performed an RNA pull-down assay and mass spectrometric analysis in MHCCLM3 cells, which suggested that 532 proteins were specifically bound to linc00261 (**Figure 6A** and Supplementary File 1). By constructing a Venn diagram comprising the 396 transcriptional factors predicted to modulate FOXA2 transcription using *JASPAR* (Supplementary File 2) [34], SMAD3, FOXO3 and CUX1 were anticipated to be recruited by linc00261 to the promoter region of *FOXA2* to regulate its transcription (**Figure 6B**). We noticed that SMAD3, and a SMAD2/3/4 complex were predicted targeting to FOXA2 promoter region. Interestingly, a previous study discovered that DEANR1 (also termed linc00261) facilitate endoderm differentiation by upregulating the expression of endoderm factor FOXA2 via inducing SMAD2/3 recruitment to

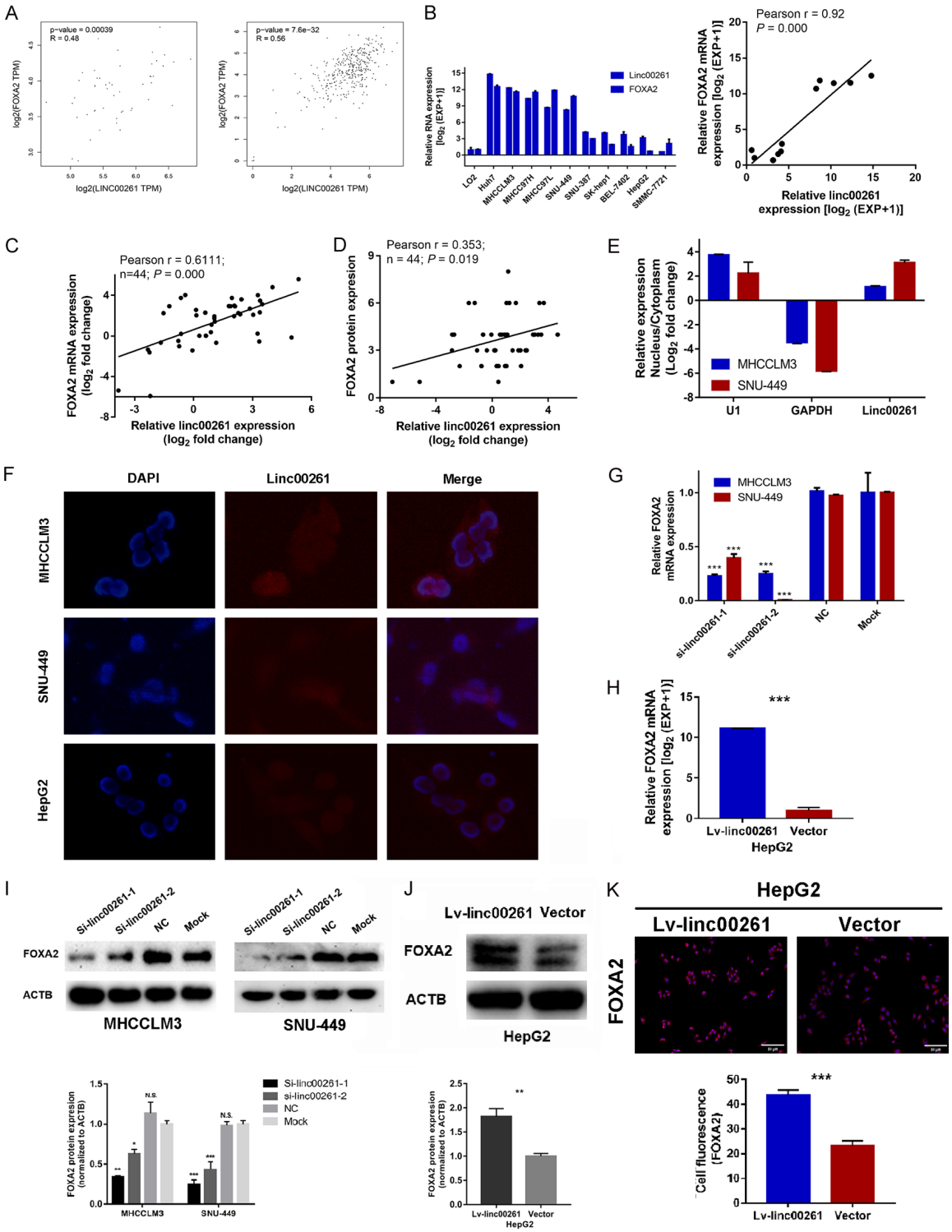

Figure 4. Correlation between linc00261 and its neighbor gene FOXA2 in HCC. (A) Correlation between linc00261 and FOXA2 mRNA expression in normal liver tissues (left; Pearson r=0.48, *P*=0.00039) and HCC tissues (right; Pearson r=0.56, *P*=7.6 10E-32) obtained from *GEPIA*; (B) Correlation between linc00261 and FOXA2 mRNA expression in a subset of HCC cell lines evaluated by RT-qPCR (n=11, Pearson r=0.92, *P*=0.000); (C) Correlation between relative linc00261 and FOXA2 mRNA expression in patients with HCC evaluated by RT-qPCR (Pearson r=0.6111, n=44, *P*=0.000); (D) Correlation between relative linc00261 expression (detected by RT-qPCR) and FOXA2 protein expression (detected by immunohistochemical staining) in patients with HCC (Pearson r=0.353, n=44, *P*=0.019); (E) Linc00261 allocation in nucleus and cytoplasm of MHCCLM3 and SNU-449 cells detected by nucleus/cytoplasm

separation followed with RT-qPCR, U1 snRNP and GAPDH were used as controls; (F) Linc00261 staining in MHCCLM3, SNU-449 and HepG2 cell lines by FISH; (G, H) FOXA2 mRNA expression after linc00261 knockdown (MHCCLM3 and SNU-449 cell lines) or after linc00261 overexpression (HepG2) examined by RT-qPCR; (I-K) FOXA2 protein expression after linc00261 knockdown (i; MHCCLM3 and SNU-449) or overexpression (J and K; HepG2) examined by western blotting (I and J) and immunofluorescence staining (K), as appropriate; the gray values of the protein bands were evaluated by image J. N.S. not significant; *$P < 0.05$; **$P < 0.01$; ***$P < 0.001$. The original western blotting images refers to Supplementary Figure 5.

the FOXA2 promoter. Therefore, we focused on SMAD3 for further research. Proteins retrieved in the RNA pull-down assay were subjected to western blotting for linc00261-protein enrichment evaluation, which verified that SMAD3 does bind to linc00261 (**Figure 6C**). RNA immunoprecipitation (RIP) followed by RT-qPCR also demonstrated that SMAD3 was specifically enriched with linc00261 in MHCCLM3 cells (**Figure 6D**); Chromatin immunoprecipitation (CHIP) showed that SMAD3 could bind to the *FOXA2* promoter in MHCCLM3 cells, and knockdown of linc00261 significantly attenuated the binding of SMAD3 to *FOXA2* promotor region (**Figure 6E**). Moreover, SMAD3, primarily located in the nucleus, was significantly downregulated in HCC tissues compared to levels in adjacent noncancerous tissues, as revealed by immunohistochemical staining of 40 randomly selected cases from cohort 2 (**Figure 6F**, **6G**), which might also attenuate linc00261-induced *FOXA2* transcription. SMAD3 expression in HCC tissues was also positively correlated with FOXA2 protein expression (**Figure 6H**; Pearson r=0.3627, n=40, *P*=0.021). Finally, the knockdown of SMAD3 in HCC cell lines significantly reduced FOXA2 expression (**Figure 6I**). These results suggest that linc00261 recruits SMAD3 to activate the transcription of *FOXA2*.

Linc00261 was repressed by EZH2 induced H3K27Me3

Accumulating studies revealed that histone methylation works cooperated with DNA methylation in silencing lncRNAs expression, which is partially induced by EZH2, a crucial co-regulator of H3K27Me3 and CpG island methylation associated-lncRNA epigenetic silencing. A recent study discovered DNMT1-mediated CpG island methylation within linc00261-FOXA2 locus is responsible for linc00261 downregulation in lung adenocarcinoma cell line [13]. We speculated that EZH2 may be participated in H3K27Me3-associated linc00261 transcription repression in HCC. Treatment with GSK126 at a concentration of 10 μM for 48 h, a selective inhibitor of EZH2 methyltransferase activity [35], significantly increased linc00261 expression in liver cancer cells (**Figure 7A**); Furthermore, western blotting revealed that H3K27Me3 expression was decreased after treatment with GSK126 (**Figure 7B**). Additionally, EZH2 was predicted to binding with linc00261 promoter region at 5 sites, and to study whether EZH2 and H3K27Me3 directly bind to the promoter region of linc00261, 5 pairs of primer were designed across the promoter (**Figure 7C**). ChIP-qPCR assay with anti-H3K27Me3 or anti-EZH2 antibodies showed that both EZH2 and H3K27Me3 enriched the promoter compared to IgG groups, which is exactly right within the CpG islands; besides, treatment with GSK126 for 48 h at a concentration of 10 μM obviously decreased the enrichments of EZH2 and H3K27Me3 (**Figure 7D**). These results indicated that linc00261 expression is partially transcriptionally controlled by EZH2-mediated H3K27Me3 level in HCC.

To determine the clinical relation of linc00261 with EZH2, H3K27Me3 expression in HCC, we detected EZH2 and H3K27me3 expression by immunohistochemical staining in tumors and adjacent normal specimens. Both EZH2 and H3K27Me3 were expressed at high levels in tumor tissues compared to non-tumor regions (**Figure 7E**, **7F**). Moreover, the Pearson correlation analysis revealed that linc00261 expression was negatively correlated with EZH2 (n=35; r=-0.3779, P=0.0252) and H3K27Me3 (n=35; r=-0.3354, P=0.0489) expression in HCC tissues (**Figure 7G**).

Discussion

In this study, we discovered that lower expression of linc00261 in tumor tissues is associated with poorer prognosis for multiple cancers including HCC. Linc00261 and its positively correlated neighbor gene *FOXA2*, were negatively associated with malignant biological behaviors, particularly MVI, and served as excellent independent prognostic factors for RFS in patients with HCC. Linc00261 inhibits migration, invasion, and EMT partially by transcrip-

A

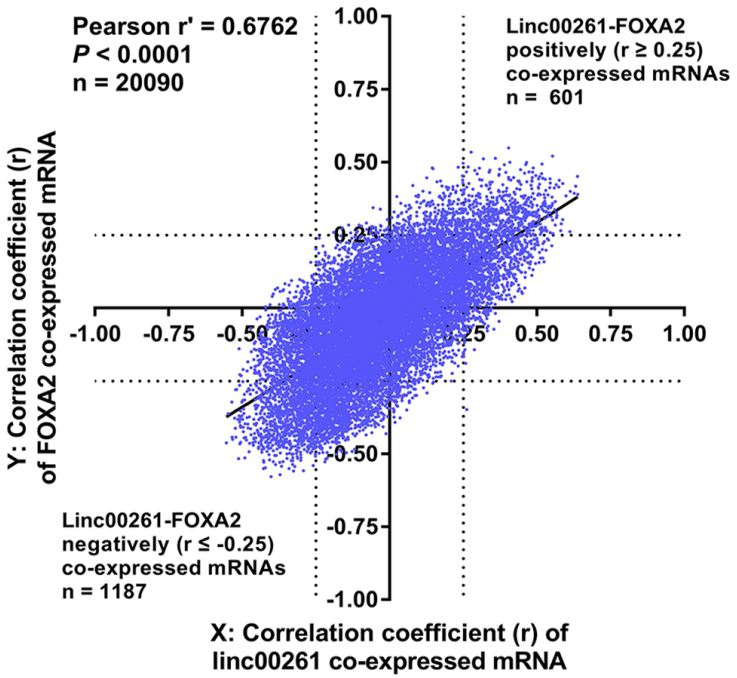
Pearson r' = 0.6762
P < 0.0001
n = 20090
Linc00261-FOXA2
positively (r ≥ 0.25)
co-expressed mRNAs
n = 601
Linc00261-FOXA2
negatively (r ≤ -0.25)
co-expressed mRNAs
n = 1187
Y: Correlation coefficient (r)
of FOXA2 co-expressed mRNA
X: Correlation coefficient (r) of
linc00261 co-expressed mRNA
1.00
0.75
0.50
0.25
-0.50
-0.75
-1.00
-1.00
-0.75
-0.50
0.50
0.75
1.00

B

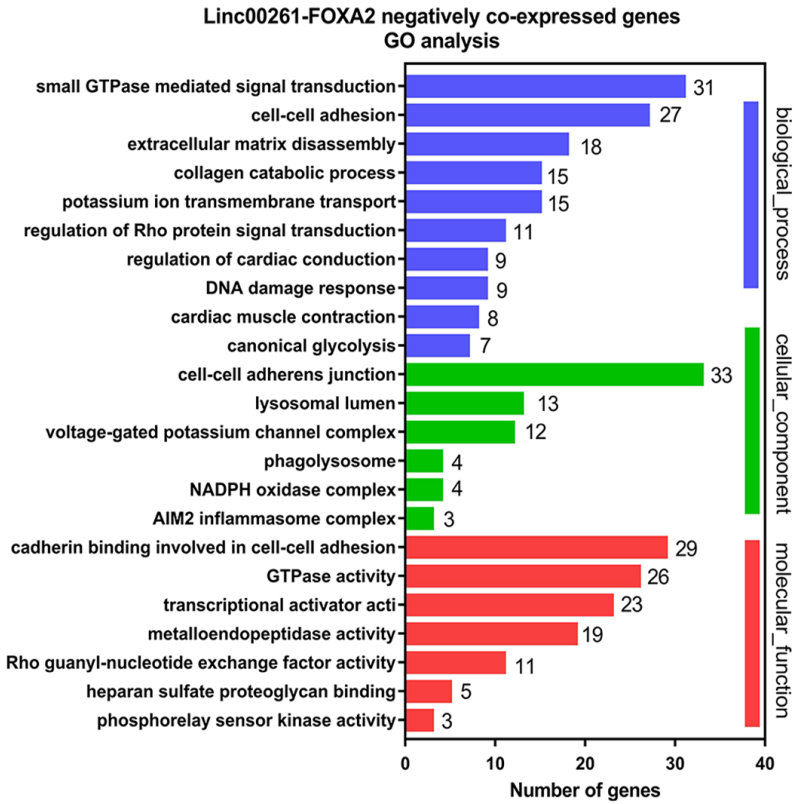
Linc00261-FOXA2 negatively co-expressed genes
GO analysis
small GTPase mediated signal transduction 31
cell-cell adhesion 27
extracellular matrix disassembly 18
collagen catabolic process 15
potassium ion transmembrane transport 15
regulation of Rho protein signal transduction 11
regulation of cardiac conduction 9
DNA damage response 9
cardiac muscle contraction 8
canonical glycolysis 7
cell-cell adherens junction 33
lysosomal lumen 13
voltage-gated potassium channel complex 12
phagolysosome 4
NADPH oxidase complex 4
AIM2 inflammasome complex 3
cadherin binding involved in cell-cell adhesion 29
GTPase activity 26
transcriptional activator acti 23
metalloendopeptidase activity 19
Rho guanyl-nucleotide exchange factor activity 11
heparan sulfate proteoglycan binding 5
phosphorelay sensor kinase activity 3
biological_process
cellular_component
molecular_function
0
10
20
30
40
Number of genes

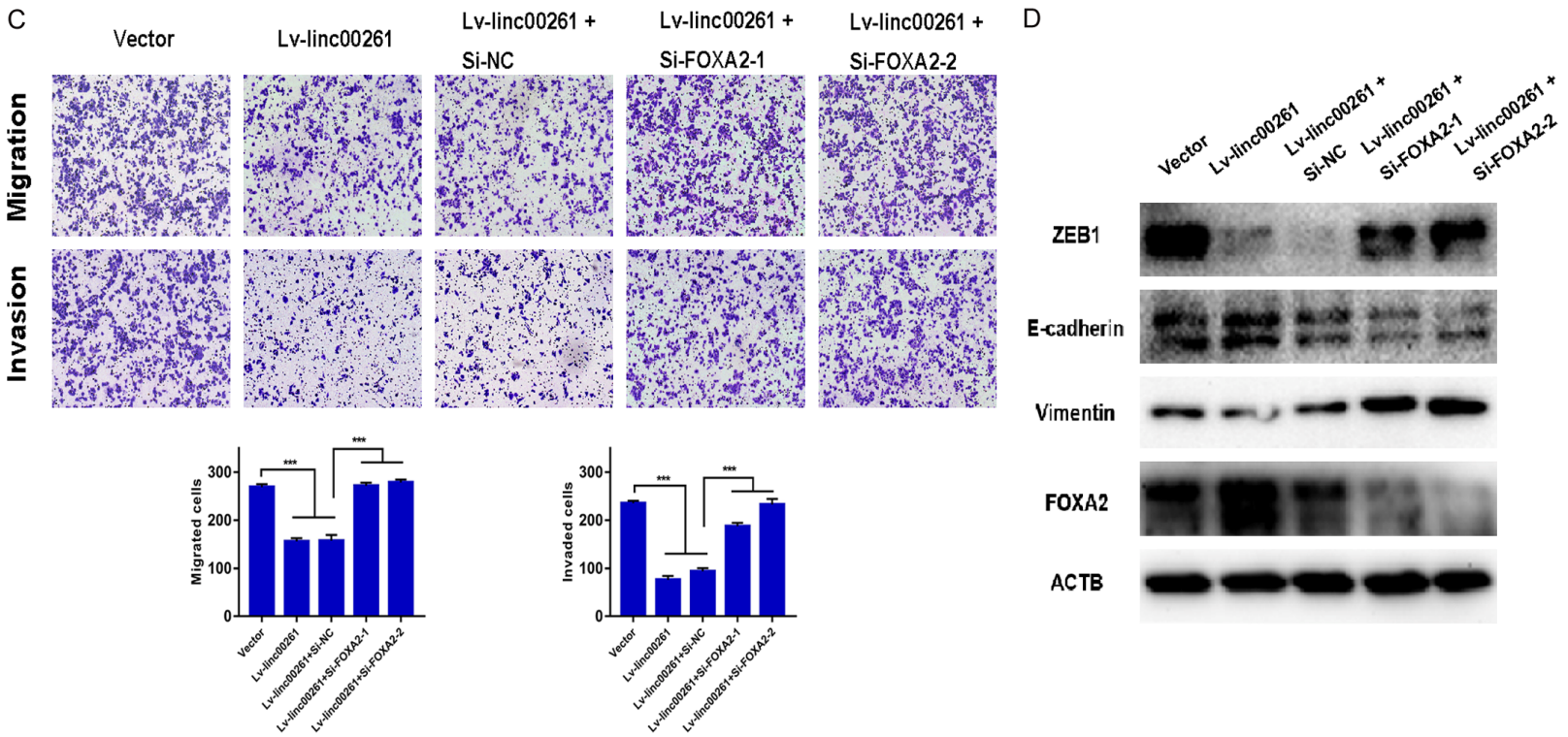

Figure 5. Bioinformatic analysis of linc00261-FOXA2 co-expressed mRNAs and the effects of linc00261/FOXA2 axis on migration, invasion and EMT in HCC. A. Pearson correlation analysis of the correlation coefficient (r) of linc00261 and FOXA2 co-expressed mRNAs obtained from *cBioPortal* (Pearson r'=0.6762, $P < 0.0001$, n=20090); B. Linc00261-FOXA2 common negatively ($r \leq -0.25$; n=1187) co-expressed mRNAs were subjected for further GO analysis conducted by *DAVID*; C. Rescue assays demonstrated that the suppressive roles in migration and invasion are reversed by FOXA2 knockdown using siRNAs in linc00261-overexpressed HepG2 evaluated by ANOVA followed LSD-t test; D. Rescue assay indicated that the effect of linc00261 overexpression on EMT associated proteins is reversed by FOXA2 knockdown using siRNAs in HepG2. GO, Gene Ontology; $***P < 0.001$. The original western blotting images refers to Supplementary Figure 6.

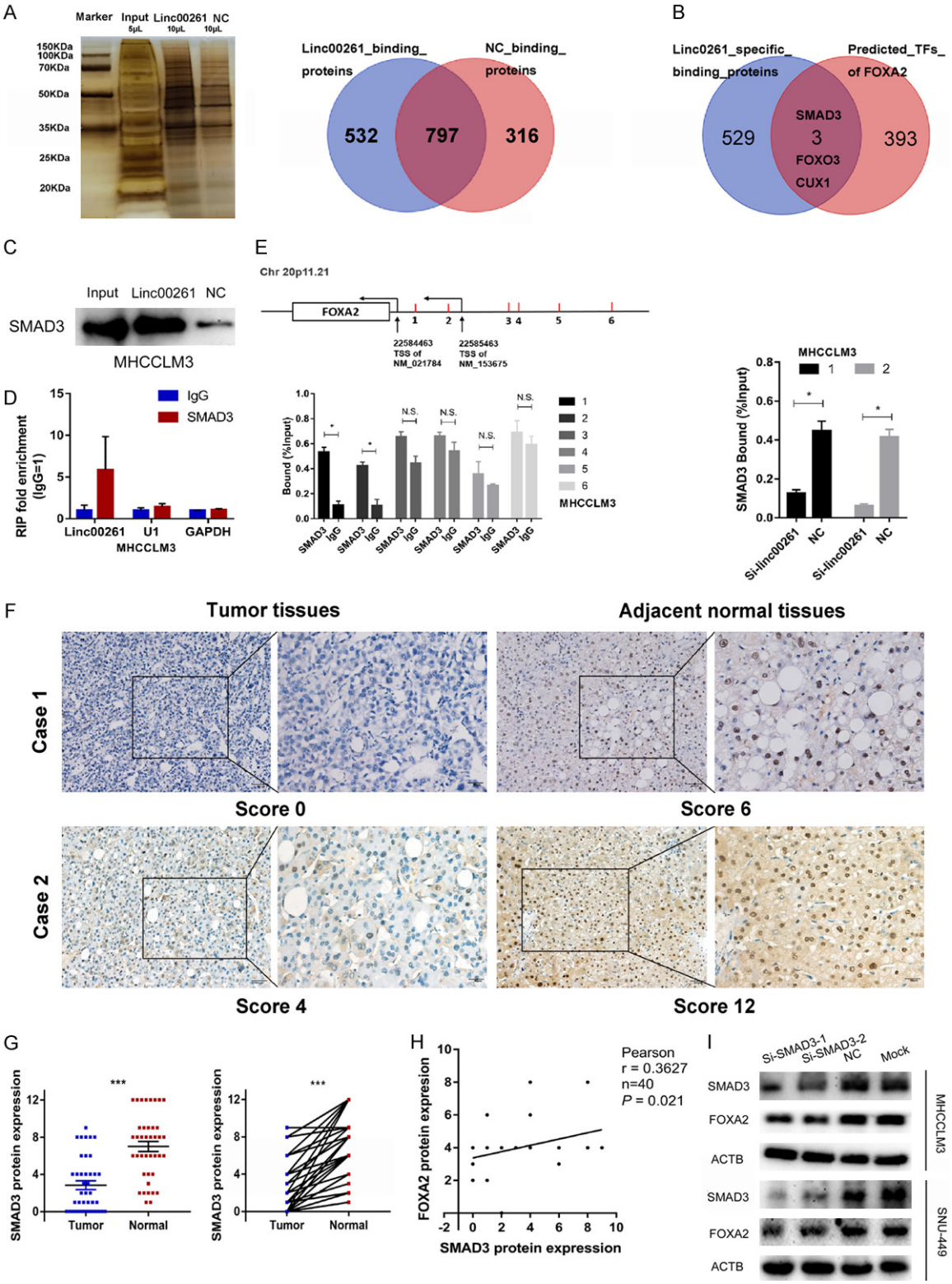

Figure 6. Linc00261 regulates FOXA2 transcription by recruiting SMAD3 to the promoter. A. SDS-PAGE electrophoresis and silver staining of linc00261 and negative control RNA binding proteins obtained from RNA pull-down assay, and the Venn diagram showed 532 linc00261 specifically binding proteins; B. Venn diagram representing the potential 3 transcription factors (SMAD3, FOXO3, and CUX1) that not only specifically binding with linc00261, but also predicted to regulate the transcription of FOXA2 using *JASPAR*; C. Proteins retrieved in the RNA pull-down assay were subjected to western blotting for linc00261-protein (SMAD3) enrichment evaluation in MHCCLM3 cells; D.

SMAD3 bound directly to linc00261 revealed by RIP assay in MHCCLM3 cells, U1 snRNP and GAPDH were used as internal control; E. CHIP demonstrated binding of SMAD3 to the promoter region of FOXA2 in MHCCLM3 cells, which was dependent on linc00261 expression; the binding positions of the promoter region are indicated in the upper diagram and Supplementary Table 6; F. Representative images of various SMAD3 protein levels in HCC and adjacent normal tissues; G. Comparison of SMAD3 protein expression in HCC and adjacent normal tissues (n=40). H. Correlation between SMAD3 and FOXA2 protein expressions in patients with HCC detected by immunohistochemical staining (Pearson r=0.3627, n=40, *P*=0.021); I. FOXA2 expression in SMAD3 knockdown MHCCLM3 and SNU-449 cells revealed by western blotting. N.S., not significant; *$P < 0.05$. The original western blotting images refers to Supplementary Figure 6.

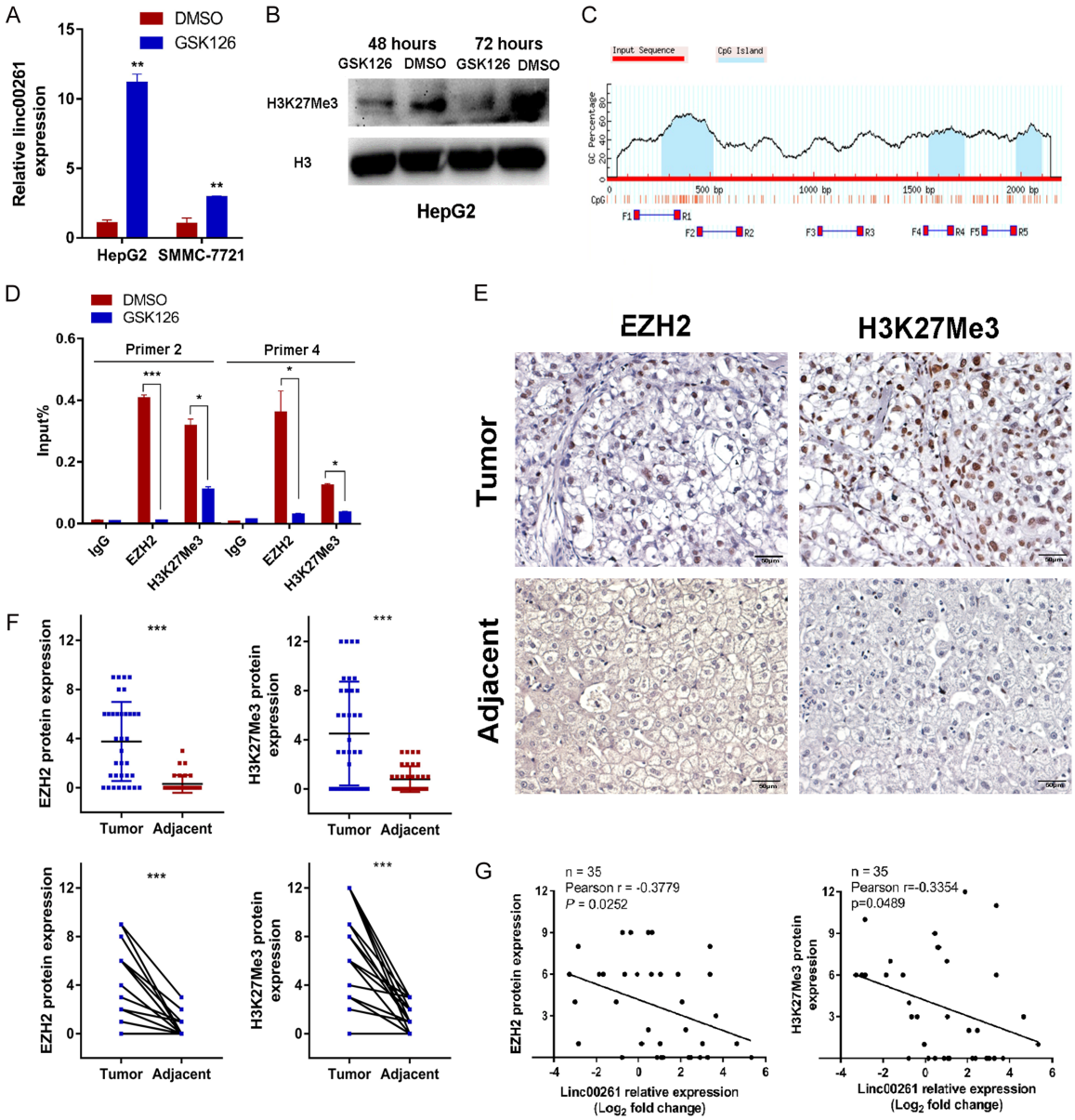

Figure 7. EZH2 represses linc00261 expression via modifying H3K27 trimethylation in liver cancer cells. A. RT-qPCR analysis of linc00261 expression in HepG2 or SMMC-7721 cells after treatment with GSK126 for 48 h at a concentration of 10 Mm; B. Treatment with GSK126 for 48 and 72 h at a concentration of 10 μM in HepG2 cell line, the H3K27Me3 expression was detected using western blotting; C. Distributions of the CpG islands (predicted by MethPrimer website) and primers for CHIP-qPCR assay in linc00261 promoter region; D. CHIP-qPCR analysis of EZH2 and H3K27me3 enrichment at the promoter of linc00261 in HepG2 cells after GSK126 treatment with GSK126 (10 μM) for 48 h; E and F. Representative images of EZH2 and H3K27Me3 staining using immunohistochemistry in human HCC and adjacent liver tissues, both of them had a higher expression in tumor tissues than that in the adjacent tissues; G. Pearson correlation analysis of linc00261 with EZH2 and H3K27Me3 proteins. *$P < 0.05$; **$P < 0.01$; ***$P < 0.001$. The original western blotting images refers to Supplementary Figure 6.

tionally upregulating *FOXA2* through an interaction with SMAD3, thereby suppressing HCC metastasis. Additionally, we identified EZH2 is responsible for linc00261 transcription repression via modulating H3K27Me3, thereby contributes to HCC progression.

To date, few lncRNAs have been successfully used as therapies or for predicting HCC metastasis. Linc00261 was found to be dysregulated in gastric cancer [36], lung cancer [13, 37], endometrial carcinoma [38], choriocarcinoma [39], and HCC [6, 7]. These studies proposed that linc00261 inhibits tumor proliferation by inducing G2-M cell cycle arrest [13] or promoting apoptosis and suppresses migration and invasion by promoting slug degradation [36] or inhibiting Notch signaling [7]. However, our present study found that the transient knockdown or reintroduction of linc00261 in HCC cells, rarely affected proliferation, and the GO enrichment results didn't show cellular proliferation, apoptosis or cell cycle associated process, which is a more comprehensive lens to look at this contradiction, and further mechanistic research is required [7]. In addition, the loss of linc00261 in cells undergoing MVI was observed; combined with the effect of lin00261 on EMT and lung metastasis suppression, we concluded that the loss of linc00261 might be a key risk factor for the generation of metastasis-initiating cells in HCC.

FOXA2 is tightly coupled with HCC initiation and progression as reported by the present results and others [14, 16, 17]. Moreover, Combining the observations that linc00261 is specifically expressed in adult endoderm-derived tissues/organs and the liver, which exhibited the highest expression level compared to other tissues, the effect of linc00261 on HCC metastasis, and the interaction between linc00261 and FOXA2 in endoderm differentiation and HCC, we propose that the linc00261-FOXA2 axis, typically involved in endoderm differentiation, is hijacked during HCC metastasis. It is thus of greater clinical significance to determine the role of the linc00261-FOXA2 axis in HCC than in other cancers. This is despite the fact that a recent study reported that the loss of linc00261, regulated by FOXA2, promotes malignant phenotypes such as G2-M cell-cycle acceleration and the activation of DNA damage in lung adenocarcinoma, whereas whether FOXA2 functions as a tumor suppressor in lung adenocarcinoma is still under controversy [13]. In brief, it is interesting and valuable to note that two neighboring development-associated genes, namely linc00261 and *FOXA2*, are strongly and positively correlated, and coincidentally play a crucial suppressive role in MVI and subsequent HCC metastasis. Much more similar mechanisms during embryonic development might be hijacked in oncogenesis and cancer metastasis.

SMAD3 contains a DNA-binding domain (Mad homology 1), followed by a proline-rich region (also known as the linker region) and a Mad homology 2 domain. Phosphorylation sites in the linker region and C-terminus integrate various signals from multiple signaling pathways such as CDKs, ERK, JNK, MAPK, and TGF-β, as well as cross-talk with these pathways. This influences the formation of heteromeric complexes with other transcription factors and the binding of SMAD3 to target promoters, ultimately resulting in divergent functions, particularly with respect to the modulation of TGF-β signaling induced EMT and cancer progression [40]. To address the molecular mechanism underlying these effects, we focused on SMAD3, and found that SMAD3 binds the promoter of *FOXA2* and promotes its transcription with the assistance of linc00261, thereby contributing to the suppression of HCC progression. Moreover, SMAD3 was found to be downregulated in HCC tissues compared to expression in adjacent normal tissues, which together with linc00261 downregulation contributed to the attenuation of *FOXA2* transcription to some extent. However, the underlying mechanism through which linc00261 transcriptionally upregulates FOXA2 requires further in-depth analysis. For example, it is unclear whether linc00261 interacts with the promoter of *FOXA2* by base pairing or if this linc00261/SMAD3 complex is sufficient for binding to the promotor and the initiation of transcription. Moreover, it remains to be determined if FOXO3, or any other factors such as SMAD3, function during this process.

Few studies demonstrated the mechanism of linc00261 downregulation in cancers. In lung adenocarcinoma, DNMT1 epigenetically silences linc00261 by promoting the CpG islands methylation that within linc00261-FOXA2 lo-

cus. Interestingly, EZH2 serves as a recruitment platform for DNMT1 and DNMT3A/3B to mediate DNA methylation. It is thus possible that EZH2 epigenetically represses linc00261 transcription by directly recruiting DNMT1 to the CpG islands. Nevertheless, we discovered for the first time that EZH2 mediated H3K27Me3 is responsible for the suppression of linc00261 transcription, and both EZH2 and H3K27Me3 bind to the CpG islands of linc00261 promoter region, indicating EZH2 as a co-regulator of two epigenetic repression systems in regulating linc00261 expression. The effect and mechanism of EZH2/linc00261 axis is essential for HCC progression and needs further investigation.

In conclusion, we demonstrated that the loss of linc00261, induced by EZH2-mediated H3K27Me3, contributes to HCC metastasis by regulating EMT, which is partially achieved via the deficiency of transcriptional upregulation of FOXA2 through an interaction between linc00261 and SMAD3. A more detailed understanding of the EZH2/linc00261 axis, linc00261/SMAD3/FOXA2 axis might reveal potential prognostic factors and therapeutic targets for HCC metastasis.

Acknowledgements

The authors thank funding support from the Guangdong Provincial Science and Technology Projects (2017A020215132) and the National Natural Science Foundation of China (81872385). The authors thank Doctor Jinhua Zhang, Department of Pathology, Nanfang Hospital, Southern Medical University for the pathological diagnosis of MVI and the analysis of immunohistochemical staining, Professor Weizhong Wu, Liver Cancer Research Institute, Zhongshan Hospital, Fudan University, Shanghai, China, for providing the HCC cell lines MHCC-LM3, MHCC-97H, and MHCC-97L as a gift, and Editage for English language editing services.

Disclosure of conflict of interest

None.

Address correspondence to: Dinghua Yang and Xianghong Li, Unit of Hepatobiliary Surgery, Department of General Surgery, Nanfang Hospital, Southern Medical University, 1838 North Guangzhou Avenue, Baiyun District, Guangzhou 510515, China. Tel: +86-13600039623; Fax: +86-020-61641706; E-mail: dhyangyd@yahoo.com; nfyangdh@163.com (DHY); Tel: +86-13632101989; Fax: +86-020-61641706; E-mail: lixh@smu.edu.cn (XHL)

References

[1] Bray F, Ferlay J, Soerjomataram I, Siegel RL, Torre LA and Jemal A. Global cancer statistics 2018: GLOBOCAN estimates of incidence and mortality worldwide for 36 cancers in 185 countries. CA Cancer J Clin 2018; 68: 394-424.

[2] Forner A, Reig M and Bruix J. Hepatocellular carcinoma. Lancet 2018; 391: 1301-1314.

[3] Fatica A and Bozzoni I. Long non-coding RNAs: new players in cell differentiation and development. Nat Rev Genet 2014; 15: 7-21.

[4] Batista PJ and Chang HY. Long noncoding RNAs: cellular address codes in development and disease. Cell 2013; 152: 1298-1307.

[5] Deniz E and Erman B. Long noncoding RNA (lincRNA), a new paradigm in gene expression control. Funct Integr Genomics 2017; 17: 135-143.

[6] Chen Z, Xiang L, Huang Y, Fang Y, Li X and Yang D. Expression of long noncoding RNA linc00261 in hepatocellular carcinoma and its association with postoperative outcomes. Nan Fang Yi Ke Da Xue Xue Bao 2018; 38: 1179-1186.

[7] Zhang HF, Li W and Han YD. LINC00261 suppresses cell proliferation, invasion and Notch signaling pathway in hepatocellular carcinoma. Cancer Biomark 2018; 21: 575-582.

[8] Celia-Terrassa T and Kang Y. Distinctive properties of metastasis-initiating cells. Genes Dev 2016; 30: 892-908.

[9] Ovcharenko I, Loots GG, Nobrega MA, Hardison RC, Miller W and Stubbs L. Evolution and functional classification of vertebrate gene deserts. Genome Res 2005; 15: 137-145.

[10] Derrien T, Johnson R, Bussotti G, Tanzer A, Djebali S, Tilgner H, Guernec G, Martin D, Merkel A, Knowles DG, Lagarde J, Veeravalli L, Ruan X, Ruan Y, Lassmann T, Carninci P, Brown JB, Lipovich L, Gonzalez JM, Thomas M, Davis CA, Shiekhattar R, Gingeras TR, Hubbard TJ, Notredame C, Harrow J and Guigo R. The GENCODE v7 catalog of human long noncoding RNAs: analysis of their gene structure, evolution, and expression. Genome Res 2012; 22: 1775-1789.

[11] Spear BT, Jin L, Ramasamy S and Dobierzewska A. Transcriptional control in the mammalian liver: liver development, perinatal repression, and zonal gene regulation. Cell Mol Life Sci 2006; 63: 2922-2938.

[12] Jiang W, Liu Y, Liu R, Zhang K and Zhang Y. The lncRNA DEANR1 facilitates human endoderm

differentiation by activating FOXA2 expression. Cell Rep 2015; 11: 137-148.
[13] Shahabi S, Kumaran V, Castillo J, Cong Z, Nandagopal G, Mullen DJ, Alvarado A, Correa MR, Saizan A, Goel R, Bhat A, Lynch SK, Zhou B, Borok Z and Marconett CN. LINC00261 is an epigenetically regulated tumor suppressor essential for activation of the DNA damage response. Cancer Res 2019; 79: 3050-3062.
[14] Li Z, Tuteja G, Schug J and Kaestner KH. Foxa1 and Foxa2 are essential for sexual dimorphism in liver cancer. Cell 2012; 148: 72-83.
[15] Yamamura N, Fugo K and Kishimoto T. Forkhead box protein A2, a pioneer factor for hepatogenesis, is involved in the expression of hepatic phenotype of alpha-fetoprotein-producing adenocarcinoma. Pathol Res Pract 2017; 213: 1082-1088.
[16] Wang J, Zhu CP, Hu PF, Qian H, Ning BF, Zhang Q, Chen F, Liu J, Shi B, Zhang X and Xie WF. FOXA2 suppresses the metastasis of hepatocellular carcinoma partially through matrix metalloproteinase-9 inhibition. Carcinogenesis 2014; 35: 2576-2583.
[17] Liang WC, Ren JL, Wong CW, Chan SO, Waye MM, Fu WM and Zhang JF. LncRNA-NEF antagonized epithelial to mesenchymal transition and cancer metastasis via cis-regulating FOXA2 and inactivating Wnt/beta-catenin signaling. Oncogene 2018; 37: 1445-1456.
[18] Francis NJ, Kingston RE and Woodcock CL. Chromatin compaction by a polycomb group protein complex. Science 2004; 306: 1574-1577.
[19] Vire E, Brenner C, Deplus R, Blanchon L, Fraga M, Didelot C, Morey L, Van Eynde A, Bernard D, Vanderwinden JM, Bollen M, Esteller M, Di Croce L, de Launoit Y and Fuks F. The Polycomb group protein EZH2 directly controls DNA methylation. Nature 2006; 439: 871-874.
[20] Au SL, Wong CC, Lee JM, Fan DN, Tsang FH, Ng IO and Wong CM. Enhancer of zeste homolog 2 epigenetically silences multiple tumor suppressor microRNAs to promote liver cancer metastasis. Hepatology 2012; 56: 622-631.
[21] Liu H, Liu Y, Liu W, Zhang W and Xu J. EZH2-mediated loss of miR-622 determines CXCR4 activation in hepatocellular carcinoma. Nat Commun 2015; 6: 8494.
[22] Sun M, Liu XH, Lu KH, Nie FQ, Xia R, Kong R, Yang JS, Xu TP, Liu YW, Zou YF, Lu BB, Yin R, Zhang EB, Xu L, De W and Wang ZX. EZH2-mediated epigenetic suppression of long noncoding RNA SPRY4-IT1 promotes NSCLC cell proliferation and metastasis by affecting the epithelial-mesenchymal transition. Cell Death Dis 2014; 5: e1298.
[23] Wei S, Liu J, Li X and Liu X. Repression of lncRNA-SVUGP2 mediated by EZH2 contributes to the development of non-small cell lung cancer via brisking Wnt/β-catenin signal. Artif Cells Nanomed Biotechnol 2019; 47: 3400-3409.
[24] Xiang LY, Ou HH, Liu XC, Chen ZJ, Li XH, Huang Y and Yang DH. Loss of tumor suppressor miR-126 contributes to the development of hepatitis B virus-related hepatocellular carcinoma metastasis through the upregulation of ADAM9. Tumour Biol 2017; 39: 1010428317709128.
[25] Anaya J. OncoLnc: linking TCGA survival data to mRNAs, miRNAs, and lncRNAs. Peer J Computer Science 2016; 2: e67.
[26] Han J, Li ZL, Xing H, Wu H, Zhu P, Lau WY, Zhou YH, Gu WM, Wang H, Chen TH, Zeng YY, Wu MC, Shen F and Yang T. The impact of resection margin and microvascular invasion on long-term prognosis after curative resection of hepatocellular carcinoma: a multi-institutional study. HPB (Oxford) 2019; 21: 962-971.
[27] Erstad DJ and Tanabe KK. Prognostic and therapeutic implications of microvascular invasion in hepatocellular carcinoma. Ann Surg Oncol 2019; 26: 1474-1493.
[28] Zhang X, Li J, Shen F and Lau WY. Significance of presence of microvascular invasion in specimens obtained after surgical treatment of hepatocellular carcinoma. J Gastroenterol Hepatol 2018; 33: 347-354.
[29] Huang da W, Sherman BT and Lempicki RA. Systematic and integrative analysis of large gene lists using DAVID bioinformatics resources. Nat Protoc 2009; 4: 44-57.
[30] Cerami E, Gao J, Dogrusoz U, Gross BE, Sumer SO, Aksoy BA, Jacobsen A, Byrne CJ, Heuer ML, Larsson E, Antipin Y, Reva B, Goldberg AP, Sander C and Schultz N. The cBio cancer genomics portal: an open platform for exploring multidimensional cancer genomics data. Cancer Discov 2012; 2: 401-404.
[31] Gao J, Aksoy BA, Dogrusoz U, Dresdner G, Gross B, Sumer SO, Sun Y, Jacobsen A, Sinha R, Larsson E, Cerami E, Sander C and Schultz N. Integrative analysis of complex cancer genomics and clinical profiles using the cBioPortal. Sci Signal 2013; 6: pl1.
[32] Ulitsky I and Bartel DP. lincRNAs: genomics, evolution, and mechanisms. Cell 2013; 154: 26-46.
[33] Tang Z, Li C, Kang B, Gao G, Li C and Zhang Z. GEPIA: a web server for cancer and normal gene expression profiling and interactive analyses. Nucleic Acids Res 2017; 45: W98-W102.
[34] Khan A, Fornes O, Stigliani A, Gheorghe M, Castro-Mondragon JA, van der Lee R, Bessy A, Cheneby J, Kulkarni SR, Tan G, Baranasic D, Arenillas DJ, Sandelin A, Vandepoele K, Lenhard B, Ballester B, Wasserman WW, Parcy F

and Mathelier A. JASPAR 2018: update of the open-access database of transcription factor binding profiles and its web framework. Nucleic Acids Res 2018; 46: D1284.
[35] Kim KH and Roberts CW. Targeting EZH2 in cancer. Nat Med 2016; 22: 128-134.
[36] Yu Y, Li L, Zheng Z, Chen S, Chen E and Hu Y. Long non-coding RNA linc00261 suppresses gastric cancer progression via promoting Slug degradation. J Cell Mol Med 2017; 21: 955-967.
[37] Liu Y, Xiao N and Xu SF. Decreased expression of long non-coding RNA LINC00261 is a prognostic marker for patients with non-small cell lung cancer: a preliminary study. Eur Rev Med Pharmacol Sci 2017; 21: 5691-5695.
[38] Fang Q, Sang L and Du S. Long noncoding RNA LINC00261 regulates endometrial carcinoma progression by modulating miRNA/FOXO1 expression. Cell Biochem Funct 2018; 36: 323-330.
[39] Wang H, Wang Y, Xue K, Guan Y, Jin Y, Liu S, Wang Y, Liu S, Wang L and Han L. Long noncoding RNA LINC00261 suppresses cell proliferation and invasion and promotes cell apoptosis in human choriocarcinoma. J Obstet Gynaecol Res 2017; 25: 733-742.
[40] Ooshima A, Park J and Kim SJ. Phosphorylation status at Smad3 linker region modulates transforming growth factor-beta-induced epithelial-mesenchymal transition and cancer progression. Cancer Sci 2019; 110: 481-488.

Supplementary Table 1. Correlation between linc00261 expression and clinicopathological characteristics of hepatocellular carcinoma (n=100)

Clinicopathological parameter		linc00261 expression		χ^2	*P* value
		High (n=50)	Low (n=50)		
Gender	Male	46	40	2.990	0.084
	Female	4	10		
Age	< 60	42	41	0.071	0.790
	≥ 60	8	9		
AFP[1] (ug/L)	< 400	36	26	4.244	0.039
	≥ 400	14	24		
Cirrhosis	Positive	38	40	0.233	0.629
	Negative	12	10		
Tumor number	1	41	39	0.250	0.617
	≥ 2	9	11		
Tumor size (cm)	< 5.0	29	16	6.828	0.009
	≥ 5.0	21	34		
Tumor capsule	Positive	36	33	0.421	0.517
	Negative	14	17		
Differentiation	Well	7	6	0.125	0.940
	Moderate	33	33		
	Poor	10	11		
MVI[2]	Positive	21	32	4.857	0.028
	Negative	29	18		
PVTT[3]	Positive	9	10	0.065	0.799
	Negative	41	40		
TNM[4] stage	I+II	39	29	4.596	0.032
	III+VI	11	21		
BCLC[5] stage	A	24	26	1.389	0.499
	B	5	2		
	C	21	22		

[1]AFP, alpha fetoprotein; [2]MVI, microvascular invasion; [3]PVTT, portal vein tumor thrombosis; [4]TNM, tumor-node-metastasis; [5]BCLC, Barcelona clinic liver cancer.

Supplementary Table 2. Univariate and multivariate Cox regression analyses for RFS of patients with HCC (n=91)[1]

Variables	HR	95% CI	*P* value
Univariate analysis			
Age (< 60 *vs.* ≥ 60 years)	1.457	0.732-2.899	0.284
Gender (male *vs.* female)	0.753	0.339-1.674	0.487
AFP[2] (< 400 *vs.* ≥ 400 μg/L)	1.203	0.718-2.018	0.483
Liver cirrhosis (Positive *vs.* Negative)	1.244	0.658-2.351	0.502
Capsule (Positive *vs.* Negative)	0.932	0.523-1.662	0.812
Tumor size (< 5.0 *vs.* ≥ 5.0 cm)	2.807	1.592-4.950	0.000
Tumor number (1 *vs.* ≥ 2)	2.186	1.191-4.012	0.012
MVI[3] (Positive *vs.* Negative)	3.031	1.749-5.255	0.000
PVTT[4] (Positive *vs.* Negative)	3.449	1.931-6.160	0.000
Differentiation (well, moderate, poor)	0.468	0.302-0.723	0.001
Expression of Linc00261 (high *vs.* low)	0.533	0.313-0.906	0.020

Multivariate analysis			
Tumor size (< 5.0 *vs.* ≥ 5.0 cm)	1.885	0.956-3.716	0.067
Tumor number (1 *vs.* ≥ 2)	2.709	1.350-5.436	0.005
MVI[3] (Positive *vs.* Negative)	2.212	1.065-4.595	0.033
PVTT[4] (Positive *vs.* Negative)	1.788	0.907-3.525	0.094
Differentiation (well, moderate, poor)	0.502	0.306-0.824	0.006
Linc00261 expression (high *vs.* low)	0.536	0.294-0.978	0.042

[1]Two patients were died because of peri-operative complications, 7 were lost to follow up; [2]AFP, alpha fetoprotein; [3]MVI, microvascular invasion; [4]PVTT, portal vein tumor thrombosis.

Supplementary Table 3. Correlation between FOXA2 protein expression and clinicopathological characteristics of hepatocellular carcinoma (n=79)

Clinicopathological parameter		FOXA2 protein		χ^2	*P* value
		High (n=26)	Low (n=53)		
Gender	Male	22 (31.0%)	49 (69.0%)	1.177	0.278
	Female	4 (50.0%)	4 (50.0%)		
Age (years old)	< 60	22 (33.8%)	43 (66.2%)	0.145	0.703
	≥ 60	4 (28.6%)	10 (71.4%)		
AFP[1] (μg/L)	< 400	14 (28.6%)	35 (71.4%)	1.101	0.294
	≥ 400	12 (40.0%)	18 (60.0%)		
Cirrhosis	Positive	21 (31.8%)	45 (68.2%)	0.020	0.886
	Negative	5 (38.5%)	8 (61.5%)		
Tumor number	=1	22 (32.4%)	46 (67.6%)	0.069	0.793
	≥ 2	4 (36.4%)	7 (63.6%)		
Tumor size (cm)	< 5.0	11 (25.6%)	32 (74.4%)	2.296	0.130
	≥ 5.0	15 (41.7%)	21 (58.3%)		
Tumor capsule	Positive	11 (28.9%)	27 (71.1%)	0.521	0.470
	Negative	15 (36.6%)	26 (63.4%)		
Differentiation	Well	1 (16.7%)	5 (83.3%)	0.871	0.647
	Moderate	22 (34.9%)	41 (65.1%)		
	Poor	3 (30.0%)	7 (70.0%)		
MVI[2]	Positive	18 (42.9%)	24 (57.1%)	4.017	0.045
	Negative	8 (21.6%)	29 (78.4%)		
PVTT[3]	Positive	11 (55.0%)	9 (45.0%)	5.918	0.015
	Negative	15 (25.4%)	44 (74.6%)		
TNM[4] stage	I+II	13 (23.6%)	42 (76.4%)	7.054	0.008
	III+IV	13 (54.2%)	11 (45.8%)		
BCLC[5] stage	A	13 (25.0%)	39 (75.0%)	4.915	0.086
	B	2 (33.3%)	4 (66.7%)		
	C	11 (52.4%)	10 (47.6%)		

[1]AFP, alpha fetoprotein; [2]MVI, microvascular invasion; [3]PVTT, portal vein tumor thrombosis; [4]TNM, tumor-node-metastasis; [5]BCLC, Barcelona clinic liver cancer.

Supplementary Table 4. Univariate and multivariate Cox regression analyses for RFS of patients with HCC (n=72)[1]

Variables	HR	95% CI	*P* value
Univariate analysis			
Age (< 60 *vs.* ≥ 60 years)	0.579	0.175-1.912	0.370
Gender (male *vs.* female)	0.693	0.165-2.910	0.617
AFP[2] (< 400 *vs.* ≥ 400)	2.026	1.006-4.083	0.048
Liver cirrhosis (Positive *vs.* Negative)	0.844	0.346-2.056	0.708
Capsule (Positive *vs.* Negative)	1.183	0.567-2.468	0.654
Tumor size (< 5.0 *vs.* ≥ 5.0 cm)	2.138	1.042-4.384	0.038
Tumor number (1 *vs.* ≥ 2)	1.685	0.739-3.843	0.215
MVI[3] (Positive *vs.* Negative)	4.230	1.883-9.505	0.000
PVTT[4] (Positive *vs.* Negative)	5.754	2.741-12.079	0.000
Differentiation (well, moderate, poor)	0.424	0.205-0.879	0.021
FOXA2 protein (high *vs.* low)	0.362	0.180-0.725	0.004
Multivariate analysis			
AFP[2] (< 400 *vs.* ≥ 400)	2.017	0.927-4.385	0.077
Tumor size (< 5.0 *vs.* ≥ 5.0 cm)	0.950	0.415-2.175	0.904
MVI[3] (Positive *vs.* Negative)	2.168	0.793-5.924	0.132
PVTT[4] (Positive *vs.* Negative)	3.144	1.330-7.432	0.009
Differentiation (well, moderate, poor)	0.231	0.091-0.586	0.002
FOXA2 protein (high *vs.* low)	0.327	0.152-0.706	0.004

[1]One patient was died because of peri-operative complication, 6 were lost to follow up; [2]AFP, alpha fetoprotein; [3]MVI, microvascular invasion; [4]PVTT, portal vein tumor thrombosis.

Supplementary Table 5. Primary antibodies and its dilutions used for western blotting, immunohistochemical, immunofluorescence staining, and CHIP

Primary antibodies	WB	IHC-P	IF	CHIP	Specificity	catalog number	Incorporation
ZEB1	1:1000	-	1:50	-	Rabbit polyclonal	21544-1-AP	Proteintech
E-cadherin	1:1000	-	1:50	-	Rabbit polyclonal	20874-1-AP	Proteintech
N-cadherin	1:1000	-	-	-	Rabbit polyclonal	22018-1-AP	Proteintech
β-catenin	1:1000	-	-	-	Rabbit monoclonal	8480	Cell signaling Technology
Vimentin	1:1000	-	1:50	-	Rabbit monoclonal	5741	Cell signaling Technology
FOXA2	1:1000	1:200	1:50	-	Rabbit polyclonal	22474-1-AP	Proteintech
SMAD3	1:1000	1:100	-	1:50	Rabbit polyclonal	ab28379	Abcam
EZH2		1:50	-	1:100	Rabbit monoclonal	5246	Cell signaling Technology
H3K27Me3	1:1000	1:200	-	1:50	Rabbit monoclonal	9733	Cell signaling Technology
ACTB	1:1000	-	-	-	Rabbit polyclonal	20536-1-AP	Proteintech

Supplementary File 1

Linc00261 specific binding proteins measured by RNA pull down and mass spectrum analysis

Gene Symbol	Accession	Score	Mass	Matches	Sequences	emPAI	Protein description
ATP2B1	AT2B1_HUMAN	141	139637	18 (3)	9 (3)	0.07	Plasma membrane calcium-transporting ATPase 1 OS=Homo sapiens GN=ATP2B1 PE=1 SV=3
ATP2B3	AT2B3_HUMAN	103	135253	25 (3)	12 (3)	0.07	Plasma membrane calcium-transporting ATPase 3 OS=Homo sapiens GN=ATP2B3 PE=1 SV=3
KRT14	K1C14_HUMAN	691	51872	34 (22)	12 (6)	0.54	Keratin, type I cytoskeletal 14 OS=Homo sapiens GN=KRT14 PE=1 SV=4
CCDC181	CC181_HUMAN	28	60408	25 (3)	7 (1)	0.05	Coiled-coil domain-containing protein 181 OS=Homo sapiens GN=CCDC181 PE=2 SV=1
KRT6A	K2C6A_HUMAN	202	60293	39 (14)	11 (5)	0.3	Keratin, type II cytoskeletal 6A OS=Homo sapiens GN=KRT6A PE=1 SV=3
KRT76	K22O_HUMAN	162	66370	40 (11)	12 (3)	0.16	Keratin, type II cytoskeletal 2 oral OS=Homo sapiens GN=KRT76 PE=1 SV=2
KRT5	K2C5_HUMAN	133	62568	28 (7)	10 (5)	0.29	Keratin, type II cytoskeletal 5 OS=Homo sapiens GN=KRT5 PE=1 SV=3
KRT79	K2C79_HUMAN	84	58085	19 (3)	6 (2)	0.12	Keratin, type II cytoskeletal 79 OS=Homo sapiens GN=KRT79 PE=1 SV=2
GOLGA3	GOGA3_HUMAN	77	167765	16 (2)	10 (2)	0.04	Golgin subfamily A member 3 OS=Homo sapiens GN=GOLGA3 PE=1 SV=2
PRPH	PERI_HUMAN	32	53732	14 (3)	3 (2)	0.13	Peripherin OS=Homo sapiens GN=PRPH PE=1 SV=2
TPM2	TPM2_HUMAN	458	32945	48 (30)	17 (10)	1.61	Tropomyosin beta chain OS=Homo sapiens GN=TPM2 PE=1 SV=1
TUBA1A	TBA1A_HUMAN	307	50788	20 (18)	6 (5)	0.37	Tubulin alpha-1A chain OS=Homo sapiens GN=TUBA1A PE=1 SV=1
ACACA	ACACA_HUMAN	282	267095	48 (17)	24 (9)	0.12	Acetyl-CoA carboxylase 1 OS=Homo sapiens GN=ACACA PE=1 SV=2
TJP2	ZO2_HUMAN	251	134104	20 (7)	16 (7)	0.18	Tight junction protein ZO-2 OS=Homo sapiens GN=TJP2 PE=1 SV=2
PPIAL4A	PAL4A_HUMAN	237	18398	20 (17)	5 (3)	0.66	Peptidyl-prolyl cis-trans isomerase A-like 4A OS=Homo sapiens GN=PPIAL4A PE=2 SV=1
RANBP2	RBP2_HUMAN	225	362365	31 (12)	19 (2)	0.02	E3 SUMO-protein ligase RanBP2 OS=Homo sapiens GN=RANBP2 PE=1 SV=2
ALDH1L1	AL1L1_HUMAN	140	99622	12 (6)	4 (1)	0.03	Cytosolic 10-formyltetrahydrofolate dehydrogenase OS=Homo sapiens GN=ALDH1L1 PE=1 SV=2
RPS27A	RS27A_HUMAN	201	18296	37 (22)	4 (4)	0.97	Ubiquitin-40S ribosomal protein S27a OS=Homo sapiens GN=RPS27A PE=1 SV=2
CAT	CATA_HUMAN	168	59947	4 (3)	3 (2)	0.11	Catalase OS=Homo sapiens GN=CAT PE=1 SV=3
CEP170	CE170_HUMAN	165	175586	29 (5)	20 (5)	0.1	Centrosomal protein of 170 kDa OS=Homo sapiens GN=CEP170 PE=1 SV=1
VBP1	PFD3_HUMAN	161	22815	10 (5)	5 (3)	0.51	Prefoldin subunit 3 OS=Homo sapiens GN=VBP1 PE=1 SV=3
CYB5B	CYB5B_HUMAN	153	16436	9 (7)	2 (2)	0.45	Cytochrome b5 type B OS=Homo sapiens GN=CYB5B PE=1 SV=2
ARHGAP17	RHG17_HUMAN	67	95776	5 (4)	5 (4)	0.14	Rho GTPase-activating protein 17 OS=Homo sapiens GN=ARHGAP17 PE=1 SV=1
SUPT5H	SPT5H_HUMAN	147	121324	16 (3)	13 (3)	0.08	Transcription elongation factor SPT5 OS=Homo sapiens GN=SUPT5H PE=1 SV=1
TNKS1BP1	TB182_HUMAN	147	182711	10 (7)	8 (6)	0.11	182 kDa tankyrase-1-binding protein OS=Homo sapiens GN=TNKS1BP1 PE=1 SV=4
EEF1A2	EF1A2_HUMAN	76	50780	11 (6)	7 (4)	0.29	Elongation factor 1-alpha 2 OS=Homo sapiens GN=EEF1A2 PE=1 SV=1
CDC42EP4	BORG4_HUMAN	140	38014	5 (2)	5 (2)	0.18	Cdc42 effector protein 4 OS=Homo sapiens GN=CDC42EP4 PE=1 SV=1
NAA10	NAA10_HUMAN	136	26613	5 (3)	4 (3)	0.42	N-alpha-acetyltransferase 10 OS=Homo sapiens GN=NAA10 PE=1 SV=1
BCAS1	BCAS1_HUMAN	132	61957	5 (5)	4 (4)	0.23	Breast carcinoma-amplified sequence 1 OS=Homo sapiens GN=BCAS1 PE=1 SV=2
CAPNS1	CPNS1_HUMAN	129	28469	5 (2)	4 (1)	0.12	Calpain small subunit 1 OS=Homo sapiens GN=CAPNS1 PE=1 SV=1
AKAP12	AKA12_HUMAN	127	191937	9 (2)	8 (2)	0.03	A-kinase anchor protein 12 OS=Homo sapiens GN=AKAP12 PE=1 SV=4
CDKN2AIP	CARF_HUMAN	124	61544	17 (3)	12 (3)	0.17	CDKN2A-interacting protein OS=Homo sapiens GN=CDKN2AIP PE=1 SV=3
DIABLO	DBLOH_HUMAN	122	27342	3 (2)	2 (1)	0.12	Diablo homolog, mitochondrial OS=Homo sapiens GN=DIABLO PE=1 SV=1
UBE2NL	UE2NL_HUMAN	119	17366	3 (2)	2 (1)	0.2	Putative ubiquitin-conjugating enzyme E2 N-like OS=Homo sapiens GN=UBE2NL PE=1 SV=1
LMCD1	LMCD1_HUMAN	118	42004	5 (3)	3 (1)	0.08	LIM and cysteine-rich domains protein 1 OS=Homo sapiens GN=LMCD1 PE=1 SV=1
TCEAL4	TCAL4_HUMAN	116	24746	4 (2)	4 (2)	0.29	Transcription elongation factor A protein-like 4 OS=Homo sapiens GN=TCEAL4 PE=1 SV=2
KLC2	KLC2_HUMAN	95	69291	10 (3)	8 (2)	0.1	Kinesin light chain 2 OS=Homo sapiens GN=KLC2 PE=1 SV=1

PPP6R1	PP6R1_HUMAN	110	97291	5 (2)	5 (2)	0.07	Serine/threonine-protein phosphatase 6 regulatory subunit 1 OS=Homo sapiens GN=PPP6R1 PE=1 SV=5
HSDL2	HSDL2_HUMAN	108	45651	8 (4)	6 (3)	0.23	Hydroxysteroid dehydrogenase-like protein 2 OS=Homo sapiens GN=HSDL2 PE=1 SV=1
SUMO4	SUMO4_HUMAN	108	10735	3 (2)	2 (1)	0.32	Small ubiquitin-related modifier 4 OS=Homo sapiens GN=SUMO4 PE=1 SV=2
ABCE1	ABCE1_HUMAN	107	68240	7 (4)	5 (2)	0.1	ATP-binding cassette sub-family E member 1 OS=Homo sapiens GN=ABCE1 PE=1 SV=1
KPNA1	IMA5_HUMAN	105	60925	2 (2)	1 (1)	0.05	Importin subunit alpha-5 OS=Homo sapiens GN=KPNA1 PE=1 SV=3
SLC25A4	ADT1_HUMAN	102	33271	21 (14)	8 (2)	0.21	ADP/ATP translocase 1 OS=Homo sapiens GN=SLC25A4 PE=1 SV=4
ARHGEF11	ARHGB_HUMAN	101	168456	7 (2)	7 (2)	0.04	Rho guanine nucleotide exchange factor 11 OS=Homo sapiens GN=ARHGEF11 PE=1 SV=1
FKBP15	FKB15_HUMAN	99	134060	6 (2)	6 (2)	0.05	FK506-binding protein 15 OS=Homo sapiens GN=FKBP15 PE=1 SV=2
FKBP3	FKBP3_HUMAN	98	25218	3 (2)	2 (1)	0.13	Peptidyl-prolyl cis-trans isomerase FKBP3 OS=Homo sapiens GN=FKBP3 PE=1 SV=1
FNBP1L	FBP1L_HUMAN	98	70478	16 (3)	11 (2)	0.1	Formin-binding protein 1-like OS=Homo sapiens GN=FNBP1L PE=1 SV=3
WASH6P	WASH6_HUMAN	96	48018	4 (1)	3 (1)	0.07	WAS protein family homolog 6 OS=Homo sapiens GN=WASH6P PE=1 SV=3
DCTN1	DCTN1_HUMAN	94	142348	23 (2)	12 (2)	0.05	Dynactin subunit 1 OS=Homo sapiens GN=DCTN1 PE=1 SV=3
FEN1	FEN1_HUMAN	94	42908	3 (1)	3 (1)	0.08	Flap endonuclease 1 OS=Homo sapiens GN=FEN1 PE=1 SV=1
CAVIN2	CAVN2_HUMAN	93	47202	6 (2)	6 (2)	0.14	Caveolae-associated protein 2 OS=Homo sapiens GN=CAVIN2 PE=1 SV=3
PICALM	PICAL_HUMAN	93	70881	8 (3)	7 (3)	0.15	Phosphatidylinositol-binding clathrin assembly protein OS=Homo sapiens GN=PICALM PE=1 SV=2
HNRNPH3	HNRH3_HUMAN	92	36960	2 (1)	2 (1)	0.09	Heterogeneous nuclear ribonucleoprotein H3 OS=Homo sapiens GN=HNRNPH3 PE=1 SV=2
NUP88	NUP88_HUMAN	91	84629	6 (2)	6 (2)	0.08	Nuclear pore complex protein Nup88 OS=Homo sapiens GN=NUP88 PE=1 SV=2
RUVBL2	RUVB2_HUMAN	90	51296	15 (3)	9 (2)	0.13	RuvB-like 2 OS=Homo sapiens GN=RUVBL2 PE=1 SV=3
EIF3I	EIF3I_HUMAN	89	36878	3 (2)	2 (2)	0.19	Eukaryotic translation initiation factor 3 subunit I OS=Homo sapiens GN=EIF3I PE=1 SV=1
SARS2	SYSM_HUMAN	88	58702	4 (1)	4 (1)	0.06	Serine--tRNA ligase, mitochondrial OS=Homo sapiens GN=SARS2 PE=1 SV=1
WASHC2A	WAC2A_HUMAN	86	147266	8 (2)	6 (1)	0.02	WASH complex subunit 2A OS=Homo sapiens GN=WASHC2A PE=1 SV=3
SDF4	CAB45_HUMAN	85	41895	2 (1)	2 (1)	0.08	45 kDa calcium-binding protein OS=Homo sapiens GN=SDF4 PE=1 SV=1
CAST	ICAL_HUMAN	83	76925	14 (3)	9 (2)	0.13	Calpastatin OS=Homo sapiens GN=CAST PE=1 SV=4
VCPIP1	VCIP1_HUMAN	83	135604	15 (2)	11 (2)	0.05	Deubiquitinating protein VCIP135 OS=Homo sapiens GN=VCPIP1 PE=1 SV=2
ZMPSTE24	FACE1_HUMAN	82	55063	7 (3)	4 (2)	0.12	CAAX prenyl protease 1 homolog OS=Homo sapiens GN=ZMPSTE24 PE=1 SV=2
FKBP1A	FKB1A_HUMAN	82	12000	2 (2)	1 (1)	0.29	Peptidyl-prolyl cis-trans isomerase FKBP1A OS=Homo sapiens GN=FKBP1A PE=1 SV=2
NPLOC4	NPL4_HUMAN	82	69046	4 (3)	3 (2)	0.1	Nuclear protein localization protein 4 homolog OS=Homo sapiens GN=NPLOC4 PE=1 SV=3
C8orf33	CH033_HUMAN	82	25319	2 (1)	2 (1)	0.13	UPF0488 protein C8orf33 OS=Homo sapiens GN=C8orf33 PE=1 SV=1
VPS37B	VP37B_HUMAN	81	31345	2 (1)	2 (1)	0.11	Vacuolar protein sorting-associated protein 37B OS=Homo sapiens GN=VPS37B PE=1 SV=1
RABGAP1	RBGP1_HUMAN	80	122915	17 (2)	14 (2)	0.05	Rab GTPase-activating protein 1 OS=Homo sapiens GN=RABGAP1 PE=1 SV=3
ZW10	ZW10_HUMAN	80	89628	4 (1)	4 (1)	0.04	Centromere/kinetochore protein zw10 homolog OS=Homo sapiens GN=ZW10 PE=1 SV=3
TRPV2	TRPV2_HUMAN	79	86838	1 (1)	1 (1)	0.04	Transient receptor potential cation channel subfamily V member 2 OS=Homo sapiens GN=TRPV2 PE=1 SV=1
SYAP1	SYAP1_HUMAN	79	39966	2 (2)	2 (2)	0.17	Synapse-associated protein 1 OS=Homo sapiens GN=SYAP1 PE=1 SV=1
WWP2	WWP2_HUMAN	77	99420	5 (1)	4 (1)	0.03	NEDD4-like E3 ubiquitin-protein ligase WWP2 OS=Homo sapiens GN=WWP2 PE=1 SV=2
OGT	OGT1_HUMAN	76	118104	3 (2)	3 (2)	0.06	UDP-N-acetylglucosamine--peptide N-acetylglucosaminyltransferase 110 kDa subunit OS=Homo sapiens GN=OGT PE=1 SV=3
PABPC3	PABP3_HUMAN	76	70215	19 (6)	12 (5)	0.26	Polyadenylate-binding protein 3 OS=Homo sapiens GN=PABPC3 PE=1 SV=2
AGPS	ADAS_HUMAN	76	73664	10 (4)	7 (3)	0.14	Alkyldihydroxyacetonephosphate synthase, peroxisomal OS=Homo sapiens GN=AGPS PE=1 SV=1
TOMM22	TOM22_HUMAN	76	15512	1 (1)	1 (1)	0.22	Mitochondrial import receptor subunit TOM22 homolog OS=Homo sapiens GN=TOMM22 PE=1 SV=3
CNN3	CNN3_HUMAN	73	36562	7 (3)	4 (2)	0.19	Calponin-3 OS=Homo sapiens GN=CNN3 PE=1 SV=1

GPRC5C	GPC5C_HUMAN	75	48732	1 (1)	1 (1)	0.07	G-protein coupled receptor family C group 5 member C OS=Homo sapiens GN=GPRC5C PE=1 SV=2
LANCL2	LANC2_HUMAN	74	51677	2 (1)	2 (1)	0.06	LanC-like protein 2 OS=Homo sapiens GN=LANCL2 PE=1 SV=1
SET	SET_HUMAN	74	33469	1 (1)	1 (1)	0.1	Protein SET OS=Homo sapiens GN=SET PE=1 SV=3
TUFT1	TUFT1_HUMAN	74	44522	5 (1)	5 (1)	0.07	Tuftelin OS=Homo sapiens GN=TUFT1 PE=1 SV=1
HMGB3	HMGB3_HUMAN	74	23137	10 (1)	7 (1)	0.15	High mobility group protein B3 OS=Homo sapiens GN=HMGB3 PE=1 SV=4
MYO1E	MYO1E_HUMAN	73	127552	3 (2)	3 (2)	0.05	Unconventional myosin-Ie OS=Homo sapiens GN=MYO1E PE=1 SV=2
ATG3	ATG3_HUMAN	73	36298	4 (1)	3 (1)	0.09	Ubiquitin-like-conjugating enzyme ATG3 OS=Homo sapiens GN=ATG3 PE=1 SV=1
ERLIN1	ERLN1_HUMAN	72	39072	4 (2)	4 (2)	0.18	Erlin-1 OS=Homo sapiens GN=ERLIN1 PE=1 SV=1
TXLNA	TXLNA_HUMAN	72	62195	9 (1)	8 (1)	0.05	Alpha-taxilin OS=Homo sapiens GN=TXLNA PE=1 SV=3
PPP4R1	PP4R1_HUMAN	71	108361	8 (3)	8 (3)	0.09	Serine/threonine-protein phosphatase 4 regulatory subunit 1 OS=Homo sapiens GN=PPP4R1 PE=1 SV=1
TJP1	ZO1_HUMAN	71	195682	8 (1)	8 (1)	0.02	Tight junction protein ZO-1 OS=Homo sapiens GN=TJP1 PE=1 SV=3
TDP2	TYDP2_HUMAN	71	41587	3 (1)	2 (1)	0.08	Tyrosyl-DNA phosphodiesterase 2 OS=Homo sapiens GN=TDP2 PE=1 SV=1
OXSM	OXSM_HUMAN	70	49439	4 (1)	4 (1)	0.07	3-oxoacyl-[acyl-carrier-protein] synthase, mitochondrial OS=Homo sapiens GN=OXSM PE=1 SV=1
HLA-A	1A02_HUMAN	70	41181	7 (2)	4 (2)	0.17	HLA class I histocompatibility antigen, A-2 alpha chain OS=Homo sapiens GN=HLA-A PE=1 SV=1
SNRPB2	RU2B_HUMAN	70	25470	5 (1)	2 (1)	0.13	U2 small nuclear ribonucleoprotein B” OS=Homo sapiens GN=SNRPB2 PE=1 SV=1
PAXX	PAXX_HUMAN	69	21968	1 (1)	1 (1)	0.15	Protein PAXX OS=Homo sapiens GN=PAXX PE=1 SV=2
LETM1	LETM1_HUMAN	69	83986	5 (1)	5 (1)	0.04	Mitochondrial proton/calcium exchanger protein OS=Homo sapiens GN=LETM1 PE=1 SV=1
MTFR1	MTFR1_HUMAN	69	37148	4 (1)	4 (1)	0.09	Mitochondrial fission regulator 1 OS=Homo sapiens GN=MTFR1 PE=1 SV=2
SH3GLB2	SHLB2_HUMAN	69	44175	10 (4)	6 (3)	0.24	Endophilin-B2 OS=Homo sapiens GN=SH3GLB2 PE=1 SV=1
ABHD12	ABD12_HUMAN	69	45524	8 (2)	3 (1)	0.07	Monoacylglycerol lipase ABHD12 OS=Homo sapiens GN=ABHD12 PE=1 SV=2
MAP2	MTAP2_HUMAN	69	199860	22 (3)	17 (3)	0.05	Microtubule-associated protein 2 OS=Homo sapiens GN=MAP2 PE=1 SV=4
GPHN	GEPH_HUMAN	69	80382	3 (1)	3 (1)	0.04	Gephyrin OS=Homo sapiens GN=GPHN PE=1 SV=1
SEC61B	SC61B_HUMAN	68	10025	3 (2)	3 (2)	0.82	Protein transport protein Sec61 subunit beta OS=Homo sapiens GN=SEC61B PE=1 SV=2
SEC16A	SC16A_HUMAN	68	234855	16 (3)	11 (3)	0.04	Protein transport protein Sec16A OS=Homo sapiens GN=SEC16A PE=1 SV=3
LUZP1	LUZP1_HUMAN	67	120772	20 (2)	17 (2)	0.05	Leucine zipper protein 1 OS=Homo sapiens GN=LUZP1 PE=1 SV=2
BIRC6	BIRC6_HUMAN	67	536192	30 (1)	20 (1)	0.01	Baculoviral IAP repeat-containing protein 6 OS=Homo sapiens GN=BIRC6 PE=1 SV=2
ASAP1	ASAP1_HUMAN	67	126390	5 (1)	4 (1)	0.03	Arf-GAP with SH3 domain, ANK repeat and PH domain-containing protein 1 OS=Homo sapiens GN=ASAP1 PE=1 SV=4
PIK3C2A	P3C2A_HUMAN	67	192156	26 (1)	15 (1)	0.02	Phosphatidylinositol 4-phosphate 3-kinase C2 domain-containing subunit alpha OS=Homo sapiens GN=PIK3C2A PE=1 SV=2
OGDH	ODO1_HUMAN	67	117059	4 (2)	4 (2)	0.06	2-oxoglutarate dehydrogenase, mitochondrial OS=Homo sapiens GN=OGDH PE=1 SV=3
IGF2BP1	IF2B1_HUMAN	67	63783	6 (2)	6 (2)	0.11	Insulin-like growth factor 2 mRNA-binding protein 1 OS=Homo sapiens GN=IGF2BP1 PE=1 SV=2
CACYBP	CYBP_HUMAN	66	26308	5 (1)	5 (1)	0.13	Calcyclin-binding protein OS=Homo sapiens GN=CACYBP PE=1 SV=2
PSMB7	PSB7_HUMAN	66	30288	4 (2)	2 (1)	0.11	Proteasome subunit beta type-7 OS=Homo sapiens GN=PSMB7 PE=1 SV=1
EXOC4	EXOC4_HUMAN	66	111170	9 (2)	8 (2)	0.06	Exocyst complex component 4 OS=Homo sapiens GN=EXOC4 PE=1 SV=1
TOR1AIP1	TOIP1_HUMAN	65	66379	6 (2)	4 (2)	0.1	Torsin-1A-interacting protein 1 OS=Homo sapiens GN=TOR1AIP1 PE=1 SV=2
PTDSS2	PTSS2_HUMAN	65	56787	1 (1)	1 (1)	0.06	Phosphatidylserine synthase 2 OS=Homo sapiens GN=PTDSS2 PE=1 SV=1
ITGA6	ITA6_HUMAN	65	127724	5 (2)	5 (2)	0.05	Integrin alpha-6 OS=Homo sapiens GN=ITGA6 PE=1 SV=5
CCDC50	CCD50_HUMAN	65	35914	8 (1)	7 (1)	0.09	Coiled-coil domain-containing protein 50 OS=Homo sapiens GN=CCDC50 PE=1 SV=1
ABHD14B	ABHEB_HUMAN	65	22446	4 (2)	3 (2)	0.32	Protein ABHD14B OS=Homo sapiens GN=ABHD14B PE=1 SV=1
CSRP1	CSRP1_HUMAN	64	21409	4 (1)	3 (1)	0.16	Cysteine and glycine-rich protein 1 OS=Homo sapiens GN=CSRP1 PE=1 SV=3

EIF4A3	IF4A3_HUMAN	64	47126	6 (1)	6 (1)	0.07	Eukaryotic initiation factor 4A-III OS=Homo sapiens GN=EIF4A3 PE=1 SV=4
NAA15	NAA15_HUMAN	64	102462	15 (1)	6 (1)	0.03	N-alpha-acetyltransferase 15, NatA auxiliary subunit OS=Homo sapiens GN=NAA15 PE=1 SV=1
CASP8	CASP8_HUMAN	64	56097	7 (1)	7 (1)	0.06	Caspase-8 OS=Homo sapiens GN=CASP8 PE=1 SV=1
ELOB	ELOB_HUMAN	63	13239	4 (3)	3 (2)	0.58	Elongin-B OS=Homo sapiens GN=ELOB PE=1 SV=1
RPS21	RS21_HUMAN	63	9220	3 (1)	2 (1)	0.38	40S ribosomal protein S21 OS=Homo sapiens GN=RPS21 PE=1 SV=1
SNRPF	RUXF_HUMAN	62	9776	1 (1)	1 (1)	0.36	Small nuclear ribonucleoprotein F OS=Homo sapiens GN=SNRPF PE=1 SV=1
ARHGEF5	ARHG5_HUMAN	62	177888	7 (2)	5 (2)	0.04	Rho guanine nucleotide exchange factor 5 OS=Homo sapiens GN=ARHGEF5 PE=1 SV=3
FAM83H	FA83H_HUMAN	62	127557	7 (1)	6 (1)	0.03	Protein FAM83H OS=Homo sapiens GN=FAM83H PE=1 SV=3
SF3A1	SF3A1_HUMAN	62	88888	12 (1)	7 (1)	0.04	Splicing factor 3A subunit 1 OS=Homo sapiens GN=SF3A1 PE=1 SV=1
PEX19	PEX19_HUMAN	62	33071	3 (2)	2 (1)	0.21	Peroxisomal biogenesis factor 19 OS=Homo sapiens GN=PEX19 PE=1 SV=1
ELAC2	RNZ2_HUMAN	61	93415	9 (1)	4 (1)	0.04	Zinc phosphodiesterase ELAC protein 2 OS=Homo sapiens GN=ELAC2 PE=1 SV=2
SRPRB	SRPRB_HUMAN	61	29912	7 (1)	6 (1)	0.11	Signal recognition particle receptor subunit beta OS=Homo sapiens GN=SRPRB PE=1 SV=3
YIPF6	YIPF6_HUMAN	61	26467	1 (1)	1 (1)	0.13	Protein YIPF6 OS=Homo sapiens GN=YIPF6 PE=1 SV=2
CNOT3	CNOT3_HUMAN	60	82050	9 (1)	5 (1)	0.04	CCR4-NOT transcription complex subunit 3 OS=Homo sapiens GN=CNOT3 PE=1 SV=1
PPP3CA	PP2BA_HUMAN	60	59335	8 (3)	6 (2)	0.11	Serine/threonine-protein phosphatase 2B catalytic subunit alpha isoform OS=Homo sapiens GN=PPP3CA PE=1 SV=1
CBX3	CBX3_HUMAN	59	20969	5 (3)	5 (3)	0.56	Chromobox protein homolog 3 OS=Homo sapiens GN=CBX3 PE=1 SV=4
AP2B1	AP2B1_HUMAN	59	105398	3 (2)	2 (2)	0.06	AP-2 complex subunit beta OS=Homo sapiens GN=AP2B1 PE=1 SV=1
WBP11	WBP11_HUMAN	59	69954	4 (1)	3 (1)	0.05	WW domain-binding protein 11 OS=Homo sapiens GN=WBP11 PE=1 SV=1
CCNDBP1	CCDB1_HUMAN	58	40636	4 (1)	4 (1)	0.08	Cyclin-D1-binding protein 1 OS=Homo sapiens GN=CCNDBP1 PE=1 SV=2
PARP1	PARP1_HUMAN	58	113811	33 (2)	16 (2)	0.06	Poly [ADP-ribose] polymerase 1 OS=Homo sapiens GN=PARP1 PE=1 SV=4
PIN4	PIN4_HUMAN	58	13858	6 (1)	6 (1)	0.25	Peptidyl-prolyl cis-trans isomerase NIMA-interacting 4 OS=Homo sapiens GN=PIN4 PE=1 SV=1
DIP2B	DIP2B_HUMAN	58	173606	12 (1)	8 (1)	0.02	Disco-interacting protein 2 homolog B OS=Homo sapiens GN=DIP2B PE=1 SV=3
PRMT1	ANM1_HUMAN	58	42059	2 (2)	2 (2)	0.16	Protein arginine N-methyltransferase 1 OS=Homo sapiens GN=PRMT1 PE=1 SV=2
SRRM2	SRRM2_HUMAN	58	300179	35 (3)	32 (3)	0.03	Serine/arginine repetitive matrix protein 2 OS=Homo sapiens GN=SRRM2 PE=1 SV=2
COPS3	CSN3_HUMAN	58	48412	5 (2)	5 (2)	0.14	COP9 signalosome complex subunit 3 OS=Homo sapiens GN=COPS3 PE=1 SV=3
PGAM1	PGAM1_HUMAN	58	28900	7 (2)	5 (1)	0.12	Phosphoglycerate mutase 1 OS=Homo sapiens GN=PGAM1 PE=1 SV=2
IARS	SYIC_HUMAN	58	145718	15 (2)	12 (1)	0.02	Isoleucine--tRNA ligase, cytoplasmic OS=Homo sapiens GN=IARS PE=1 SV=2
ADIRF	ADIRF_HUMAN	57	7850	2 (1)	2 (1)	0.45	Adipogenesis regulatory factor OS=Homo sapiens GN=ADIRF PE=1 SV=1
OSBPL10	OSB10_HUMAN	57	84716	6 (1)	5 (1)	0.04	Oxysterol-binding protein-related protein 10 OS=Homo sapiens GN=OSBPL10 PE=1 SV=2
TBL2	TBL2_HUMAN	57	50393	3 (1)	2 (1)	0.07	Transducin beta-like protein 2 OS=Homo sapiens GN=TBL2 PE=1 SV=1
LIN7C	LIN7C_HUMAN	57	21935	6 (1)	2 (1)	0.15	Protein lin-7 homolog C OS=Homo sapiens GN=LIN7C PE=1 SV=1
GRIPAP1	GRAP1_HUMAN	57	96273	13 (1)	8 (1)	0.03	GRIP1-associated protein 1 OS=Homo sapiens GN=GRIPAP1 PE=1 SV=1
FAM107B	F107B_HUMAN	57	15548	1 (1)	1 (1)	0.22	Protein FAM107B OS=Homo sapiens GN=FAM107B PE=1 SV=1
ARFGAP1	ARFG1_HUMAN	57	44982	1 (1)	1 (1)	0.07	ADP-ribosylation factor GTPase-activating protein 1 OS=Homo sapiens GN=ARFGAP1 PE=1 SV=2
CTPS1	PYRG1_HUMAN	57	67332	6 (2)	6 (2)	0.1	CTP synthase 1 OS=Homo sapiens GN=CTPS1 PE=1 SV=2
ITPR3	ITPR3_HUMAN	56	306820	26 (1)	22 (1)	0.01	Inositol 1,4,5-trisphosphate receptor type 3 OS=Homo sapiens GN=ITPR3 PE=1 SV=2
ACTL6A	ACL6A_HUMAN	56	47944	5 (1)	4 (1)	0.07	Actin-like protein 6A OS=Homo sapiens GN=ACTL6A PE=1 SV=1
SLC9A3R2	NHRF2_HUMAN	56	37619	2 (1)	2 (1)	0.09	Na(+)/H(+) exchange regulatory cofactor NHE-RF2 OS=Homo sapiens GN=SLC9A3R2 PE=1 SV=2
MISP	MISP_HUMAN	56	75482	2 (1)	2 (1)	0.04	Mitotic interactor and substrate of PLK1 OS=Homo sapiens GN=MISP PE=1 SV=1
OTUB1	OTUB1_HUMAN	56	31492	1 (1)	1 (1)	0.11	Ubiquitin thioesterase OTUB1 OS=Homo sapiens GN=OTUB1 PE=1 SV=2

TAGLN	TAGL_HUMAN	56	22653	7 (2)	4 (2)	0.32	Transgelin OS=Homo sapiens GN=TAGLN PE=1 SV=4
SSH3	SSH3_HUMAN	56	73293	2 (1)	1 (1)	0.04	Protein phosphatase Slingshot homolog 3 OS=Homo sapiens GN=SSH3 PE=1 SV=2
GPS1	CSN1_HUMAN	56	56071	9 (2)	6 (2)	0.12	COP9 signalosome complex subunit 1 OS=Homo sapiens GN=GPS1 PE=1 SV=4
CLPX	CLPX_HUMAN	56	69922	10 (1)	4 (1)	0.05	ATP-dependent Clp protease ATP-binding subunit clpX-like, mitochondrial OS=Homo sapiens GN=CLPX PE=1 SV=2
SQSTM1	SQSTM_HUMAN	56	48455	2 (1)	1 (1)	0.07	Sequestosome-1 OS=Homo sapiens GN=SQSTM1 PE=1 SV=1
FKBP5	FKBP5_HUMAN	56	51693	13 (1)	11 (1)	0.06	Peptidyl-prolyl cis-trans isomerase FKBP5 OS=Homo sapiens GN=FKBP5 PE=1 SV=2
HTATIP2	HTAI2_HUMAN	55	27260	8 (2)	4 (2)	0.26	Oxidoreductase HTATIP2 OS=Homo sapiens GN=HTATIP2 PE=1 SV=2
SAMHD1	SAMH1_HUMAN	55	72896	6 (1)	3 (1)	0.05	Deoxynucleoside triphosphate triphosphohydrolase SAMHD1 OS=Homo sapiens GN=SAMHD1 PE=1 SV=2
DAZAP1	DAZP1_HUMAN	55	43584	1 (1)	1 (1)	0.08	DAZ-associated protein 1 OS=Homo sapiens GN=DAZAP1 PE=1 SV=1
MIA3	TGO1_HUMAN	55	214255	12 (1)	11 (1)	0.02	Transport and Golgi organization protein 1 homolog OS=Homo sapiens GN=MIA3 PE=1 SV=1
RFC2	RFC2_HUMAN	54	39588	1 (1)	1 (1)	0.08	Replication factor C subunit 2 OS=Homo sapiens GN=RFC2 PE=1 SV=3
MAP7	MAP7_HUMAN	54	84116	27 (1)	11 (1)	0.04	Ensconsin OS=Homo sapiens GN=MAP7 PE=1 SV=1
NT5C2	5NTC_HUMAN	54	65384	4 (1)	3 (1)	0.05	Cytosolic purine 5'-nucleotidase OS=Homo sapiens GN=NT5C2 PE=1 SV=1
REXO2	ORN_HUMAN	53	27044	6 (2)	4 (1)	0.12	Oligoribonuclease, mitochondrial OS=Homo sapiens GN=REXO2 PE=1 SV=3
ELP2	ELP2_HUMAN	53	94266	2 (1)	2 (1)	0.03	Elongator complex protein 2 OS=Homo sapiens GN=ELP2 PE=1 SV=2
SRP54	SRP54_HUMAN	53	55953	11 (2)	8 (2)	0.12	Signal recognition particle 54 kDa protein OS=Homo sapiens GN=SRP54 PE=1 SV=1
NUDT5	NUDT5_HUMAN	53	24597	4 (3)	3 (2)	0.29	ADP-sugar pyrophosphatase OS=Homo sapiens GN=NUDT5 PE=1 SV=1
NRBP1	NRBP_HUMAN	53	60377	1 (1)	1 (1)	0.05	Nuclear receptor-binding protein OS=Homo sapiens GN=NRBP1 PE=1 SV=1
MRPL46	RM46_HUMAN	53	31799	8 (1)	6 (1)	0.1	39S ribosomal protein L46, mitochondrial OS=Homo sapiens GN=MRPL46 PE=1 SV=1
GGCT	GGCT_HUMAN	53	21222	4 (1)	3 (1)	0.16	Gamma-glutamylcyclotransferase OS=Homo sapiens GN=GGCT PE=1 SV=1
GOLPH3	GOLP3_HUMAN	53	34075	2 (1)	2 (1)	0.1	Golgi phosphoprotein 3 OS=Homo sapiens GN=GOLPH3 PE=1 SV=1
CLUH	CLU_HUMAN	53	148003	9 (1)	6 (1)	0.02	Clustered mitochondria protein homolog OS=Homo sapiens GN=CLUH PE=1 SV=2
DNPEP	DNPEP_HUMAN	52	53022	6 (1)	5 (1)	0.06	Aspartyl aminopeptidase OS=Homo sapiens GN=DNPEP PE=1 SV=1
EXOSC6	EXOS6_HUMAN	52	28503	6 (1)	4 (1)	0.12	Exosome complex component MTR3 OS=Homo sapiens GN=EXOSC6 PE=1 SV=1
WDHD1	WDHD1_HUMAN	52	127371	8 (1)	6 (1)	0.03	WD repeat and HMG-box DNA-binding protein 1 OS=Homo sapiens GN=WDHD1 PE=1 SV=1
MARK2	MARK2_HUMAN	52	88255	2 (1)	2 (1)	0.04	Serine/threonine-protein kinase MARK2 OS=Homo sapiens GN=MARK2 PE=1 SV=2
STXBP1	STXB1_HUMAN	52	67925	3 (1)	3 (1)	0.05	Syntaxin-binding protein 1 OS=Homo sapiens GN=STXBP1 PE=1 SV=1
CNOT1	CNOT1_HUMAN	52	269106	7 (2)	6 (2)	0.02	CCR4-NOT transcription complex subunit 1 OS=Homo sapiens GN=CNOT1 PE=1 SV=2
CGN	CING_HUMAN	52	136532	18 (2)	16 (2)	0.05	Cingulin OS=Homo sapiens GN=CGN PE=1 SV=2
NAGK	NAGK_HUMAN	52	37694	6 (1)	4 (1)	0.09	N-acetyl-D-glucosamine kinase OS=Homo sapiens GN=NAGK PE=1 SV=4
MRPS27	RT27_HUMAN	51	47924	6 (1)	6 (1)	0.07	28S ribosomal protein S27, mitochondrial OS=Homo sapiens GN=MRPS27 PE=1 SV=3
CASP14	CASPE_HUMAN	51	27947	7 (1)	3 (1)	0.12	Caspase-14 OS=Homo sapiens GN=CASP14 PE=1 SV=2
PLEC	PLEC_HUMAN	51	533462	73 (2)	55 (2)	0.01	Plectin OS=Homo sapiens GN=PLEC PE=1 SV=3
UBR4	UBR4_HUMAN	51	580547	39 (2)	26 (2)	0.01	E3 ubiquitin-protein ligase UBR4 OS=Homo sapiens GN=UBR4 PE=1 SV=1
PITPNA	PIPNA_HUMAN	51	32014	6 (2)	6 (2)	0.22	Phosphatidylinositol transfer protein alpha isoform OS=Homo sapiens GN=PITPNA PE=1 SV=2
PTPN2	PTN2_HUMAN	50	48842	12 (1)	8 (1)	0.07	Tyrosine-protein phosphatase non-receptor type 2 OS=Homo sapiens GN=PTPN2 PE=1 SV=2
SEPT8	SEPT8_HUMAN	50	56234	6 (1)	3 (1)	0.06	Septin-8 OS=Homo sapiens GN=SEPT8 PE=1 SV=4
RAB14	RAB14_HUMAN	50	24110	7 (4)	5 (3)	0.48	Ras-related protein Rab-14 OS=Homo sapiens GN=RAB14 PE=1 SV=4
DNAJB1	DNJB1_HUMAN	50	38191	5 (1)	5 (1)	0.09	DnaJ homolog subfamily B member 1 OS=Homo sapiens GN=DNAJB1 PE=1 SV=4
EPB41L2	E41L2_HUMAN	50	113032	6 (1)	6 (1)	0.03	Band 4.1-like protein 2 OS=Homo sapiens GN=EPB41L2 PE=1 SV=1

UBE2C	UBE2C_HUMAN	49	19754	3 (2)	2 (2)	0.37	Ubiquitin-conjugating enzyme E2 C OS=Homo sapiens GN=UBE2C PE=1 SV=1
CPNE1	CPNE1_HUMAN	49	59649	5 (1)	4 (1)	0.06	Copine-1 OS=Homo sapiens GN=CPNE1 PE=1 SV=1
ERAL1	ERAL1_HUMAN	49	48833	1 (1)	1 (1)	0.07	GTPase Era, mitochondrial OS=Homo sapiens GN=ERAL1 PE=1 SV=2
EIF2B2	EI2BB_HUMAN	49	39193	1 (1)	1 (1)	0.08	Translation initiation factor eIF-2B subunit beta OS=Homo sapiens GN=EIF2B2 PE=1 SV=3
HNMT	HNMT_HUMAN	49	33616	1 (1)	1 (1)	0.1	Histamine N-methyltransferase OS=Homo sapiens GN=HNMT PE=1 SV=1
TEX264	TX264_HUMAN	49	34452	1 (1)	1 (1)	0.1	Testis-expressed protein 264 OS=Homo sapiens GN=TEX264 PE=1 SV=1
CORO7	CORO7_HUMAN	49	101626	2 (1)	2 (1)	0.03	Coronin-7 OS=Homo sapiens GN=CORO7 PE=1 SV=2
DDX1	DDX1_HUMAN	48	83349	4 (1)	4 (1)	0.04	ATP-dependent RNA helicase DDX1 OS=Homo sapiens GN=DDX1 PE=1 SV=2
MLPH	MELPH_HUMAN	48	66593	3 (1)	3 (1)	0.05	Melanophilin OS=Homo sapiens GN=MLPH PE=1 SV=1
IMUP	IMUP_HUMAN	48	10891	1 (1)	1 (1)	0.32	Immortalization up-regulated protein OS=Homo sapiens GN=IMUP PE=1 SV=1
SMAD3	SMAD3_HUMAN	48	48905	3 (1)	3 (1)	0.07	Mothers against decapentaplegic homolog 3 OS=Homo sapiens GN=SMAD3 PE=1 SV=1
DHCR24	DHC24_HUMAN	48	60803	2 (1)	2 (1)	0.05	Delta(24)-sterol reductase OS=Homo sapiens GN=DHCR24 PE=1 SV=2
TMOD3	TMOD3_HUMAN	48	39741	2 (1)	2 (1)	0.08	Tropomodulin-3 OS=Homo sapiens GN=TMOD3 PE=1 SV=1
PAPSS1	PAPS1_HUMAN	48	71586	4 (1)	3 (1)	0.05	Bifunctional 3'-phosphoadenosine 5'-phosphosulfate synthase 1 OS=Homo sapiens GN=PAPSS1 PE=1 SV=2
CTAGE15	CTGEF_HUMAN	47	88212	15 (1)	8 (1)	0.04	cTAGE family member 15 OS=Homo sapiens GN=CTAGE15 PE=2 SV=1
ARL6IP1	AR6P1_HUMAN	47	23518	4 (2)	3 (1)	0.14	ADP-ribosylation factor-like protein 6-interacting protein 1 OS=Homo sapiens GN=ARL6IP1 PE=1 SV=2
TMEM33	TMM33_HUMAN	47	28302	1 (1)	1 (1)	0.12	Transmembrane protein 33 OS=Homo sapiens GN=TMEM33 PE=1 SV=2
MRPL19	RM19_HUMAN	47	33799	7 (1)	4 (1)	0.1	39S ribosomal protein L19, mitochondrial OS=Homo sapiens GN=MRPL19 PE=1 SV=2
CSTF2	CSTF2_HUMAN	47	61035	16 (2)	10 (2)	0.11	Cleavage stimulation factor subunit 2 OS=Homo sapiens GN=CSTF2 PE=1 SV=1
HMGCL	HMGCL_HUMAN	46	34794	3 (1)	3 (1)	0.1	Hydroxymethylglutaryl-CoA lyase, mitochondrial OS=Homo sapiens GN=HMGCL PE=1 SV=2
CCAR2	CCAR2_HUMAN	46	103465	11 (1)	8 (1)	0.03	Cell cycle and apoptosis regulator protein 2 OS=Homo sapiens GN=CCAR2 PE=1 SV=2
USP47	UBP47_HUMAN	46	158581	11 (1)	8 (1)	0.02	Ubiquitin carboxyl-terminal hydrolase 47 OS=Homo sapiens GN=USP47 PE=1 SV=3
RNMT	MCES_HUMAN	46	55494	7 (1)	7 (1)	0.06	mRNA cap guanine-N7 methyltransferase OS=Homo sapiens GN=RNMT PE=1 SV=1
TMEM245	TM245_HUMAN	46	101508	6 (1)	3 (1)	0.03	Transmembrane protein 245 OS=Homo sapiens GN=TMEM245 PE=1 SV=2
SIRT5	SIR5_HUMAN	46	34543	2 (1)	2 (1)	0.1	NAD-dependent protein deacylase sirtuin-5, mitochondrial OS=Homo sapiens GN=SIRT5 PE=1 SV=2
NDUFB10	NDUBA_HUMAN	46	21048	6 (1)	5 (1)	0.16	NADH dehydrogenase [ubiquinone] 1 beta subcomplex subunit 10 OS=Homo sapiens GN=NDUFB10 PE=1 SV=3
STX12	STX12_HUMAN	46	31736	9 (2)	5 (2)	0.22	Syntaxin-12 OS=Homo sapiens GN=STX12 PE=1 SV=1
RAB32	RAB32_HUMAN	46	25210	8 (1)	4 (1)	0.13	Ras-related protein Rab-32 OS=Homo sapiens GN=RAB32 PE=1 SV=3
ISG15	ISG15_HUMAN	45	17933	3 (1)	2 (1)	0.19	Ubiquitin-like protein ISG15 OS=Homo sapiens GN=ISG15 PE=1 SV=5
MT-CO2	COX2_HUMAN	45	25719	1 (1)	1 (1)	0.13	Cytochrome c oxidase subunit 2 OS=Homo sapiens GN=MT-CO2 PE=1 SV=1
GNA13	GNA13_HUMAN	45	44364	2 (2)	2 (2)	0.15	Guanine nucleotide-binding protein subunit alpha-13 OS=Homo sapiens GN=GNA13 PE=1 SV=2
METTL2B	MET2B_HUMAN	45	44140	7 (1)	3 (1)	0.07	Methyltransferase-like protein 2B OS=Homo sapiens GN=METTL2B PE=1 SV=3
ADD1	ADDA_HUMAN	45	81304	4 (1)	4 (1)	0.04	Alpha-adducin OS=Homo sapiens GN=ADD1 PE=1 SV=2
TNS3	TENS3_HUMAN	45	156366	4 (1)	4 (1)	0.02	Tensin-3 OS=Homo sapiens GN=TNS3 PE=1 SV=2
GRSF1	GRSF1_HUMAN	45	53606	6 (2)	6 (2)	0.13	G-rich sequence factor 1 OS=Homo sapiens GN=GRSF1 PE=1 SV=3
EMD	EMD_HUMAN	45	29033	1 (1)	1 (1)	0.11	Emerin OS=Homo sapiens GN=EMD PE=1 SV=1
DCTN3	DCTN3_HUMAN	45	21220	4 (2)	2 (1)	0.16	Dynactin subunit 3 OS=Homo sapiens GN=DCTN3 PE=1 SV=1
PNKP	PNKP_HUMAN	44	57554	4 (1)	4 (1)	0.06	Bifunctional polynucleotide phosphatase/kinase OS=Homo sapiens GN=PNKP PE=1 SV=1
GIPC1	GIPC1_HUMAN	44	36141	6 (1)	3 (1)	0.09	PDZ domain-containing protein GIPC1 OS=Homo sapiens GN=GIPC1 PE=1 SV=2
COX6B1	CX6B1_HUMAN	44	10414	8 (2)	4 (1)	0.33	Cytochrome c oxidase subunit 6B1 OS=Homo sapiens GN=COX6B1 PE=1 SV=2

LZIC	LZIC_HUMAN	44	21538	1 (1)	1 (1)	0.16	Protein LZIC OS=Homo sapiens GN=LZIC PE=1 SV=1
PPM1G	PPM1G_HUMAN	44	59919	4 (2)	4 (2)	0.11	Protein phosphatase 1G OS=Homo sapiens GN=PPM1G PE=1 SV=1
OTUD7B	OTU7B_HUMAN	44	93152	7 (1)	6 (1)	0.04	OTU domain-containing protein 7B OS=Homo sapiens GN=OTUD7B PE=1 SV=1
NDE1	NDE1_HUMAN	44	38842	10 (1)	7 (1)	0.09	Nuclear distribution protein nudE homolog 1 OS=Homo sapiens GN=NDE1 PE=1 SV=2
ACAA1	THIK_HUMAN	44	44834	1 (1)	1 (1)	0.07	3-ketoacyl-CoA thiolase, peroxisomal OS=Homo sapiens GN=ACAA1 PE=1 SV=2
PSMD1	PSMD1_HUMAN	44	106795	4 (1)	4 (1)	0.03	26S proteasome non-ATPase regulatory subunit 1 OS=Homo sapiens GN=PSMD1 PE=1 SV=2
SF3B2	SF3B2_HUMAN	44	100279	16 (1)	10 (1)	0.03	Splicing factor 3B subunit 2 OS=Homo sapiens GN=SF3B2 PE=1 SV=2
ARIH1	ARI1_HUMAN	44	65900	7 (1)	4 (1)	0.05	E3 ubiquitin-protein ligase ARIH1 OS=Homo sapiens GN=ARIH1 PE=1 SV=2
LRP1	LRP1_HUMAN	44	523150	14 (1)	12 (1)	0.01	Prolow-density lipoprotein receptor-related protein 1 OS=Homo sapiens GN=LRP1 PE=1 SV=2
RAB3GAP2	RBGPR_HUMAN	44	157482	5 (1)	4 (1)	0.02	Rab3 GTPase-activating protein non-catalytic subunit OS=Homo sapiens GN=RAB3GAP2 PE=1 SV=1
MYO6	MYO6_HUMAN	44	150965	9 (1)	8 (1)	0.02	Unconventional myosin-VI OS=Homo sapiens GN=MYO6 PE=1 SV=4
CUX1	CASP_HUMAN	43	77636	13 (1)	5 (1)	0.04	Protein CASP OS=Homo sapiens GN=CUX1 PE=1 SV=2
CCDC9	CCDC9_HUMAN	43	59781	7 (1)	5 (1)	0.05	Coiled-coil domain-containing protein 9 OS=Homo sapiens GN=CCDC9 PE=1 SV=1
PRPSAP2	KPRB_HUMAN	43	41299	8 (1)	5 (1)	0.08	Phosphoribosyl pyrophosphate synthase-associated protein 2 OS=Homo sapiens GN=PRPSAP2 PE=1 SV=1
YTHDF2	YTHD2_HUMAN	43	62467	3 (1)	3 (1)	0.05	YTH domain-containing family protein 2 OS=Homo sapiens GN=YTHDF2 PE=1 SV=2
PEF1	PEF1_HUMAN	43	30646	3 (1)	2 (1)	0.11	Peflin OS=Homo sapiens GN=PEF1 PE=1 SV=1
RBMS2	RBMS2_HUMAN	43	44159	2 (1)	2 (1)	0.07	RNA-binding motif, single-stranded-interacting protein 2 OS=Homo sapiens GN=RBMS2 PE=1 SV=1
MSH2	MSH2_HUMAN	43	105418	4 (1)	4 (1)	0.03	DNA mismatch repair protein Msh2 OS=Homo sapiens GN=MSH2 PE=1 SV=1
LYN	LYN_HUMAN	43	58993	3 (1)	3 (1)	0.06	Tyrosine-protein kinase Lyn OS=Homo sapiens GN=LYN PE=1 SV=3
DNAJB11	DJB11_HUMAN	42	40774	6 (2)	4 (2)	0.17	DnaJ homolog subfamily B member 11 OS=Homo sapiens GN=DNAJB11 PE=1 SV=1
CD47	CD47_HUMAN	42	35590	2 (1)	2 (1)	0.09	Leukocyte surface antigen CD47 OS=Homo sapiens GN=CD47 PE=1 SV=1
CCDC93	CCD93_HUMAN	42	73437	10 (1)	7 (1)	0.04	Coiled-coil domain-containing protein 93 OS=Homo sapiens GN=CCDC93 PE=1 SV=2
GINS3	PSF3_HUMAN	42	24576	2 (1)	2 (1)	0.14	DNA replication complex GINS protein PSF3 OS=Homo sapiens GN=GINS3 PE=1 SV=1
HMOX1	HMOX1_HUMAN	42	32798	3 (2)	1 (1)	0.1	Heme oxygenase 1 OS=Homo sapiens GN=HMOX1 PE=1 SV=1
RRAS2	RRAS2_HUMAN	42	23613	4 (1)	3 (1)	0.14	Ras-related protein R-Ras2 OS=Homo sapiens GN=RRAS2 PE=1 SV=1
PSMC4	PRS6B_HUMAN	42	47451	1 (1)	1 (1)	0.07	26S proteasome regulatory subunit 6B OS=Homo sapiens GN=PSMC4 PE=1 SV=2
EIF2B4	EI2BD_HUMAN	42	58035	4 (1)	3 (1)	0.06	Translation initiation factor eIF-2B subunit delta OS=Homo sapiens GN=EIF2B4 PE=1 SV=2
FNBP1	FNBP1_HUMAN	42	71718	11 (1)	7 (1)	0.05	Formin-binding protein 1 OS=Homo sapiens GN=FNBP1 PE=1 SV=2
ERH	ERH_HUMAN	41	12422	2 (2)	1 (1)	0.28	Enhancer of rudimentary homolog OS=Homo sapiens GN=ERH PE=1 SV=1
EMC1	EMC1_HUMAN	41	112145	8 (1)	5 (1)	0.03	ER membrane protein complex subunit 1 OS=Homo sapiens GN=EMC1 PE=1 SV=1
GHITM	GHITM_HUMAN	41	37352	8 (2)	4 (2)	0.18	Growth hormone-inducible transmembrane protein OS=Homo sapiens GN=GHITM PE=1 SV=2
CAB39	CAB39_HUMAN	41	40015	5 (2)	4 (2)	0.17	Calcium-binding protein 39 OS=Homo sapiens GN=CAB39 PE=1 SV=1
VPS18	VPS18_HUMAN	41	111484	5 (1)	4 (1)	0.03	Vacuolar protein sorting-associated protein 18 homolog OS=Homo sapiens GN=VPS18 PE=1 SV=2
RAB5B	RAB5B_HUMAN	40	23920	2 (2)	1 (1)	0.14	Ras-related protein Rab-5B OS=Homo sapiens GN=RAB5B PE=1 SV=1
ATP6AP2	RENR_HUMAN	40	38983	2 (1)	2 (1)	0.08	Renin receptor OS=Homo sapiens GN=ATP6AP2 PE=1 SV=2
CHCHD3	MIC19_HUMAN	40	26421	6 (1)	3 (1)	0.13	MICOS complex subunit MIC19 OS=Homo sapiens GN=CHCHD3 PE=1 SV=1
LOC112268437	YJ005_HUMAN	40	38181	1 (1)	1 (1)	0.09	Uncharacterized protein FLJ45252 OS=Homo sapiens PE=2 SV=2
SNX6	SNX6_HUMAN	40	46905	3 (1)	3 (1)	0.07	Sorting nexin-6 OS=Homo sapiens GN=SNX6 PE=1 SV=1
DIAPH2	DIAP2_HUMAN	40	126231	11 (1)	11 (1)	0.03	Protein diaphanous homolog 2 OS=Homo sapiens GN=DIAPH2 PE=1 SV=1
GPAT3	GPAT3_HUMAN	40	49187	8 (1)	7 (1)	0.07	Glycerol-3-phosphate acyltransferase 3 OS=Homo sapiens GN=GPAT3 PE=1 SV=2
PDXDC1	PDXD1_HUMAN	40	87565	6 (1)	4 (1)	0.04	Pyridoxal-dependent decarboxylase domain-containing protein 1 OS=Homo sapiens GN=PDXDC1 PE=1 SV=2

STK39	STK39_HUMAN	40	59950	3 (1)	3 (1)	0.05	STE20/SPS1-related proline-alanine-rich protein kinase OS=Homo sapiens GN=STK39 PE=1 SV=3
STT3A	STT3A_HUMAN	39	81104	2 (1)	2 (1)	0.04	Dolichyl-diphosphooligosaccharide--protein glycosyltransferase subunit STT3A OS=Homo sapiens GN=STT3A PE=1 SV=2
PIK3C3	PK3C3_HUMAN	39	102169	8 (1)	5 (1)	0.03	Phosphatidylinositol 3-kinase catalytic subunit type 3 OS=Homo sapiens GN=PIK3C3 PE=1 SV=1
HNRNPA0	ROA0_HUMAN	39	30993	2 (1)	2 (1)	0.11	Heterogeneous nuclear ribonucleoprotein A0 OS=Homo sapiens GN=HNRNPA0 PE=1 SV=1
PTCHD3	PTHD3_HUMAN	39	87842	10 (2)	4 (1)	0.04	Patched domain-containing protein 3 OS=Homo sapiens GN=PTCHD3 PE=1 SV=3
SDSL	SDSL_HUMAN	39	35222	1 (1)	1 (1)	0.09	Serine dehydratase-like OS=Homo sapiens GN=SDSL PE=1 SV=1
TNRC6A	TNR6A_HUMAN	39	210967	10 (1)	7 (1)	0.02	Trinucleotide repeat-containing gene 6A protein OS=Homo sapiens GN=TNRC6A PE=1 SV=2
EPN1	EPN1_HUMAN	39	60370	6 (1)	5 (1)	0.05	Epsin-1 OS=Homo sapiens GN=EPN1 PE=1 SV=2
EPB41L1	E41L1_HUMAN	39	99012	8 (1)	8 (1)	0.03	Band 4.1-like protein 1 OS=Homo sapiens GN=EPB41L1 PE=1 SV=2
CHMP4C	CHM4C_HUMAN	38	26394	2 (1)	2 (1)	0.13	Charged multivesicular body protein 4c OS=Homo sapiens GN=CHMP4C PE=1 SV=1
DDX39A	DX39A_HUMAN	38	49611	6 (1)	6 (1)	0.07	ATP-dependent RNA helicase DDX39A OS=Homo sapiens GN=DDX39A PE=1 SV=2
ELMO2	ELMO2_HUMAN	38	83018	5 (1)	3 (1)	0.04	Engulfment and cell motility protein 2 OS=Homo sapiens GN=ELMO2 PE=1 SV=2
SLAIN2	SLAI2_HUMAN	38	62733	5 (1)	5 (1)	0.05	SLAIN motif-containing protein 2 OS=Homo sapiens GN=SLAIN2 PE=1 SV=2
BCL2L1	B2CL1_HUMAN	38	26090	2 (1)	2 (1)	0.13	Bcl-2-like protein 1 OS=Homo sapiens GN=BCL2L1 PE=1 SV=1
HNRNPUL2	HNRL2_HUMAN	38	85622	7 (1)	6 (1)	0.04	Heterogeneous nuclear ribonucleoprotein U-like protein 2 OS=Homo sapiens GN=HNRNPUL2 PE=1 SV=1
NAA50	NAA50_HUMAN	38	19614	2 (1)	1 (1)	0.17	N-alpha-acetyltransferase 50 OS=Homo sapiens GN=NAA50 PE=1 SV=1
UBAP2	UBAP2_HUMAN	38	117614	7 (1)	6 (1)	0.03	Ubiquitin-associated protein 2 OS=Homo sapiens GN=UBAP2 PE=1 SV=1
TXNDC5	TXND5_HUMAN	38	48283	4 (2)	3 (1)	0.07	Thioredoxin domain-containing protein 5 OS=Homo sapiens GN=TXNDC5 PE=1 SV=2
MRPL11	RM11_HUMAN	37	20727	4 (1)	2 (1)	0.16	39S ribosomal protein L11, mitochondrial OS=Homo sapiens GN=MRPL11 PE=1 SV=1
ZC3H4	ZC3H4_HUMAN	37	140797	13 (1)	6 (1)	0.02	Zinc finger CCCH domain-containing protein 4 OS=Homo sapiens GN=ZC3H4 PE=1 SV=3
MCM4	MCM4_HUMAN	37	97068	10 (1)	5 (1)	0.03	DNA replication licensing factor MCM4 OS=Homo sapiens GN=MCM4 PE=1 SV=5
SCRIB	SCRIB_HUMAN	37	175748	11 (1)	9 (1)	0.02	Protein scribble homolog OS=Homo sapiens GN=SCRIB PE=1 SV=4
IGF2R	MPRI_HUMAN	37	281155	13 (2)	11 (2)	0.02	Cation-independent mannose-6-phosphate receptor OS=Homo sapiens GN=IGF2R PE=1 SV=3
RUFY1	RUFY1_HUMAN	37	80851	8 (2)	6 (2)	0.08	RUN and FYVE domain-containing protein 1 OS=Homo sapiens GN=RUFY1 PE=1 SV=2
SETD3	SETD3_HUMAN	37	67557	7 (1)	4 (1)	0.05	Histone-lysine N-methyltransferase setd3 OS=Homo sapiens GN=SETD3 PE=1 SV=1
ATL2	ATLA2_HUMAN	37	66814	3 (1)	3 (1)	0.05	Atlastin-2 OS=Homo sapiens GN=ATL2 PE=1 SV=2
PRKAG1	AAKG1_HUMAN	37	37727	3 (1)	1 (1)	0.09	5'-AMP-activated protein kinase subunit gamma-1 OS=Homo sapiens GN=PRKAG1 PE=1 SV=1
NOMO3	NOMO3_HUMAN	37	135019	8 (1)	7 (1)	0.02	Nodal modulator 3 OS=Homo sapiens GN=NOMO3 PE=3 SV=2
EPB41	41_HUMAN	37	97528	3 (1)	3 (1)	0.03	Protein 4.1 OS=Homo sapiens GN=EPB41 PE=1 SV=4
SIAE	SIAE_HUMAN	37	58961	3 (1)	3 (1)	0.06	Sialate O-acetylesterase OS=Homo sapiens GN=SIAE PE=1 SV=1
NAXE	NNRE_HUMAN	36	31996	4 (3)	1 (1)	0.1	NAD(P)H-hydrate epimerase OS=Homo sapiens GN=NAXE PE=1 SV=2
WIPF2	WIPF2_HUMAN	36	46317	2 (1)	2 (1)	0.07	WAS/WASL-interacting protein family member 2 OS=Homo sapiens GN=WIPF2 PE=1 SV=1
MAP2K2	MP2K2_HUMAN	36	44681	2 (1)	1 (1)	0.07	Dual specificity mitogen-activated protein kinase kinase 2 OS=Homo sapiens GN=MAP2K2 PE=1 SV=1
XRCC1	XRCC1_HUMAN	36	69776	3 (1)	3 (1)	0.05	DNA repair protein XRCC1 OS=Homo sapiens GN=XRCC1 PE=1 SV=2
GOLGA4	GOGA4_HUMAN	36	261892	34 (1)	29 (1)	0.01	Golgin subfamily A member 4 OS=Homo sapiens GN=GOLGA4 PE=1 SV=1
KIF15	KIF15_HUMAN	36	161030	19 (1)	16 (1)	0.02	Kinesin-like protein KIF15 OS=Homo sapiens GN=KIF15 PE=1 SV=1
ORMDL1	ORML1_HUMAN	36	17360	2 (1)	2 (1)	0.2	ORM1-like protein 1 OS=Homo sapiens GN=ORMDL1 PE=1 SV=1
BIN2	BIN2_HUMAN	36	62008	7 (1)	5 (1)	0.05	Bridging integrator 2 OS=Homo sapiens GN=BIN2 PE=1 SV=3
SPCS3	SPCS3_HUMAN	36	20358	1 (1)	1 (1)	0.17	Signal peptidase complex subunit 3 OS=Homo sapiens GN=SPCS3 PE=1 SV=1

CC2D1A	C2D1A_HUMAN	36	104397	11 (1)	6 (1)	0.03	Coiled-coil and C2 domain-containing protein 1A OS=Homo sapiens GN=CC2D1A PE=1 SV=1
CNOT9	CNOT9_HUMAN	35	33952	4 (1)	3 (1)	0.1	CCR4-NOT transcription complex subunit 9 OS=Homo sapiens GN=CNOT9 PE=1 SV=1
TRIP10	CIP4_HUMAN	35	68538	4 (1)	3 (1)	0.05	Cdc42-interacting protein 4 OS=Homo sapiens GN=TRIP10 PE=1 SV=3
TSHZ3	TSH3_HUMAN	35	119518	24 (4)	8 (1)	0.03	Teashirt homolog 3 OS=Homo sapiens GN=TSHZ3 PE=1 SV=2
CORO1B	COR1B_HUMAN	35	54885	10 (1)	4 (1)	0.06	Coronin-1B OS=Homo sapiens GN=CORO1B PE=1 SV=1
SMC4	SMC4_HUMAN	35	147775	11 (2)	10 (2)	0.04	Structural maintenance of chromosomes protein 4 OS=Homo sapiens GN=SMC4 PE=1 SV=2
RPL26L1	RL26L_HUMAN	35	17246	1 (1)	1 (1)	0.2	60S ribosomal protein L26-like 1 OS=Homo sapiens GN=RPL26L1 PE=1 SV=1
MPST	THTM_HUMAN	35	33443	5 (1)	3 (1)	0.1	3-mercaptopyruvate sulfurtransferase OS=Homo sapiens GN=MPST PE=1 SV=3
SARNP	SARNP_HUMAN	35	23713	5 (1)	4 (1)	0.14	SAP domain-containing ribonucleoprotein OS=Homo sapiens GN=SARNP PE=1 SV=3
TRIP12	TRIPC_HUMAN	35	222234	12 (1)	10 (1)	0.01	E3 ubiquitin-protein ligase TRIP12 OS=Homo sapiens GN=TRIP12 PE=1 SV=1
ITSN2	ITSN2_HUMAN	34	194423	16 (1)	16 (1)	0.02	Intersectin-2 OS=Homo sapiens GN=ITSN2 PE=1 SV=3
ACACB	ACACB_HUMAN	34	278361	12 (1)	9 (1)	0.01	Acetyl-CoA carboxylase 2 OS=Homo sapiens GN=ACACB PE=1 SV=3
ST13P5	F10A5_HUMAN	34	41579	4 (1)	4 (1)	0.08	Putative protein FAM10A5 OS=Homo sapiens GN=ST13P5 PE=5 SV=1
KLC4	KLC4_HUMAN	34	69054	7 (1)	6 (1)	0.05	Kinesin light chain 4 OS=Homo sapiens GN=KLC4 PE=1 SV=3
TTLL12	TTL12_HUMAN	34	75154	2 (1)	2 (1)	0.04	Tubulin--tyrosine ligase-like protein 12 OS=Homo sapiens GN=TTLL12 PE=1 SV=2
DHFR	DYR_HUMAN	34	21496	10 (1)	7 (1)	0.16	Dihydrofolate reductase OS=Homo sapiens GN=DHFR PE=1 SV=2
KIAA1211	K1211_HUMAN	34	137248	22 (1)	14 (1)	0.02	Uncharacterized protein KIAA1211 OS=Homo sapiens GN=KIAA1211 PE=1 SV=3
UPF1	RENT1_HUMAN	34	125578	4 (2)	3 (2)	0.05	Regulator of nonsense transcripts 1 OS=Homo sapiens GN=UPF1 PE=1 SV=2
RTF1	RTF1_HUMAN	34	80493	15 (1)	8 (1)	0.04	RNA polymerase-associated protein RTF1 homolog OS=Homo sapiens GN=RTF1 PE=1 SV=4
ASL	ARLY_HUMAN	34	51910	3 (1)	3 (1)	0.06	Argininosuccinate lyase OS=Homo sapiens GN=ASL PE=1 SV=4
FAM91A1	F91A1_HUMAN	34	94648	4 (1)	3 (1)	0.03	Protein FAM91A1 OS=Homo sapiens GN=FAM91A1 PE=1 SV=3
TPD52L1	TPD53_HUMAN	34	22492	3 (1)	3 (1)	0.15	Tumor protein D53 OS=Homo sapiens GN=TPD52L1 PE=1 SV=1
AHSA1	AHSA1_HUMAN	33	38421	3 (1)	2 (1)	0.09	Activator of 90 kDa heat shock protein ATPase homolog 1 OS=Homo sapiens GN=AHSA1 PE=1 SV=1
PFAS	PUR4_HUMAN	33	146297	10 (1)	4 (1)	0.02	Phosphoribosylformylglycinamidine synthase OS=Homo sapiens GN=PFAS PE=1 SV=4
CYP4F2	CP4F2_HUMAN	33	60442	5 (2)	3 (1)	0.05	Phylloquinone omega-hydroxylase CYP4F2 OS=Homo sapiens GN=CYP4F2 PE=1 SV=1
DDX39B	DX39B_HUMAN	33	49416	7 (1)	6 (1)	0.07	Spliceosome RNA helicase DDX39B OS=Homo sapiens GN=DDX39B PE=1 SV=1
GSTA1	GSTA1_HUMAN	33	25672	3 (1)	2 (1)	0.13	Glutathione S-transferase A1 OS=Homo sapiens GN=GSTA1 PE=1 SV=3
PPP4R3A	P4R3A_HUMAN	33	95935	5 (1)	5 (1)	0.03	Serine/threonine-protein phosphatase 4 regulatory subunit 3A OS=Homo sapiens GN=PPP4R3A PE=1 SV=1
RPL7	RL7_HUMAN	33	29264	7 (1)	5 (1)	0.11	60S ribosomal protein L7 OS=Homo sapiens GN=RPL7 PE=1 SV=1
HIP1	HIP1_HUMAN	33	117232	7 (1)	7 (1)	0.03	Huntingtin-interacting protein 1 OS=Homo sapiens GN=HIP1 PE=1 SV=5
NAPG	SNAG_HUMAN	33	35066	2 (1)	2 (1)	0.09	Gamma-soluble NSF attachment protein OS=Homo sapiens GN=NAPG PE=1 SV=1
STOML2	STML2_HUMAN	33	38624	3 (1)	3 (1)	0.09	Stomatin-like protein 2, mitochondrial OS=Homo sapiens GN=STOML2 PE=1 SV=1
IDH3A	IDH3A_HUMAN	33	40022	4 (1)	4 (1)	0.08	Isocitrate dehydrogenase [NAD] subunit alpha, mitochondrial OS=Homo sapiens GN=IDH3A PE=1 SV=1
DNAJA2	DNJA2_HUMAN	33	46344	2 (1)	1 (1)	0.07	DnaJ homolog subfamily A member 2 OS=Homo sapiens GN=DNAJA2 PE=1 SV=1
CAMKV	CAMKV_HUMAN	33	54662	6 (4)	2 (1)	0.06	CaM kinase-like vesicle-associated protein OS=Homo sapiens GN=CAMKV PE=2 SV=2
OCRL	OCRL_HUMAN	33	105392	19 (1)	6 (1)	0.03	Inositol polyphosphate 5-phosphatase OCRL-1 OS=Homo sapiens GN=OCRL PE=1 SV=3
XPO5	XPO5_HUMAN	33	138332	4 (1)	4 (1)	0.02	Exportin-5 OS=Homo sapiens GN=XPO5 PE=1 SV=1
SNX9	SNX9_HUMAN	33	66949	3 (1)	3 (1)	0.05	Sorting nexin-9 OS=Homo sapiens GN=SNX9 PE=1 SV=1
UBE2V2	UB2V2_HUMAN	32	16409	10 (2)	3 (1)	0.21	Ubiquitin-conjugating enzyme E2 variant 2 OS=Homo sapiens GN=UBE2V2 PE=1 SV=4
S100A2	S10A2_HUMAN	32	11337	1 (1)	1 (1)	0.3	Protein S100-A2 OS=Homo sapiens GN=S100A2 PE=1 SV=3

DDAH2	DDAH2_HUMAN	32	29911	2 (1)	2 (1)	0.11	N(G),N(G)-dimethylarginine dimethylaminohydrolase 2 OS=Homo sapiens GN=DDAH2 PE=1 SV=1
GBP2	GBP2_HUMAN	32	67680	13 (1)	7 (1)	0.05	Guanylate-binding protein 2 OS=Homo sapiens GN=GBP2 PE=1 SV=3
DGCR8	DGCR8_HUMAN	32	86789	4 (1)	4 (1)	0.04	Microprocessor complex subunit DGCR8 OS=Homo sapiens GN=DGCR8 PE=1 SV=1
ATP2C1	AT2C1_HUMAN	32	101653	6 (1)	4 (1)	0.03	Calcium-transporting ATPase type 2C member 1 OS=Homo sapiens GN=ATP2C1 PE=1 SV=3
PGRMC1	PGRC1_HUMAN	32	21772	1 (1)	1 (1)	0.15	Membrane-associated progesterone receptor component 1 OS=Homo sapiens GN=PGRMC1 PE=1 SV=3
FNTA	FNTA_HUMAN	32	44495	4 (1)	3 (1)	0.07	Protein farnesyltransferase/geranylgeranyltransferase type-1 subunit alpha OS=Homo sapiens GN=FNTA PE=1 SV=1
AK3	KAD3_HUMAN	32	25550	6 (1)	3 (1)	0.13	GTP:AMP phosphotransferase AK3, mitochondrial OS=Homo sapiens GN=AK3 PE=1 SV=4
HIP1R	HIP1R_HUMAN	31	119999	12 (1)	11 (1)	0.03	Huntingtin-interacting protein 1-related protein OS=Homo sapiens GN=HIP1R PE=1 SV=2
ATP6V0A1	VPP1_HUMAN	31	97148	6 (1)	5 (1)	0.03	V-type proton ATPase 116 kDa subunit a isoform 1 OS=Homo sapiens GN=ATP6V0A1 PE=1 SV=3
AFDN	AFAD_HUMAN	31	207702	17 (1)	14 (1)	0.02	Afadin OS=Homo sapiens GN=AFDN PE=1 SV=3
NUP50	NUP50_HUMAN	31	50512	5 (1)	3 (1)	0.07	Nuclear pore complex protein Nup50 OS=Homo sapiens GN=NUP50 PE=1 SV=2
TCOF1	TCOF_HUMAN	31	152243	15 (1)	11 (1)	0.02	Treacle protein OS=Homo sapiens GN=TCOF1 PE=1 SV=3
GFM1	EFGM_HUMAN	31	84103	12 (1)	11 (1)	0.04	Elongation factor G, mitochondrial OS=Homo sapiens GN=GFM1 PE=1 SV=2
WDR82	WDR82_HUMAN	31	35456	1 (1)	1 (1)	0.09	WD repeat-containing protein 82 OS=Homo sapiens GN=WDR82 PE=1 SV=1
NHLRC2	NHLC2_HUMAN	31	80249	3 (1)	3 (1)	0.04	NHL repeat-containing protein 2 OS=Homo sapiens GN=NHLRC2 PE=1 SV=1
ANKHD1	ANKH1_HUMAN	31	271286	13 (1)	9 (1)	0.01	Ankyrin repeat and KH domain-containing protein 1 OS=Homo sapiens GN=ANKHD1 PE=1 SV=1
SLC35B2	S35B2_HUMAN	31	48054	6 (1)	2 (1)	0.07	Adenosine 3'-phospho 5'-phosphosulfate transporter 1 OS=Homo sapiens GN=SLC35B2 PE=1 SV=1
NUP62	NUP62_HUMAN	31	53394	2 (1)	2 (1)	0.06	Nuclear pore glycoprotein p62 OS=Homo sapiens GN=NUP62 PE=1 SV=3
GM2A	SAP3_HUMAN	31	21281	1 (1)	1 (1)	0.16	Ganglioside GM2 activator OS=Homo sapiens GN=GM2A PE=1 SV=4
ERAP1	ERAP1_HUMAN	31	107736	8 (1)	5 (1)	0.03	Endoplasmic reticulum aminopeptidase 1 OS=Homo sapiens GN=ERAP1 PE=1 SV=3
CUL2	CUL2_HUMAN	31	87554	2 (1)	2 (1)	0.04	Cullin-2 OS=Homo sapiens GN=CUL2 PE=1 SV=2
HSD17B12	DHB12_HUMAN	31	34416	4 (1)	3 (1)	0.1	Very-long-chain 3-oxoacyl-CoA reductase OS=Homo sapiens GN=HSD17B12 PE=1 SV=2
FIS1	FIS1_HUMAN	31	16984	3 (1)	2 (1)	0.2	Mitochondrial fission 1 protein OS=Homo sapiens GN=FIS1 PE=1 SV=2
PCCB	PCCB_HUMAN	30	58806	3 (1)	3 (1)	0.06	Propionyl-CoA carboxylase beta chain, mitochondrial OS=Homo sapiens GN=PCCB PE=1 SV=3
OTULIN	OTUL_HUMAN	30	40636	5 (1)	5 (1)	0.08	Ubiquitin thioesterase otulin OS=Homo sapiens GN=OTULIN PE=1 SV=3
CD59	CD59_HUMAN	30	14795	1 (1)	1 (1)	0.23	CD59 glycoprotein OS=Homo sapiens GN=CD59 PE=1 SV=1
IMPAD1	IMPA3_HUMAN	30	38828	1 (1)	1 (1)	0.09	Inositol monophosphatase 3 OS=Homo sapiens GN=IMPAD1 PE=1 SV=1
ABR	ABR_HUMAN	30	98106	8 (1)	5 (1)	0.03	Active breakpoint cluster region-related protein OS=Homo sapiens GN=ABR PE=2 SV=2
TLN2	TLN2_HUMAN	30	273781	30 (2)	21 (2)	0.02	Talin-2 OS=Homo sapiens GN=TLN2 PE=1 SV=4
DTYMK	KTHY_HUMAN	30	23976	2 (1)	2 (1)	0.14	Thymidylate kinase OS=Homo sapiens GN=DTYMK PE=1 SV=4
ZMYND10	ZMY10_HUMAN	30	51167	6 (1)	2 (1)	0.06	Zinc finger MYND domain-containing protein 10 OS=Homo sapiens GN=ZMYND10 PE=1 SV=2
PLXNB2	PLXB2_HUMAN	30	207734	17 (1)	12 (1)	0.02	Plexin-B2 OS=Homo sapiens GN=PLXNB2 PE=1 SV=3
MGST3	MGST3_HUMAN	30	16734	1 (1)	1 (1)	0.2	Microsomal glutathione S-transferase 3 OS=Homo sapiens GN=MGST3 PE=1 SV=1
ABCC2	MRP2_HUMAN	30	175237	11 (1)	11 (1)	0.02	Canalicular multispecific organic anion transporter 1 OS=Homo sapiens GN=ABCC2 PE=1 SV=3
LOC642696	YP010_HUMAN	30	21022	7 (1)	4 (1)	0.16	Putative uncharacterized protein FLJ32790 OS=Homo sapiens PE=2 SV=2
LIMCH1	LIMC1_HUMAN	30	122818	13 (1)	10 (1)	0.03	LIM and calponin homology domains-containing protein 1 OS=Homo sapiens GN=LIMCH1 PE=1 SV=4
PHLDB2	PHLB2_HUMAN	29	142812	17 (1)	12 (1)	0.02	Pleckstrin homology-like domain family B member 2 OS=Homo sapiens GN=PHLDB2 PE=1 SV=2
SMAD1	SMAD1_HUMAN	29	53025	4 (1)	2 (1)	0.06	Mothers against decapentaplegic homolog 1 OS=Homo sapiens GN=SMAD1 PE=1 SV=1
PODN	PODN_HUMAN	29	69162	4 (1)	2 (1)	0.05	Podocan OS=Homo sapiens GN=PODN PE=1 SV=2
ARHGEF2	ARHG2_HUMAN	29	112386	8 (1)	7 (1)	0.03	Rho guanine nucleotide exchange factor 2 OS=Homo sapiens GN=ARHGEF2 PE=1 SV=4

CCNK	CCNK_HUMAN	29	64598	1 (1)	1 (1)	0.05	Cyclin-K OS=Homo sapiens GN=CCNK PE=1 SV=2
BCL9L	BCL9L_HUMAN	29	157427	7 (1)	5 (1)	0.02	B-cell CLL/lymphoma 9-like protein OS=Homo sapiens GN=BCL9L PE=1 SV=1
ZC3H14	ZC3HE_HUMAN	29	83793	8 (1)	3 (1)	0.04	Zinc finger CCCH domain-containing protein 14 OS=Homo sapiens GN=ZC3H14 PE=1 SV=1
RGPD2	RGPD2_HUMAN	29	198667	16 (1)	13 (1)	0.02	RANBP2-like and GRIP domain-containing protein 2 OS=Homo sapiens GN=RGPD2 PE=2 SV=1
IFI16	IF16_HUMAN	29	88656	7 (1)	5 (1)	0.04	Gamma-interferon-inducible protein 16 OS=Homo sapiens GN=IFI16 PE=1 SV=3
EMC8	EMC8_HUMAN	29	24214	1 (1)	1 (1)	0.14	ER membrane protein complex subunit 8 OS=Homo sapiens GN=EMC8 PE=1 SV=1
SMC3	SMC3_HUMAN	29	141853	16 (1)	12 (1)	0.02	Structural maintenance of chromosomes protein 3 OS=Homo sapiens GN=SMC3 PE=1 SV=2
YES1	YES_HUMAN	29	61276	3 (1)	3 (1)	0.05	Tyrosine-protein kinase Yes OS=Homo sapiens GN=YES1 PE=1 SV=3
RSAD1	RSAD1_HUMAN	29	49139	4 (1)	3 (1)	0.07	Radical S-adenosyl methionine domain-containing protein 1, mitochondrial OS=Homo sapiens GN=RSAD1 PE=2 SV=2
CLIC3	CLIC3_HUMAN	29	26917	1 (1)	1 (1)	0.12	Chloride intracellular channel protein 3 OS=Homo sapiens GN=CLIC3 PE=1 SV=2
CAMSAP3	CAMP3_HUMAN	28	135464	11 (1)	8 (1)	0.02	Calmodulin-regulated spectrin-associated protein 3 OS=Homo sapiens GN=CAMSAP3 PE=1 SV=2
OBSCN	OBSCN_HUMAN	28	879630	52 (4)	34 (1)		Obscurin OS=Homo sapiens GN=OBSCN PE=1 SV=3
GULP1	GULP1_HUMAN	28	34925	3 (1)	3 (1)	0.09	PTB domain-containing engulfment adapter protein 1 OS=Homo sapiens GN=GULP1 PE=1 SV=1
PMPCB	MPPB_HUMAN	28	55073	2 (1)	2 (1)	0.06	Mitochondrial-processing peptidase subunit beta OS=Homo sapiens GN=PMPCB PE=1 SV=2
ZNFX1	ZNFX1_HUMAN	28	225102	19 (1)	10 (1)	0.01	NFX1-type zinc finger-containing protein 1 OS=Homo sapiens GN=ZNFX1 PE=2 SV=2
SLIRP	SLIRP_HUMAN	28	12398	1 (1)	1 (1)	0.28	SRA stem-loop-interacting RNA-binding protein, mitochondrial OS=Homo sapiens GN=SLIRP PE=1 SV=1
LMAN2	LMAN2_HUMAN	28	40545	2 (1)	2 (1)	0.08	Vesicular integral-membrane protein VIP36 OS=Homo sapiens GN=LMAN2 PE=1 SV=1
DHCR7	DHCR7_HUMAN	28	55195	1 (1)	1 (1)	0.06	7-dehydrocholesterol reductase OS=Homo sapiens GN=DHCR7 PE=1 SV=1
SHMT1	GLYC_HUMAN	28	53619	3 (1)	3 (1)	0.06	Serine hydroxymethyltransferase, cytosolic OS=Homo sapiens GN=SHMT1 PE=1 SV=1
MPHOSPH10	MPP10_HUMAN	28	78930	13 (1)	7 (1)	0.04	U3 small nucleolar ribonucleoprotein protein MPP10 OS=Homo sapiens GN=MPHOSPH10 PE=1 SV=2
TTC9	TTC9A_HUMAN	28	24706	3 (1)	3 (1)	0.14	Tetratricopeptide repeat protein 9A OS=Homo sapiens GN=TTC9 PE=1 SV=3
TPST2	TPST2_HUMAN	28	42284	4 (2)	2 (1)	0.08	Protein-tyrosine sulfotransferase 2 OS=Homo sapiens GN=TPST2 PE=1 SV=1
HCFC1	HCFC1_HUMAN	28	210598	18 (1)	9 (1)	0.02	Host cell factor 1 OS=Homo sapiens GN=HCFC1 PE=1 SV=2
ACYP2	ACYP2_HUMAN	28	11190	4 (1)	1 (1)	0.31	Acylphosphatase-2 OS=Homo sapiens GN=ACYP2 PE=1 SV=2
RAB27B	RB27B_HUMAN	28	24820	1 (1)	1 (1)	0.13	Ras-related protein Rab-27B OS=Homo sapiens GN=RAB27B PE=1 SV=4
TSG101	TS101_HUMAN	28	44088	14 (1)	5 (1)	0.07	Tumor susceptibility gene 101 protein OS=Homo sapiens GN=TSG101 PE=1 SV=2
RETREG3	RETR3_HUMAN	28	51763	5 (1)	2 (1)	0.06	Reticulophagy regulator 3 OS=Homo sapiens GN=RETREG3 PE=1 SV=1
DHRS7	DHRS7_HUMAN	27	38673	4 (1)	4 (1)	0.09	Dehydrogenase/reductase SDR family member 7 OS=Homo sapiens GN=DHRS7 PE=1 SV=1
CMPK1	KCY_HUMAN	27	22436	4 (1)	4 (1)	0.15	UMP-CMP kinase OS=Homo sapiens GN=CMPK1 PE=1 SV=3
CD99	CD99_HUMAN	27	18893	3 (1)	1 (1)	0.18	CD99 antigen OS=Homo sapiens GN=CD99 PE=1 SV=1
SPNS1	SPNS1_HUMAN	27	57050	2 (1)	2 (1)	0.06	Protein spinster homolog 1 OS=Homo sapiens GN=SPNS1 PE=1 SV=1
CLNK	CLNK_HUMAN	27	49808	4 (1)	3 (1)	0.07	Cytokine-dependent hematopoietic cell linker OS=Homo sapiens GN=CLNK PE=1 SV=2
ACTR1A	ACTZ_HUMAN	27	42701	6 (3)	3 (3)	0.25	Alpha-centractin OS=Homo sapiens GN=ACTR1A PE=1 SV=1
IPO5	IPO5_HUMAN	27	125032	6 (1)	4 (1)	0.03	Importin-5 OS=Homo sapiens GN=IPO5 PE=1 SV=4
BROX	BROX_HUMAN	27	46960	2 (1)	2 (1)	0.07	BRO1 domain-containing protein BROX OS=Homo sapiens GN=BROX PE=1 SV=1
MGAT1	MGAT1_HUMAN	27	51132	3 (1)	2 (1)	0.06	Alpha-1,3-mannosyl-glycoprotein 2-beta-N-acetylglucosaminyltransferase OS=Homo sapiens GN=MGAT1 PE=1 SV=2
XPO1	XPO1_HUMAN	27	124447	2 (1)	2 (1)	0.03	Exportin-1 OS=Homo sapiens GN=XPO1 PE=1 SV=1
SEC23IP	S23IP_HUMAN	27	111691	9 (1)	7 (1)	0.03	SEC23-interacting protein OS=Homo sapiens GN=SEC23IP PE=1 SV=1
FAM50A	FA50A_HUMAN	27	40216	9 (1)	6 (1)	0.08	Protein FAM50A OS=Homo sapiens GN=FAM50A PE=1 SV=2

TLE3	TLE3_HUMAN	27	84162	5 (1)	2 (1)	0.04	Transducin-like enhancer protein 3 OS=Homo sapiens GN=TLE3 PE=1 SV=2
CNGB1	CNGB1_HUMAN	27	140502	12 (1)	6 (1)	0.02	Cyclic nucleotide-gated cation channel beta-1 OS=Homo sapiens GN=CNGB1 PE=1 SV=2
CCDC33	CCD33_HUMAN	27	107548	5 (1)	5 (1)	0.03	Coiled-coil domain-containing protein 33 OS=Homo sapiens GN=CCDC33 PE=1 SV=3
TMUB1	TMUB1_HUMAN	27	26530	1 (1)	1 (1)	0.13	Transmembrane and ubiquitin-like domain-containing protein 1 OS=Homo sapiens GN=TMUB1 PE=1 SV=1
POLDIP2	PDIP2_HUMAN	26	42235	3 (1)	3 (1)	0.08	Polymerase delta-interacting protein 2 OS=Homo sapiens GN=POLDIP2 PE=1 SV=1
CHUK	IKKA_HUMAN	26	85725	6 (1)	6 (1)	0.04	Inhibitor of nuclear factor kappa-B kinase subunit alpha OS=Homo sapiens GN=CHUK PE=1 SV=2
RRN3P2	RN3P2_HUMAN	26	38352	1 (1)	1 (1)	0.09	Putative RRN3-like protein RRN3P2 OS=Homo sapiens GN=RRN3P2 PE=5 SV=3
HUS1B	HUS1B_HUMAN	26	31305	10 (1)	3 (1)	0.11	Checkpoint protein HUS1B OS=Homo sapiens GN=HUS1B PE=1 SV=2
XPNPEP1	XPP1_HUMAN	26	70558	3 (1)	3 (1)	0.05	Xaa-Pro aminopeptidase 1 OS=Homo sapiens GN=XPNPEP1 PE=1 SV=3
PPIE	PPIE_HUMAN	26	33695	4 (1)	4 (1)	0.1	Peptidyl-prolyl cis-trans isomerase E OS=Homo sapiens GN=PPIE PE=1 SV=1
CUL3	CUL3_HUMAN	26	89444	13 (1)	6 (1)	0.04	Cullin-3 OS=Homo sapiens GN=CUL3 PE=1 SV=2
TMEM41B	TM41B_HUMAN	26	32663	4 (1)	4 (1)	0.1	Transmembrane protein 41B OS=Homo sapiens GN=TMEM41B PE=1 SV=1
TMF1	TMF1_HUMAN	26	123280	13 (1)	10 (1)	0.03	TATA element modulatory factor OS=Homo sapiens GN=TMF1 PE=1 SV=2
NDUFS4	NDUS4_HUMAN	26	20095	3 (1)	3 (1)	0.17	NADH dehydrogenase [ubiquinone] iron-sulfur protein 4, mitochondrial OS=Homo sapiens GN=NDUFS4 PE=1 SV=1
PDCD10	PDC10_HUMAN	26	24686	2 (1)	2 (1)	0.14	Programmed cell death protein 10 OS=Homo sapiens GN=PDCD10 PE=1 SV=1
FN3KRP	KT3K_HUMAN	26	34618	7 (1)	6 (1)	0.1	Ketosamine-3-kinase OS=Homo sapiens GN=FN3KRP PE=1 SV=2
UBXN7	UBXN7_HUMAN	26	55227	4 (1)	4 (1)	0.06	UBX domain-containing protein 7 OS=Homo sapiens GN=UBXN7 PE=1 SV=2
VPS45	VPS45_HUMAN	26	65435	13 (1)	5 (1)	0.05	Vacuolar protein sorting-associated protein 45 OS=Homo sapiens GN=VPS45 PE=1 SV=1
VAPB	VAPB_HUMAN	25	27439	3 (1)	3 (1)	0.12	Vesicle-associated membrane protein-associated protein B/C OS=Homo sapiens GN=VAPB PE=1 SV=3
ASPM	ASPM_HUMAN	25	413189	26 (2)	23 (2)	0.02	Abnormal spindle-like microcephaly-associated protein OS=Homo sapiens GN=ASPM PE=1 SV=2
CLTB	CLCB_HUMAN	25	25289	3 (1)	2 (1)	0.13	Clathrin light chain B OS=Homo sapiens GN=CLTB PE=1 SV=1
GRAMD1A	GRM1A_HUMAN	25	81314	6 (1)	6 (1)	0.04	GRAM domain-containing protein 1A OS=Homo sapiens GN=GRAMD1A PE=1 SV=2
RTN1	RTN1_HUMAN	25	83851	16 (2)	3 (2)	0.08	Reticulon-1 OS=Homo sapiens GN=RTN1 PE=1 SV=1
ACOX1	ACOX1_HUMAN	25	74889	3 (1)	2 (1)	0.04	Peroxisomal acyl-coenzyme A oxidase 1 OS=Homo sapiens GN=ACOX1 PE=1 SV=3
UBXN1	UBXN1_HUMAN	25	33419	5 (1)	4 (1)	0.1	UBX domain-containing protein 1 OS=Homo sapiens GN=UBXN1 PE=1 SV=2
NPAS1	NPAS1_HUMAN	25	63005	4 (1)	3 (1)	0.05	Neuronal PAS domain-containing protein 1 OS=Homo sapiens GN=NPAS1 PE=2 SV=2
FOXO3	FOXO3_HUMAN	25	71517	8 (1)	4 (1)	0.05	Forkhead box protein O3 OS=Homo sapiens GN=FOXO3 PE=1 SV=1
C14orf166	CN166_HUMAN	25	28165	5 (1)	3 (1)	0.12	UPF0568 protein C14orf166 OS=Homo sapiens GN=C14orf166 PE=1 SV=1
SVIL	SVIL_HUMAN	25	249417	16 (1)	14 (1)	0.01	Supervillin OS=Homo sapiens GN=SVIL PE=1 SV=2
PPIL3	PPIL3_HUMAN	25	18371	4 (1)	3 (1)	0.18	Peptidyl-prolyl cis-trans isomerase-like 3 OS=Homo sapiens GN=PPIL3 PE=1 SV=1
NEDD8	NEDD8_HUMAN	25	9066	4 (1)	3 (1)	0.38	NEDD8 OS=Homo sapiens GN=NEDD8 PE=1 SV=1
ZCCHC6	TUT7_HUMAN	25	173288	13 (1)	9 (1)	0.02	Terminal uridylyltransferase 7 OS=Homo sapiens GN=ZCCHC6 PE=1 SV=1
NFE2	NFE2_HUMAN	25	41675	3 (1)	3 (1)	0.08	Transcription factor NF-E2 45 kDa subunit OS=Homo sapiens GN=NFE2 PE=1 SV=1
KIF2A	KIF2A_HUMAN	25	80589	4 (1)	4 (1)	0.04	Kinesin-like protein KIF2A OS=Homo sapiens GN=KIF2A PE=1 SV=3
ZC3H13	ZC3HD_HUMAN	25	197203	29 (1)	17 (1)	0.02	Zinc finger CCCH domain-containing protein 13 OS=Homo sapiens GN=ZC3H13 PE=1 SV=1
LCMT1	LCMT1_HUMAN	25	39152	10 (1)	5 (1)	0.08	Leucine carboxyl methyltransferase 1 OS=Homo sapiens GN=LCMT1 PE=1 SV=2
MEGF9	MEGF9_HUMAN	24	65338	2 (1)	1 (1)	0.05	Multiple epidermal growth factor-like domains protein 9 OS=Homo sapiens GN=MEGF9 PE=2 SV=3
PPFIBP1	LIPB1_HUMAN	24	114523	12 (1)	7 (1)	0.03	Liprin-beta-1 OS=Homo sapiens GN=PPFIBP1 PE=1 SV=2
OSBPL7	OSBL7_HUMAN	24	96398	10 (1)	6 (1)	0.03	Oxysterol-binding protein-related protein 7 OS=Homo sapiens GN=OSBPL7 PE=1 SV=1

CETN2	CETN2_HUMAN	24	19726	7 (1)	5 (1)	0.17	Centrin-2 OS=Homo sapiens GN=CETN2 PE=1 SV=1
COL4A3BP	C43BP_HUMAN	24	71475	2 (1)	2 (1)	0.05	Collagen type IV alpha-3-binding protein OS=Homo sapiens GN=COL4A3BP PE=1 SV=1
KDELC2	KDEL2_HUMAN	24	58934	3 (1)	3 (1)	0.06	KDEL motif-containing protein 2 OS=Homo sapiens GN=KDELC2 PE=1 SV=2
MAPK1	MK01_HUMAN	24	41762	2 (1)	2 (1)	0.08	Mitogen-activated protein kinase 1 OS=Homo sapiens GN=MAPK1 PE=1 SV=3
IWS1	IWS1_HUMAN	24	91956	11 (1)	5 (1)	0.04	Protein IWS1 homolog OS=Homo sapiens GN=IWS1 PE=1 SV=2
RUFY3	RUFY3_HUMAN	24	53216	4 (1)	4 (1)	0.06	Protein RUFY3 OS=Homo sapiens GN=RUFY3 PE=1 SV=1
TRIM72	TRI72_HUMAN	24	53609	4 (1)	4 (1)	0.06	Tripartite motif-containing protein 72 OS=Homo sapiens GN=TRIM72 PE=1 SV=2
PPP2R2D	2ABD_HUMAN	24	52580	11 (1)	8 (1)	0.06	Serine/threonine-protein phosphatase 2A 55 kDa regulatory subunit B delta isoform OS=Homo sapiens GN=PPP2R2D PE=1 SV=1
HEXA	HEXA_HUMAN	23	61120	2 (1)	1 (1)	0.05	Beta-hexosaminidase subunit alpha OS=Homo sapiens GN=HEXA PE=1 SV=2
TEP1	TEP1_HUMAN	23	293500	17 (1)	12 (1)	0.01	Telomerase protein component 1 OS=Homo sapiens GN=TEP1 PE=1 SV=2
FXR1	FXR1_HUMAN	23	70020	7 (1)	5 (1)	0.05	Fragile X mental retardation syndrome-related protein 1 OS=Homo sapiens GN=FXR1 PE=1 SV=3
MUT	MUTA_HUMAN	23	83538	5 (1)	5 (1)	0.04	Methylmalonyl-CoA mutase, mitochondrial OS=Homo sapiens GN=MUT PE=1 SV=4
MTAP	MTAP_HUMAN	23	31729	4 (1)	4 (1)	0.1	S-methyl-5'-thioadenosine phosphorylase OS=Homo sapiens GN=MTAP PE=1 SV=2
CYP51A1	CP51A_HUMAN	23	57169	3 (1)	3 (1)	0.06	Lanosterol 14-alpha demethylase OS=Homo sapiens GN=CYP51A1 PE=1 SV=3
SORD	DHSO_HUMAN	23	38927	1 (1)	1 (1)	0.08	Sorbitol dehydrogenase OS=Homo sapiens GN=SORD PE=1 SV=4
MCTS1	MCTS1_HUMAN	23	20770	5 (1)	2 (1)	0.16	Malignant T-cell-amplified sequence 1 OS=Homo sapiens GN=MCTS1 PE=1 SV=1
PABPN1	PABP2_HUMAN	23	32843	3 (1)	3 (1)	0.1	Polyadenylate-binding protein 2 OS=Homo sapiens GN=PABPN1 PE=1 SV=3
SCFD1	SCFD1_HUMAN	23	72676	3 (1)	3 (1)	0.05	Sec1 family domain-containing protein 1 OS=Homo sapiens GN=SCFD1 PE=1 SV=4
PUF60	PUF60_HUMAN	23	60009	5 (1)	5 (1)	0.05	Poly(U)-binding-splicing factor PUF60 OS=Homo sapiens GN=PUF60 PE=1 SV=1
ADSS	PURA2_HUMAN	23	50465	12 (1)	9 (1)	0.07	Adenylosuccinate synthetase isozyme 2 OS=Homo sapiens GN=ADSS PE=1 SV=3
ILF3	ILF3_HUMAN	23	95678	6 (2)	3 (1)	0.03	Interleukin enhancer-binding factor 3 OS=Homo sapiens GN=ILF3 PE=1 SV=3
ABLIM1	ABLM1_HUMAN	22	89513	11 (1)	7 (1)	0.04	Actin-binding LIM protein 1 OS=Homo sapiens GN=ABLIM1 PE=1 SV=3
FBXO38	FBX38_HUMAN	22	135740	7 (1)	5 (1)	0.02	F-box only protein 38 OS=Homo sapiens GN=FBXO38 PE=1 SV=3
MATR3	MATR3_HUMAN	22	95078	4 (1)	4 (1)	0.03	Matrin-3 OS=Homo sapiens GN=MATR3 PE=1 SV=2
CHD4	CHD4_HUMAN	22	219407	29 (1)	15 (1)	0.01	Chromodomain-helicase-DNA-binding protein 4 OS=Homo sapiens GN=CHD4 PE=1 SV=2
TAF15	RBP56_HUMAN	22	62021	4 (1)	4 (1)	0.05	TATA-binding protein-associated factor 2N OS=Homo sapiens GN=TAF15 PE=1 SV=1
UBE2L3	UB2L3_HUMAN	22	18021	1 (1)	1 (1)	0.19	Ubiquitin-conjugating enzyme E2 L3 OS=Homo sapiens GN=UBE2L3 PE=1 SV=1
NPC2	NPC2_HUMAN	22	16902	2 (1)	1 (1)	0.2	Epididymal secretory protein E1 OS=Homo sapiens GN=NPC2 PE=1 SV=1
ALDH7A1	AL7A1_HUMAN	22	59020	5 (1)	4 (1)	0.06	Alpha-aminoadipic semialdehyde dehydrogenase OS=Homo sapiens GN=ALDH7A1 PE=1 SV=5
HMGB1	HMGB1_HUMAN	22	25049	4 (1)	3 (1)	0.13	High mobility group protein B1 OS=Homo sapiens GN=HMGB1 PE=1 SV=3
ARL6IP4	AR6P4_HUMAN	21	45287	10 (1)	2 (1)	0.07	ADP-ribosylation factor-like protein 6-interacting protein 4 OS=Homo sapiens GN=ARL6IP4 PE=1 SV=2
ITGA3	ITA3_HUMAN	21	117735	5 (1)	2 (1)	0.03	Integrin alpha-3 OS=Homo sapiens GN=ITGA3 PE=1 SV=5
LPCAT3	MBOA5_HUMAN	21	56511	2 (1)	2 (1)	0.06	Lysophospholipid acyltransferase 5 OS=Homo sapiens GN=LPCAT3 PE=1 SV=1
S100A10	S10AA_HUMAN	21	11310	2 (1)	1 (1)	0.3	Protein S100-A10 OS=Homo sapiens GN=S100A10 PE=1 SV=2
TTC28	TTC28_HUMAN	20	272653	11 (1)	7 (1)	0.01	Tetratricopeptide repeat protein 28 OS=Homo sapiens GN=TTC28 PE=1 SV=4
CNNM2	CNNM2_HUMAN	20	97531	14 (2)	9 (1)	0.03	Metal transporter CNNM2 OS=Homo sapiens GN=CNNM2 PE=1 SV=2
AP2M1	AP2M1_HUMAN	20	49965	4 (1)	4 (1)	0.07	AP-2 complex subunit mu OS=Homo sapiens GN=AP2M1 PE=1 SV=2
MESD	MESD_HUMAN	20	26231	3 (1)	3 (1)	0.13	LRP chaperone MESD OS=Homo sapiens GN=MESD PE=1 SV=2
ATP9B	ATP9B_HUMAN	20	130760	5 (1)	4 (1)	0.02	Probable phospholipid-transporting ATPase IIB OS=Homo sapiens GN=ATP9B PE=2 SV=4
TECRL	TECRL_HUMAN	20	42609	3 (1)	3 (1)	0.08	Trans-2,3-enoyl-CoA reductase-like OS=Homo sapiens GN=TECRL PE=1 SV=1
RPL3	RL3_HUMAN	20	46365	9 (1)	8 (1)	0.07	60S ribosomal protein L3 OS=Homo sapiens GN=RPL3 PE=1 SV=2

GOLGA6L6	GG6L6_HUMAN	20	91124	8 (1)	7 (1)	0.04	Golgin subfamily A member 6-like protein 6 OS=Homo sapiens GN=GOLGA6L6 PE=3 SV=4
CDC23	CDC23_HUMAN	20	69588	4 (1)	3 (1)	0.05	Cell division cycle protein 23 homolog OS=Homo sapiens GN=CDC23 PE=1 SV=3
PRSS42	PRS42_HUMAN	19	32613	5 (1)	4 (1)	0.1	Serine protease 42 OS=Homo sapiens GN=PRSS42 PE=1 SV=1
TTN	TITIN_HUMAN	19	3842904	243 (1)	152 (1)		Titin OS=Homo sapiens GN=TTN PE=1 SV=4
MICAL3	MICA3_HUMAN	19	225297	15 (1)	13 (1)	0.01	[F-actin]-monooxygenase MICAL3 OS=Homo sapiens GN=MICAL3 PE=1 SV=2
FREM3	FREM3_HUMAN	19	238943	17 (1)	6 (1)	0.01	FRAS1-related extracellular matrix protein 3 OS=Homo sapiens GN=FREM3 PE=3 SV=2
NSF	NSF_HUMAN	18	83055	7 (1)	6 (1)	0.04	Vesicle-fusing ATPase OS=Homo sapiens GN=NSF PE=1 SV=3
UBE4B	UBE4B_HUMAN	18	147460	13 (1)	6 (1)	0.02	Ubiquitin conjugation factor E4 B OS=Homo sapiens GN=UBE4B PE=1 SV=1
IMPACT	IMPCT_HUMAN	18	37023	1 (1)	1 (1)	0.09	Protein IMPACT OS=Homo sapiens GN=IMPACT PE=1 SV=2
SPAST	SPAST_HUMAN	18	67497	8 (1)	6 (1)	0.05	Spastin OS=Homo sapiens GN=SPAST PE=1 SV=1
COPS4	CSN4_HUMAN	17	46525	8 (1)	4 (1)	0.07	COP9 signalosome complex subunit 4 OS=Homo sapiens GN=COPS4 PE=1 SV=1
GPRIN3	GRIN3_HUMAN	17	83357	9 (1)	5 (1)	0.04	G protein-regulated inducer of neurite outgrowth 3 OS=Homo sapiens GN=GPRIN3 PE=2 SV=2
SESTD1	SESD1_HUMAN	17	80040	3 (1)	3 (1)	0.04	SEC14 domain and spectrin repeat-containing protein 1 OS=Homo sapiens GN=SESTD1 PE=1 SV=2
TASP1	TASP1_HUMAN	16	45225	5 (1)	2 (1)	0.07	Threonine aspartase 1 OS=Homo sapiens GN=TASP1 PE=1 SV=1
IKZF5	IKZF5_HUMAN	16	47393	10 (1)	2 (1)	0.07	Zinc finger protein Pegasus OS=Homo sapiens GN=IKZF5 PE=1 SV=1
CDC149	CC149_HUMAN	15	52992	10 (1)	4 (1)	0.06	Coiled-coil domain-containing protein 149 OS=Homo sapiens GN=CCDC149 PE=2 SV=2
ATXN1L	ATX1L_HUMAN	15	73774	2 (1)	2 (1)	0.04	Ataxin-1-like OS=Homo sapiens GN=ATXN1L PE=1 SV=1
CD63	CD63_HUMAN	15	26474	6 (1)	4 (1)	0.13	CD63 antigen OS=Homo sapiens GN=CD63 PE=1 SV=2

Supplementary Table 6. Primers for CHIP-RT-qPCR analysis

Targets	Forward (5'-3')	Reverse (5'-3')	Product (bp)	Position of products
FOXA2_1	CTGGTCGAGCCCCCTTTC	AGAGGGTGGTTTCCTCCCAG	77	22584975...22585051
FOXA2_2	GCCCCTCCCTGTTACAGTTC	GGTGTCTGAGGAGTCGGAGA	94	22585305...22585398
FOXA2_3	TTCCAGCCTCACCCTTACT	CCTCAGACACAGAGAATGCATAG	138	22585907...22586022
FOXA2_4	TGCCTACTGCTACCTCCTC	GCAGAAGACAGGCGAGATG	93	22585956...22586048
FOXA2_5	GCACAGACTAGGTCAACCATAA	GGAAAGAGGAGTAAGCATTGGA	142	22586454...22586595
FOXA2_6	AAATCAGAACTCCGGGAAGG	GGGTCTACGGTTAGCTTTAGG	141	22587155...22587295
Linc00261_1	CAGCACTTTGCCTGTTCACC	AGTGTCTCGCCATTTCTGGG	186	22580309...22580494
Linc00261_2	TCTGGCCAATGGACCATGAC	CTGGATTGCCAACCTCACCT	122	22580062...22580183
Linc00261_3	TTGAGTGCTACCTTGCTGGG	GAGGAGAGACGGCCTGATTG	246	22579380...22579625
Linc00261_4	AAAAGGATGTCGGGGAGCAG	AGTAGAGTTGGGGAAAGCGC	149	22578983...22579131
Linc00261_5	TTCCATGCCACGTCACACTT	GCAAAGATTTCACTGCCCGC	180	22578650...22578829

Supplementary Materials and Methods

Cell lines and culture conditions

Liver cancer cell lines MHCC-LM3, MHCC-97H, MHCC-97L were obtained from Liver Cancer Research Institute, Zhongshan Hospital affiliated to Fudan University, Shanghai, China as a gift. Huh7, BEL-7402, SMMC-7721 cancer cell lines and human immortalized liver cell line LO2 were bought from the Institutes of Biological Sciences, Chinese Academy of Sciences, Shanghai, China. SNU-449, SNU-387, SK-hep1 and HepG2 were purchased from American Type Culture Collection (ATCC; VA, USA).

Huh7, MHCC-LM3, MHCC-97H, MHCC-97L, SK-hep1, HepG2 were cultured in Dulbecco's modified Eagle medium (DMEM) medium (Gibco, CA, USA) supplemented with 10% fetal bovine serum (Gibco). LO2, SNU-449, SNU-387, BEL-7402 and SMMC-7721 were maintained in Roswell Park Memorial Institute (RPMI) -1640 medium (Gibco). All cell lines were maintained at 37°C in a humidified atmosphere with 5% CO_2.

Cell proliferation assay, plate colony-forming assay, Transwell migration and invasion assays

The cell viability and colony formation ability were detected using Cell counting Kit-8 (CCK-8; Dojindo Laboratories, Kumamoto, Japan) assay and plate colony-forming assay, respectively. Cell migration and invasion abilities were evaluated by Transwell assay. All experiments were repeated for 3 times.

For the CCK-8 assay, cells (3,000/well) were seeded into 96-wells plates. After adhesion, cell viability was assessed after 0, 24, 48, 72 and 96 hours according to the manufacturer's protocol.

For the plate colony-forming assay, cells (200/well) were seeded into 6-well plates and incubated for another two weeks. Then, the colonies were fixed in 4% paraformaldehyde, stained with 0.5% crystal violet, captured with FluorChem E system (ProteinSimple, CA, USA) and manually counted.

For Transwell assays, cells were harvested, suspended in serum-free media, and seeded into the upper compartments of chambers (Corning, NY, USA) without (for migration) or with Matrigel (at a dilution of 1:8 with serum-free medium for invasion; Corning) -coated that inserted in 24-well plates (5×10^4/well), the complete medium was added into the lower chambers. After 24 hours incubation, cells migrated and invaded to the other side of the membranes were fixed, stained with 0.5% crystal violet and digitally imaged under microscope (Olympus, Tokyo, Japan).

RNA extraction and RT-qPCR

Total RNA was extracted from tissues and cell lines using RNAiso Plus reagent (Takara, Dalian, China) and then converted into cDNA (PrimeScript first-strand cDNA synthesis kit; Takara), which was subsequently applied for RT-qPCR detection on StepOne plus system (Applied Biosystems, CA, USA) using SYBR Premix Ex Taq™ kit (Takara) according to the manufacturer's instructions. The RT-qPCR primer sequences were listed as follow: linc00261, 5'-GTCAGAAGGAAAGGCCGTGA-3' (forward), 5'-TGAGCCGAGATGAACAGGTG-3' (reverse); FOXA2, 5'-GGAGCAGCTACTATGCAGAGC-3' (forward), 5'-CGTGTTCATGCCGTTCATCC-3' (reverse); SMAD3, 5'-TGTGCGGCTCTACTACATCG-3' (forward), 5'-GCAGCAAATTCCTGGTTGTT-3' (reverse); 18S rRNA, 5'-GTAACCCGTTGAACCCCATT-3' (forward), 5'-CCATCCAATCGGTAGTAGCG-3' (reverse). 18S rRNA was used as internal control, and $2^{-\Delta\Delta CT}$ method was applied to analyze expression of target genes.

Western blotting

Cells were harvested and lysed with RIPA lysis buffer (Beyotime, Shanghai, China) containing 1 mM protein inhibitor, Phenylmethanesulfonyl fluoride (Beyotime) after washed with ice-cold PBS solution. The protein concentrations were determined using bicinchoninic acid (BCA; Beyotime) and equivalent total protein was then separated with 10% sodium dodecyl sulfate polyacrylamide gel electrophoresis gel, transferred to polyvinylidene fluoride membrane (PVDF; Millipore, MA, USA). Followed with blocking non-specific antigens by TBST solution containing 5% skimmed milk for 1 hour at room temperature, the

membranes were incubated with primary antibodies (Supplementary Table 5) overnight at 4°C, and subsequently incubated with horseradish peroxidase-conjugated goat-anti-rabbit secondary antibody (1:10,000; Proteintech, MA, USA) for 1 hour at room temperature. Detection was performed using ECL substrate kit (Fdbio Science, Hangzhou, China) under FluorChem E system (ProteinSimple).

Subcellular fractionation and quantification of RNAs

Cytoplasm and nuclear fraction of MHCCLM3 and SNU-449 cells were separated using a cytoplasmic and nuclear extraction kit (BestBio, Shanghai, China). After removal of DNA using DNase, the cytoplasmic and nuclear RNA were respectively extracted from cytoplasmic and nuclear fraction with the assistance of HiPure total RNA nano kit (Magen, Guangzhou, China). Linc00261, GAPDH (known as primary located at cytoplasm) and U1 snRNP (known as primary located at nucleus) expressions in cytoplasm and nucleus were determined by RT-qPCR, and the values were normalized to β-actin mRNA. The primers used were listed as follow: GAPDH, 5'-CAGGAGGCATTGCTGATGAT-3' (forward), 5'-GAAGGCTGGGGCTCATTT-3' (reverse); U1 snRNP, 5'-ATACTTACCTGGCAGGGGAG-3' (forward), 5'-CAGGGGGAAAGCGCGAACGCA-3' (reverse); β-actin, 5'-CGTCACCAACTGGGACGACA-3' (forward), 5'-CTTCTCGCGGTTGGCCTTGG-3' (reverse); primers of linc00261 were the same as above.

Establishment of transient knockdown models

Small interfering RNAs (siRNAs) for human linc00261, FOXA2 and SMAD3 were designed and synthesized by GenePharma (Shanghai, China) and were used to establish the transient knockdown models with the aid of Lipofectamine 3000 transfection reagent (Invitrogen, CA, USA) in MHCC-LM3 and SNU-449 cells. After 48-72 hours incubation, cells were collected for knockdown efficiency validation or other assays. The sense strand of the siRNAs were listed as follow: linc00261-1, 5'-GAAAGCTGTAGCCATTCAA-3'; linc00261-2, 5'-GCAATTAATTCAGGACACT-3'; FOXA2-1, 5'-GAAAGCTGTAGCCATTCAA-3'; FOXA2-2, 5'-GCAATTAATTCAGGACACT-3'; SMAD3-1, 5'-GGAUUGAGCUGCACCUGAATT-3'; SMAD3-2, 5'-GGAGAAAUGGUGCGAGAAGTT-3'; Negative control (NC), 5'-TTCTCCGAACGTGTCACGTTT-3'.

Lentivirus construction and transfection

For the construction of stably linc00261-overexpression model, the full length of linc00261 (NR.001558.3) was synthesized and then cloned into a lentivirus (Ubi-MCS-SV40-EGFP-IRES-puromycin) by Genechem (Shanghai, China). HepG2 and SMMC-7721 cells were infected with either linc00261-overexpression lentiviral vectors or empty vectors at a multiplicity of infection (MOI) of 20. The antibiotic-resistant transfected cells were enriched by applying 2 ug/mL puromycin culture media for 7 days, and the overexpression of linc00261 were confirmed by RT-qPCR.

In situ tumor model

The animal experiment was approved by the Institutional Animal Care and Use Committee of Southern Medical University. Male Biocytogen-NOD-*Prkdc*^{scid}*IL2rg*^{tm1}/Bcgen (B-NDG; age, 4-6 weeks) mice were purchased from Beijing Biocytogen corporation and kept in specific pathogen-free (SPF) grade conditions with free access to sterilized food and water. For the construction of orthotopic xenograft tumor model of HCC, a small transverse incision was made at the upper abdomen of the mice to expose the liver after anesthesia. Then, about 2 × 10^6 linc00261-overexpression (7 mice) or -vector SMMC-7721 cells (9 mice) that pre-transfected with another vector-lentivirus (Ubi-MCS-firefly-Luciferase-IRES-Puromycin; Genechem) were suspended in 20 μL of PBS and injected into the upper left lobe of the liver. After confirmation of hemostasis of the injection site, the abdominal cavity was closed with silk thread.

To observe the growth of intra- and extra-hepatic tumors, mice were anesthetized and intraperitoneal injected with D-Luciferin, Potassium salt (Yeasen, Shanghai, China). After 10 mins, the intra- and extra-hepatic tumors were viewed under bioluminescence IVIS Lumina II Imaging System (Xenogen, CA, USA). After 30 days, the mice were scarified and the livers and lungs were collected for further detection.

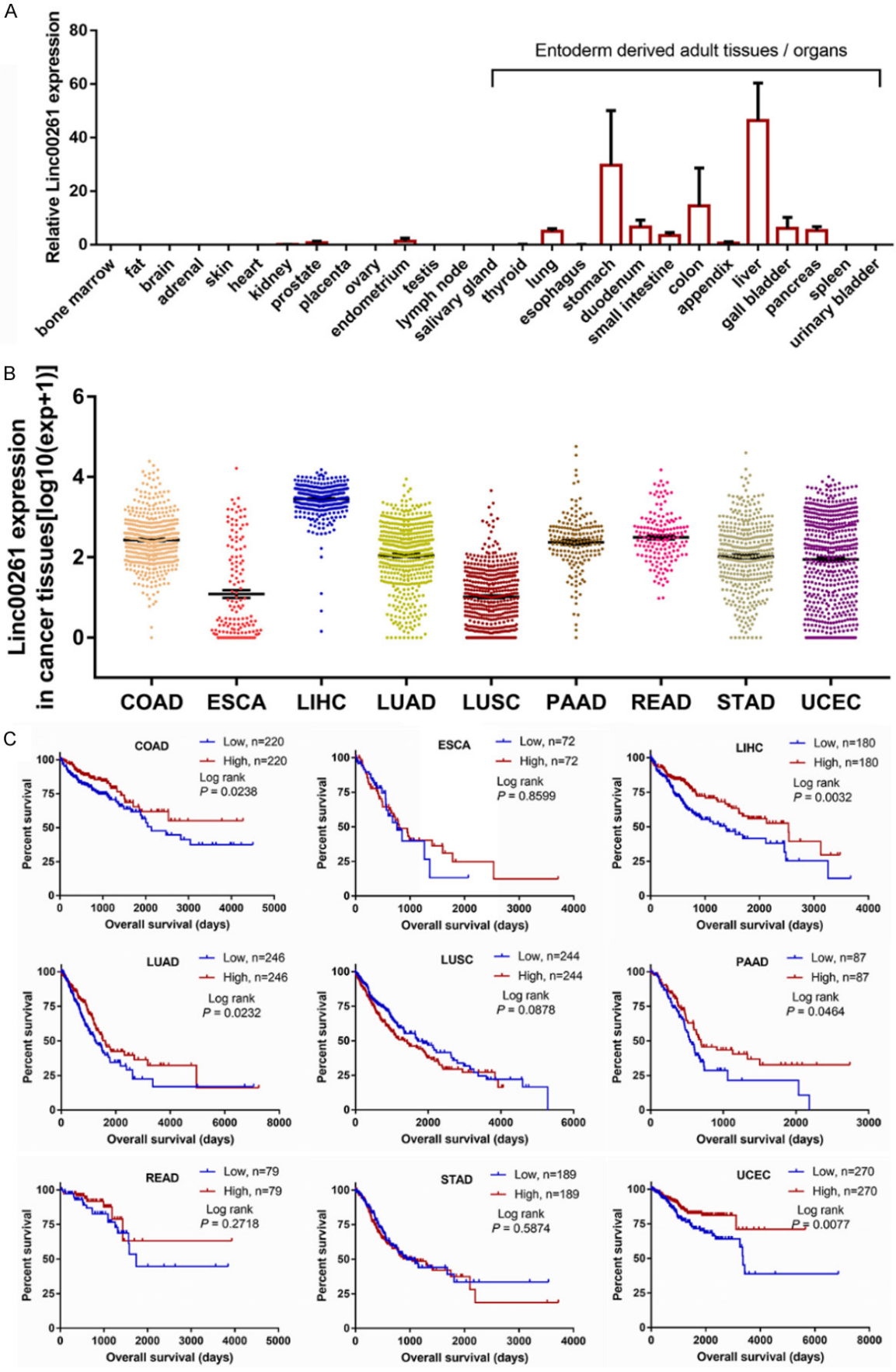
A
Relative Linc00261 expression
Entoderm derived adult tissues / organs
bone marrow
fat
brain
adrenal
skin
heart
kidney
prostate
placenta
ovary
endometrium
testis
lymph node
salivary gland
thyroid
lung
esophagus
stomach
duodenum
small intestine
colon
appendix
liver
gall bladder
pancreas
spleen
urinary bladder
B
Linc00261 expression in cancer tissues[log10(exp+1)]
COAD
ESCA
LIHC
LUAD
LUSC
PAAD
READ
STAD
UCEC
C
COAD
Low, n=220
High, n=220
Log rank P = 0.0238
ESCA
Low, n=72
High, n=72
Log rank P = 0.8599
LIHC
Low, n=180
High, n=180
Log rank P = 0.0032
LUAD
Low, n=246
High, n=246
Log rank P = 0.0232
LUSC
Low, n=244
High, n=244
Log rank P = 0.0878
PAAD
Low, n=87
High, n=87
Log rank P = 0.0464
READ
Low, n=79
High, n=79
Log rank P = 0.2718
STAD
Low, n=189
High, n=189
Log rank P = 0.5874
UCEC
Low, n=270
High, n=270
Log rank P = 0.0077
Percent survival
Overall survival (days)

Supplementary Figure 1. Linc00261 expression in normal tissues/organs and the survival analysis in 9 common cancers. A. Linc00261 expression in 27 normal tissues/organs derived from different germinal layers during embryo development obtained from NCBI gene database; B. Linc00261 expression in 9 common cancers obtained from *oncoInc*; C. Kaplan-Meier analysis of overall survival in cancers with different linc00261 expression. COAD, Colon adenocarcinoma; ESCA, Esophageal carcinoma; LIHC, Liver hepatocellular carcinoma; LUAD, Lung adenocarcinoma; LUSC, Lung squamous cell carcinoma; PAAD, Pancreatic adenocarcinoma; READ, Rectum adenocarcinoma; STAD, Stomach adenocarcinoma; UCEC, Uterine corpus endometrial carcinoma.

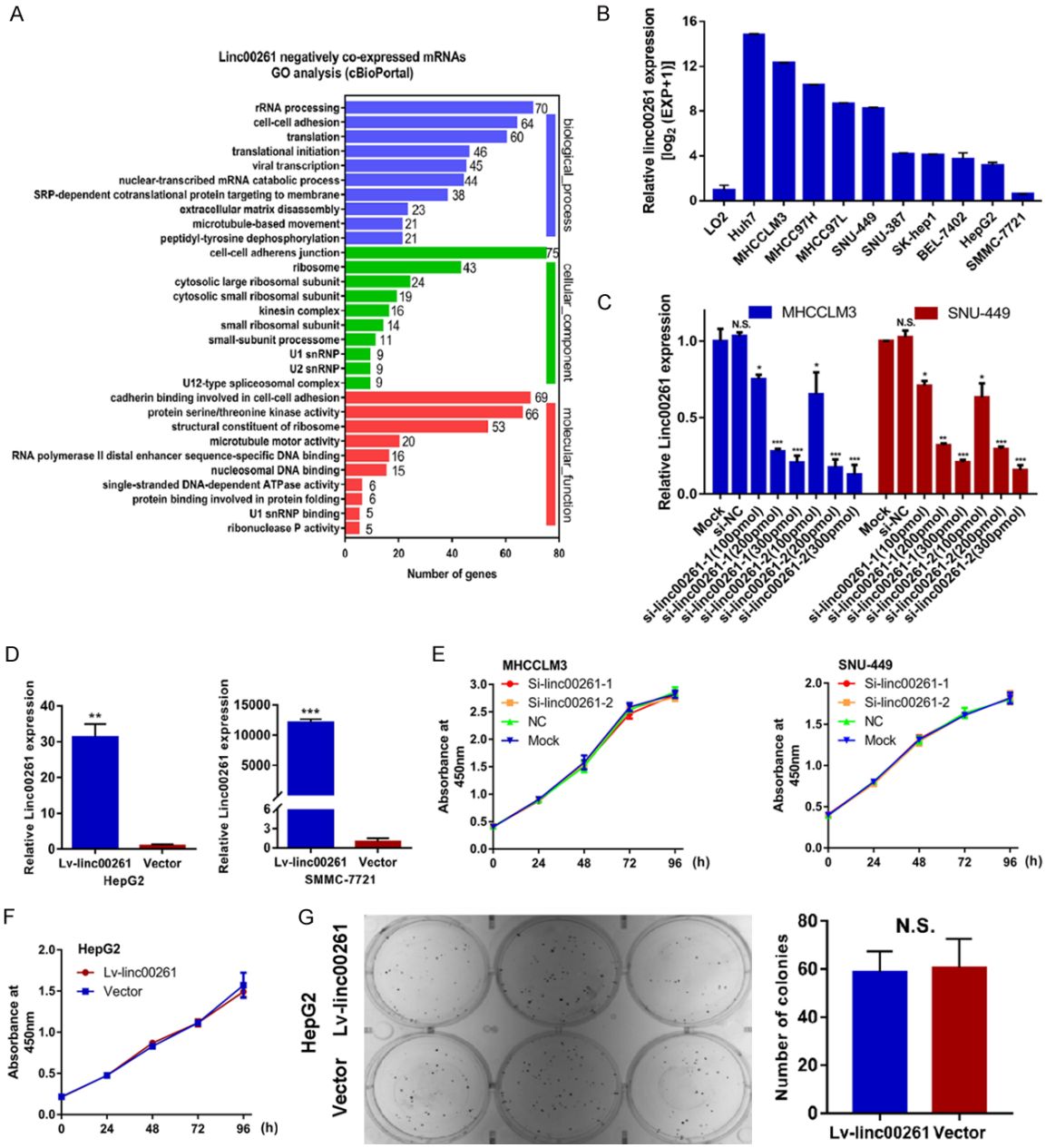

Supplementary Figure 2. Bioinformatic analysis of linc00261 co-expressed genes and its effect on cell proliferation. (A) GO analysis conducted by *DAVID* using linc00261 negatively co-expressed mRNAs obtained from *cBioPortal*; (B) Linc00261 expression in a subset of HCC cell lines; (C) Successfully knockdown of linc00261 using gradient amounts of siRNAs in MHCCLM3 and SNU-449 cell lines determined by RT-qPCR and ANOVA; (D) Lentivirus-mediated overexpression of linc00261 in HepG2 and SMMC-7721 evaluated by RT-qPCR and t-test; (E, F) Cell proliferation after linc00261 knockdown (E; MHCCLM3 and SNU-449) or overexpression (F; HepG2) revealed by CCK-8 assay; (G) Plate colony-forming assay and statistical analyses after overexpression of linc00261 in HepG2. GO, Gene Ontology; N.S., not significant; $*P < 0.05$; $**P < 0.01$; $***P < 0.001$.

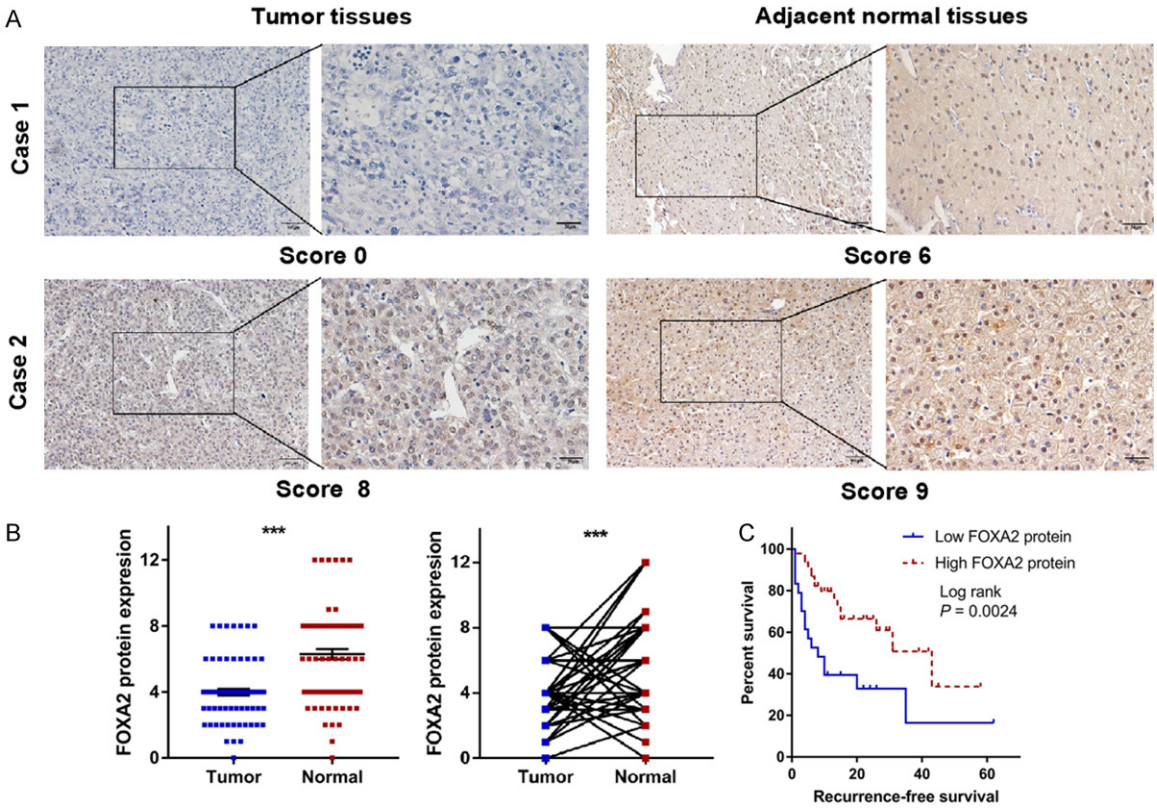

Supplementary Figure 3. FOXA2 protein expression in patients with HCC and the survival analysis. A. Representative images of various FOXA2 protein levels in HCC and adjacent normal tissues; B. Comparison of FOXA2 protein expression in HCC and adjacent normal tissues (n=79); C. Recurrence-free survival was analyzed by Kaplan-Meier method in HCC patients with different FOXA2 protein levels (n=72, P=0.0024). ***$P < 0.001$.

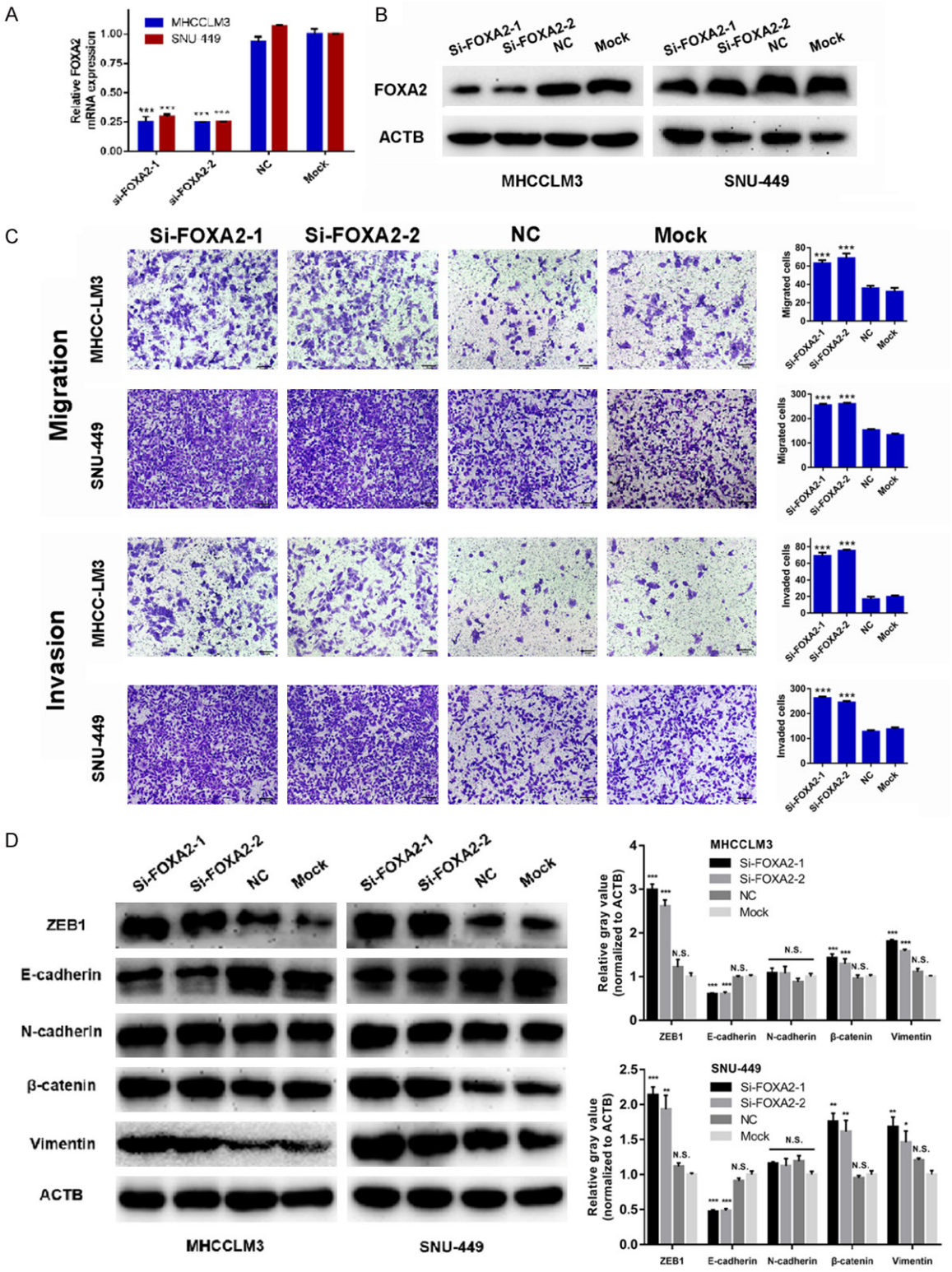

Supplementary Figure 4. Transient knockdown of FOXA2 promoted migration, invasion and EMT in HCC cells. A and B. Successfully knockdown of FOXA2 using siRNAs in MHCCLM3 and SNU-449 cell lines determined by RT-qPCR and western blotting; C. Representative images and statistical analyses of migration and invasion assays after FOXA2 knockdown by siRNAs in MHCCLM3 and SNU-449 cell lines; D. The protein expressions of epithelial (E-cadherin) and mesenchymal associated markers (N-cadherin, β-catenin and Vimentin)/transcription factor (ZEB1) determined by western blotting after transient knockdown of FOXA2 in MHCCLM3 and SNU-449 cell lines; the gray values of protein bands were evaluated by image J. N.S. not significant; *$P < 0.05$; **$P < 0.01$; ***$P < 0.001$. The original western blotting images refers to Supplementary Figure 7.

Supplementary File 2

Transcriptional factors predicted to modulate FOXA2 transcription using JASPAR

BHLHE22
CLOCK
BARHL2
EGR4
FOXD2
DBP
EHF
FOSL2
CEBPD
FOXL1
HIC2
FOXP2
ERG
EGR2
GSC
ESX1
ARNT::HIF1A
GATA3
HEY2
ETV5
ELF5
CENPB
FOXC2
ELK1
GATA2
CREB3
ETV4
FOXP1
HINFP
ETV3
GSX2
FOXH1
FEV
FOXO4
E2F6
FIGLA
CUX1
FOXP3
DUX4
ELF4
GCM1
ELF1
EBF1
FOXD1
E2F4
FOXA1
CREB1
GSX1
FOXC1
DMRT3

FOS
FLI1
HESX1
ESRRB
BSX
FOXO3
ELK3
EMX2
EN1
ETV6
CEBPB
FOXI1
GSC2
GCM2
ESRRA
ETV1
FOXB1
CEBPG
E2F1
EVX1
AR
CUX2
BHLHE23
ESR2
CEBPE
GBX2
ETS1
GLIS2
GATA5
CDX2
EGR3
BHLHE40
HLF
GABPA
ALX3
GATA1::TAL1
FOXO6
BARX1
EVX2
EGR1
EN2
ELK4
GMEB2
BATF::JUN
HEY1
CEBPA
FOS::JUN
EMX1
CDX1
ERF
GBX1
FOXG1
DLX6
CREB3L1

GRHL1
HES5
ELF3
EOMES
HES7
BHLHE41
Bhlha15
Foxd3
Atf1
Barhl1
Esrra
Gabpa
Bhlhe40
Foxa2
Hes1
Arid5a
Gmeb1
Egr1
Gata4
Crem
FOSL1::JUND
Dlx3
Dux
Creb3l2
Hic1
FOXK2
Erg
Cebpa
Gata1
Arid3b
Gfi1b
GATA6
Dlx4
ASCL1
CTCFL
En1
Bcl6
Esrrg
Ascl2
Arnt
Creb5
Ddit3::Cebpa
Hes2
Dmbx1
Atoh1
E2F3
Esrrb
Foxj2
Foxo1
HIF1A
Crx
Arid3a
FOSL1::JUND(var.2)
Dlx1

Atf3
FOSB::JUNB(var.2)
Hand1::Tcf3
FOSL1::JUN(var.2)
Dlx2
Ahr::Arnt
Gfi1
Ets1
YY1
PAX7
TFEC
ZNF263
SP3
SPIB
TBX21
TCF3
TAL1::TCF3
SOX9
TP53
REL
MNT
MZF1(var.2)
MSC
HOXD11
RFX5
ZEB1
ZIC1
HOXC13
TFAP2A(var.3)
RHOXF1
ZNF354C
MEIS1
MIXL1
USF2
UNCX
STAT1::STAT2
TBX4
LM43
MAX
NR4A2
PAX1
RORA
PAX4
TCF7L2
HOXA13
TFE3
TEAD1
NFIA
NR2F1
PHOX2A
VSX2
LBX1
SOX10
HOXA10

ONECUT1
INSM1
RUNX3
NEUROD2
POU3F4
POU3F1
NKX2-8
HOXC11
STAT3
LM168
LM59
LM165
RARA::RXRA
HOXA2
HOXD12
ID4
NKX2-3
HSF4
MEOX1
OTX2
VAX1
LM142
NFIX
SMAD3
PAX3
PITX3
TBX5
TFEB
SPI1
T
POU1F1
LMX1B
HOXA5
MLXIPL
SHOX
RREB1
NFKB1
HOXC12
NRL
SP1
RAX2
KLF16
ZBTB33
MGA
NHLH1
TBX1
TFAP4
SP8
HNF4G
LM33
LBX2
NKX3-1
ZNF740
ZBTB7A

NOTO
PDX1
TFCP2
RFX4
OLIG1
ZBTB7B
OLIG3
TBR1
PLAG1
LM205
JUNB
SREBF1
RFX3
TFAP2B(var.2)
HMBOX1
VAX2
MEIS2
POU6F2
NFATC3
NFKB2
LM114
TEAD3
HOXC10
NKX6-1
MEOX2
SPDEF
MAFK
TFAP2C(var.3)
POU3F3
TFAP2C
POU2F1
MSX1
SREBF2
MYF6
PAX9
KLF5
VENTX
MEF2A
ZBTB7C
NKX3-2
LM141
ZIC3
TBX2
NFIC
LHX2
JUN
HOXB3
MEIS3
LHX6
THAP1
LMX1A
ONECUT2
SP2
POU3F2

SPIC
SNAI2
HOXB2
ZBTB18
TFAP2A(var.2)
OLIG2
LM216
POU6F1
SP4
PAX5
HOXB13
NKX6-2
LHX9
POU2F2
NFIL3
MAFF
TFAP2B
TBX15
HNF4A
ISL2
TBX19
RAX
NEUROG2
RELA
SRF
STAT1
TFAP2C(var.2)
HOXD13
TCF4
NR2C2
MZF1
ONECUT3
VSX1
KLF14
JUND(var.2)
TBX20
POU5F1B
MNX1
HSF1
TFAP2B(var.3)
NFATC2
OTX1
TEF
NFYA
LM130
XBP1
ZIC4
TFAP2A
MSX2
PRDM1
USF1
TEAD4
RUNX2
SMAD2::SMAD3::SMAD4

RORA(var.2)
MEF2C
NFE2L2
LM112
NRF1
NR3C1
PRRX1
ISX
SRY
Alx4
ESR1
DUXA
BACH2
Alx1
FOSB::JUNB
CTCF
FOSL1
ETV2
FOSL2::JUNB
Arntl
Foxj3
FOSL2::JUN

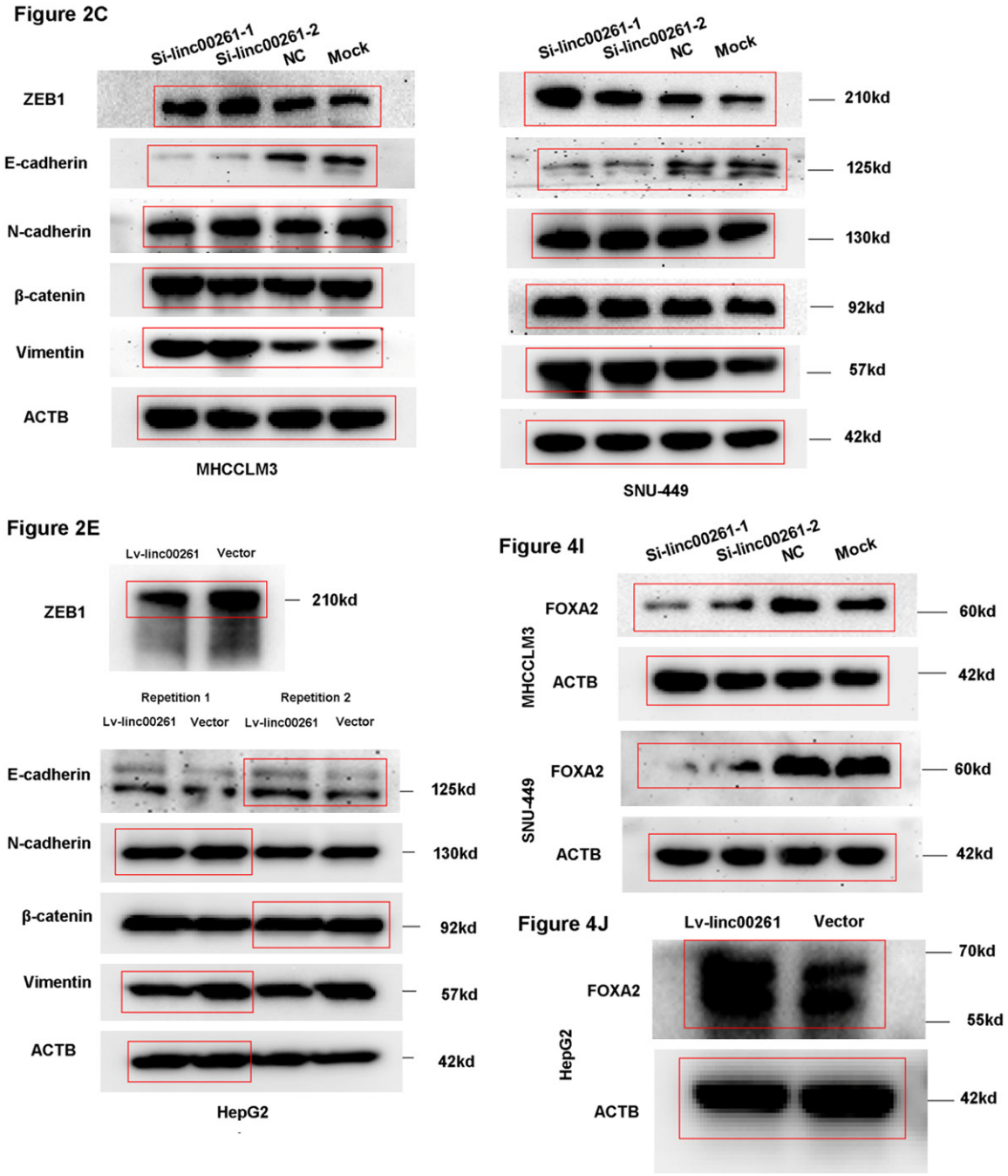

Supplementary Figure 5. Original western blotting images of **Figures 2C**, **2E**, **4I** and **4J**.

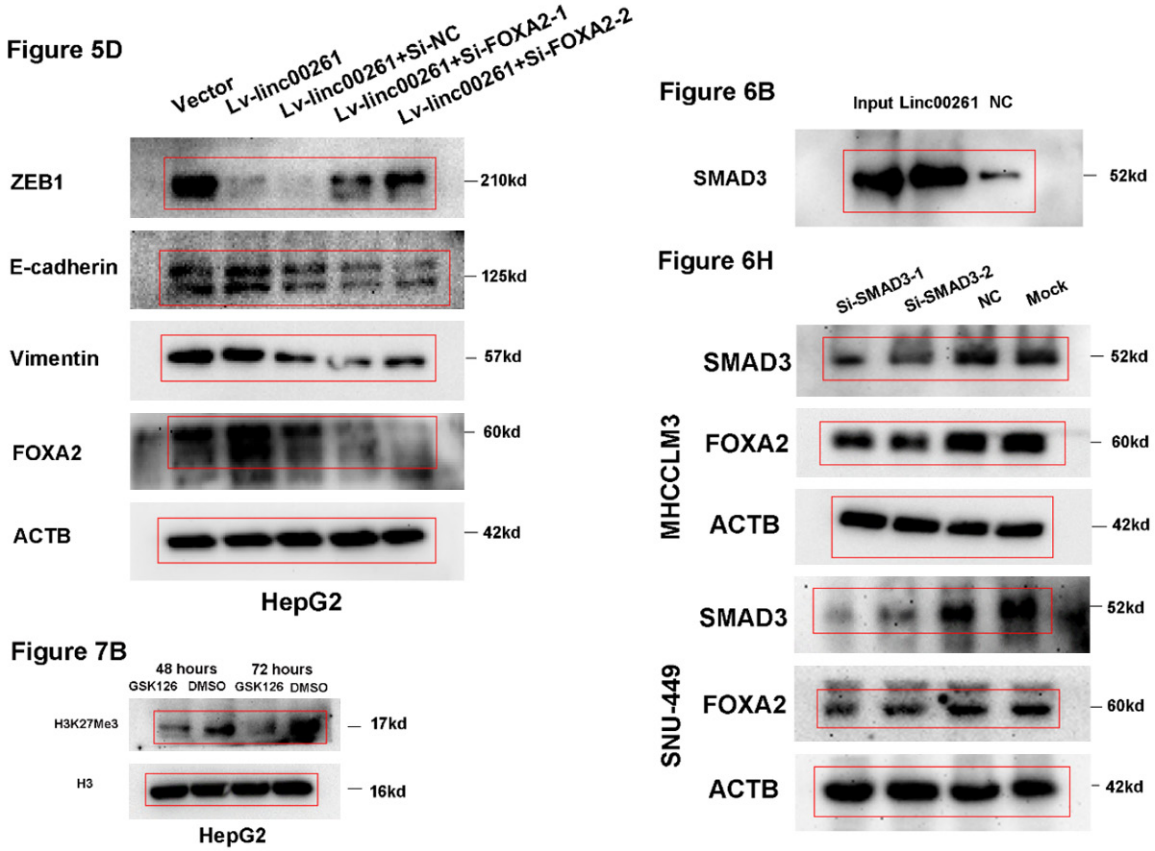

Supplementary Figure 6. Original western blotting images of **Figures 5D**, **6B**, **6H** and **7B**.

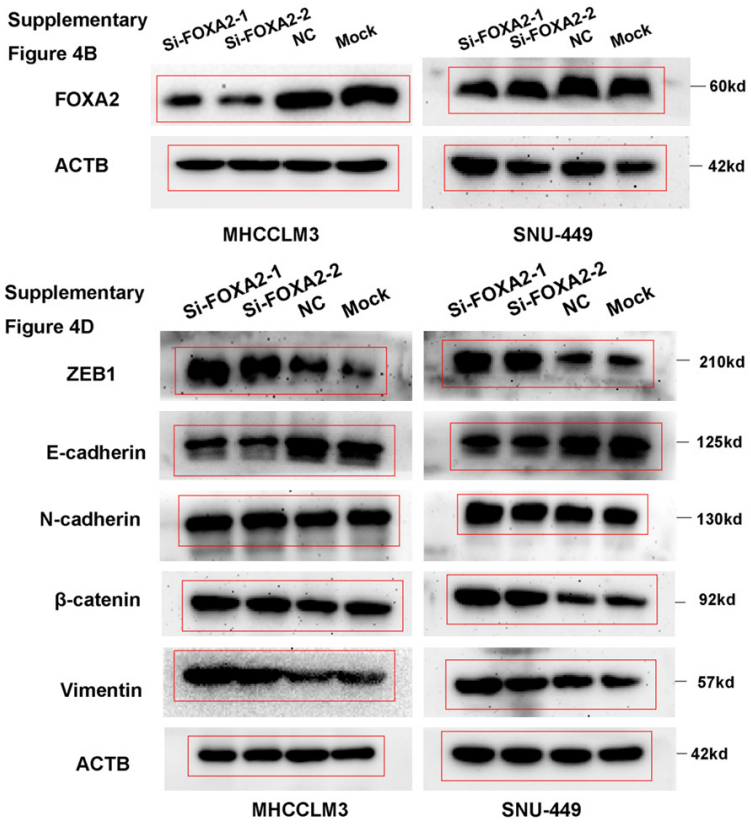

Supplementary Figure 7. Original western blotting images of Supplementary Figure 4B and 4D.